Monte Carlo Simulation and Statistical Mechanics Modelling of Mixture Adsorption in Silicalite

Seyed Ebrahim Jalili

March 2011

Chemical Engineering Department
University College London

A thesis submitted to University College London for the degree of Doctor of Philosophy

DECLARATION

The work presented in this thesis was carried out in department of chemical engineering, University College London, and is the original and independent research work of the author, except where specifically acknowledged in the text.

No part of this thesis has previously has been submitted in candidature for a degree in any other university.

Seyed Ebrahim Jalili

March 2010

ACKNOWLEDGEMENT

Firstly, I would like to express my deepest thanks to my supervisor, Dr George Manos; thank you for your excellent supervision, warm encouragement and invaluable advice.

I am also very grateful to Professor Lawrence J. Dunne from London South Bank University for his guidance and help.

My gratitude is also towards all of my colleagues.

I am further greatly indebted to my wife, Mandana, for her understanding and continual encouragement through both the smooth and difficult times.

CONFERENCE AND PUBLICATIONS

1. Ayache Khettar, Seyed E. Jalili, Lawrence J. Dunne, George Manos and Zhimei Du, **"Monte-Carlo simulation and mean-field theory interpretation of adsorption preference reversal in isotherms of alkenes binary mixtures in zeolites at elevated pressures",** Chemical Physics Letters, Volume 362, Issues 5-6, 26 August 2002, Pages 414-418

2. Seyed E. Jalili, Lawrence J. Dunne, George Manos and Ayache Khettar, **"Statistical mechanics of a two-dimensional lattice model of benzene adsorption in zeolites",** Chemical Physics Letters, Volume 367, Issues 3-4, 6 January 2003, Pages 324-329

3. Seyed E. Jalili, George Manos, Lawrence J. Dunne, **"Statistical Mechanical Treatment of Hydrocarbon Adsorption in Zeolites. Adsorption in Silicalite of Benzene and Alkane Binary mixtures"**, International Symposia on Chemical Reaction Engineering, ISCRE 18, Chicago, June 6-9, 2004

4. Georeg Manos, Lawrence J. Dunne, Seyed E. Jalili, **"Matrix computation of the statistical mechanics of a lattice model of multistep benzene adsorption isotherms in silicalite"**, Chemical Physics Letters, Volume 401, Issues 4-6, 11 January 2005, Pages 430-434

5. Seyed E. Jalili, **"Statistical mechanics of adsorption of hydrocarbons on zeolites"** , 7th World Congress of Chemical Engineering, Glasgow, Scotland, 12 July 2005

6. Lawrence J Dunne, Akrem Furgani, Seyed Jalili, George Manos; **"Monte Carlo simulations of methane/carbon dioxide and ethane/carbon dioxide mixture adsorption in zeolites and comparison with matrix treatment of statistical mechanical lattice model"**, Chemical Physics, Volume 359, Issues 1-3, 18 May 2009, Pages 27-30

7. Lawrence J. Dunne, Akrem Furgani, Seyed Jalili and George Manos "**Monte Carlo Simulation and Lattice Model Studies of Adsorption of Methane, Ethane, Carbon Dioxide and Their Binary and Ternary Mixtures in the Silicalite Zeolite"**, in "Adsorption and Phase Behaviour in Nanochannels and Nanotubes" Eds: L.J. Dunne, G. Manos, Springer, 2010, Pages 147-169.

ABSTRACT

Adsorption in zeolites is widely and increasingly used in many industrial processes. For the design of new processes and improvement of the performance of existing ones, basic adsorption data is needed but due to the difficulties of experimentation it is lacking.

In this thesis, different methods have been used to calculate the adsorption isotherms of benzene, methane, ethane and CO_2 mixtures as well as Propane, i-butane and n-butane and their binary and ternary mixtures in zeolites.

Firstly, Lattice Model has been used to calculate benzene adsorption isotherms in silicalite zeolite whose experimental adsorption isotherms exhibit unusual features. The zeolite is modelled as two types of quasi one-dimensional pores. The lattice model has dimer states to represent molecules lying in extended states with the aromatic ring on average parallel to the pore wall, the monomer state to represent molecules standing perpendicular to the principle axis of the pores. Vacant sites or holes allow

for incomplete filling of the lattice sites. For a wide range of interaction parameters the model gives steps in the adsorption isotherms similar to those observed experimentally for benzene adsorption in silicalite. The model attributes the experimentally observed steps in the level of adsorption with rising pressure, to re-orientational transitions amongst molecules in the adsorbed phase.

Secondly Conventional Grand Canonical Monte Carlo techniques have been used to calculate methane, ethane and CO_2 binary mixture adsorption isotherms in silicalite as well as propane, i-butane and n-butane equimolar binary and ternary mixture adsorption in silicalite.

In the last part of the thesis, studies have made of lattice models of CH_4 / C_2H_6 and CO_2 adsorption in silicalite and the results compared with the Monte Carlo data. One dimensional lattice models have also been used to calculate the binary and ternary mixture adsorption of propane, i-butane and n-butane. The isotherms were compared with the Monte Carlo results.

TABLE OF CONTENTS

1- INTRODUCTION

Adsorption is a process with great fundamental and technical significance in which molecules of a bulk phase adhere to a solid surface. The study of surfaces has developed to become an existing area of research. Surface science has benefited from the increased power of analytical instruments for probing surfaces, and on the theoretical side from a deeper understanding of the basic intermolecular forces involved in adsorption and the wide availability of powerful computing facilities. In this thesis, theoretical studies are presented which have been made of adsorption isotherms for hydrocarbon in silicalite using computer simulation techniques, and the theoretical derivation of several analytical models of adsorption.

1.1 Physical and chemical adsorption

The molecules that bind to surface are called the adsorbate while the substance holding the adsorbate is called the adsorbent. Adsorption leads to loss of degree of freedom of molecules and a decrease in entropy. Regardless of the nature of the molecules or the type of adsorbent surface,

adsorption is always exothermic. According to the forces involved, there are two types of adsorption, namely physical adsorption and chemical adsorption. In the former the molecules retain their identity while in the latter dissociation may occur. Physical adsorption is non-specific and similar to the process of condensation of a fluid. The forces involved in physical adsorption are Van der Waals (dispersion) forces and electrostatic interactions (e.g. dipole, polarisation interactions). The Van der Waals force is always important, while the electrostatic interactions are usually only significant for adsorbents which have a marked polar or ionic structure. The heat of adsorption is the same order of magnitude as the heat of condensation, normally about $-20\ kJmol^{-1}$, as for example, the heat of methane adsorption in silicalite at low coverage (Atkins, 1998). In general, the physical process is rapid and reversible. The amount of adsorption decreases rapidly as the temperature is raised and is generally small above the critical temperature of the adsorbed component. Physical adsorption is not highly dependent on the irregularities in the nature of the surface, but is usually direct proportional to surface area.

In contrast, chemical adsorption is specific and involves chemical bonding forces that are much stronger than Van der Waals forces. The sharing of electrons between adsorbent and adsorbate leads to the formation of a chemical bond. Chemical adsorption refers to higher heats of adsorption than physical adsorption at least an order of magnitude. For example the heat of adsorption of ethane on CR is $-427\ kJmol^{-1}$ (Atkins, 1998).

The general features, which distinguish physical adsorption and chemical adsorption, are shown in Table 1-1:

Table 1-1 Physical and Chemical adsorption characteristic

Physical adsorption	Chemical adsorption
Low heat of adsorption (<2 or 3 times latent heat of evaporation)	High heat of adsorption (>2 or 3 times latent heat of evaporation)
None specific	Highly specific
Monolayer or multilayer. No dissociation of adsorbed species. Only significant at relatively low temp.	Monolayer only May involve dissociation. Possible over a wide range of temp.
Rapid, non-activated, reversible. No electron transfer although polarisation of adsorbate may occur.	Activated, may be slow and irreversible. Electron transfer leading to bond formation between adsorbate and surface.

1.2 Application of adsorption

Adsorption phenomena are operative in many physical, biological and chemical systems. Adsorption on solids such as synthetic zeolites or activated carbon is of great scientific interest since they are involved in many industrial processes. From the early days of using bone char for decolourisation of sugar solutions and other foods, to the later implementation of activated carbon for removing nerve gases from battlefield, adsorption presently has many applications.

There are three main groups of adsorption applications, namely catalysis, separation of gases and purification of gases.

Catalysis- Adsorption plays a key role in heterogeneous catalysis. A typical mechanism of catalytic reaction on a solid involves adsorption of reactant

components on the catalyst surface, surface reaction and desorption of the products (Smith, 1981).

Separation of gases- Adsorptive separation of mixtures is based on the preferential adsorption of one component of the mixture. It has been used for the separation of the noble gases, the extraction of gasoline from natural gas, the recovery of benzene and light oil from illuminating gas, etc.

Purification of gases- Pure gases are required in many applications such as in anaesthesia. Other processes include the purification of carbon dioxide to make it usable for carbonated water, the purification of hydrogen before catalytic hydrogenation, the purification of ammonia before catalytic oxidation, the refining of helium, the drying of air and other gases, the purification of air in submarines and so on. In all of these applications, adsorption plays a central role.

Furthermore, adsorption of supercritical fluids is now widely used to regenerate adsorbents (DeFilippi et al., 1983), decontaminate soils (Brady et al., 1987), separate and purify gases, e.g. hydrogen and light hydrocarbons and displace adsorbed compounds (Tan & Liou, 1988). In recent years adsorption and catalysis under supercritical conditions have received more attention since several advantages over conventional adsorption and catalysis processes have been exploited (Johnston & Haynes, 1987).

1.3 Adsorption in zeolites

Zeolites are microporous crystalline materials with pores that have about the same size as small molecules like water or n-hexane (pore size is usually 3-12

Å). The structure of a zeolites is based on a covalently bonded TO_4 tetrahedra in which the tetrahedral atom T is usually silicium or aluminium (See Figure 1-1) .

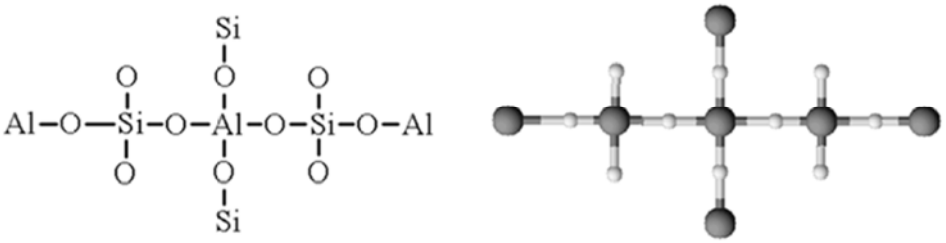

Figure 1-1 Basic Zeolites Chemical Structure (left) Crystal structure (right)

As all corners of a tetrahedral have connections to other tetrahedra, a three dimensional pore network of channels and/or cavities is formed (see Figure 1-2).

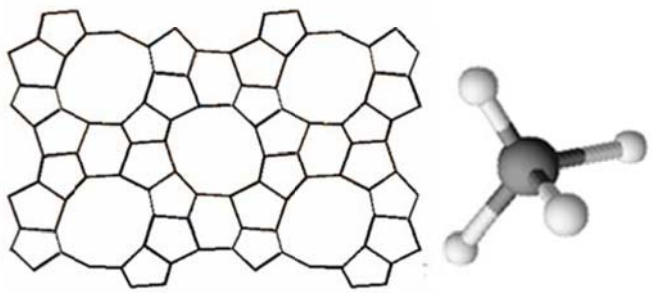

Figure 1-2 All zeolites crystal structures is a framework (left) (International Zeolite Association, 2010a) built up by silicon and aluminium atoms (black) surrounded by 4 oxygen (white) atoms in "tetrahedral" configurations (right).

Many occur naturally as minerals, and are extensively mined in many parts of the world. Others are synthetic, and are made commercially for specific uses, or produced by research scientists trying to understand more about their chemistry. (International Zeolite Association, 2010b)

Because of their unique porous properties, varieties of applications with a global market of several million tonnes per annum use zeolites. In the western world, major uses are in petrochemical cracking, ion-exchange (water softening and purification), and in the separation and removal of

gases and solvents. Other applications are in agriculture, animal husbandry and construction. They are often also referred to as molecular sieves (British Zeolite Association, 2006).

Of many existing zeolitic structures, silicalite[1] is perhaps the most studied, best characterised and most widely used in practice. Silicalite provides a non polar structure for adsorption of relatively small molecules and has been used as membranes for separation of mixtures of light hydrocarbons (Funke *et al.*, 1997b;Funke *et al.*, 1997a;Gump *et al.*, 1999;Krishna & Paschek, 2001a;Lin *et al.*, 1998;van de Graaf *et al.*, 1999). Silicalite has a high ratio of silica to alumina, is hydrophobic and stable up to high temperatures(Krishna & Paschek, 2001b). Figure 1-3 shows a schematic of the structure of silicalite which consists of a system of intersecting channels composed of zigzag channels along x, cross-linked by straight channels along y. Both channels are defined by 10-rings. The straight channels are approximately elliptical in

[1] In 1978, an article appeared in *Nature* which was to have wide-ranging consequences. A new polymorph of silica (silicalite, refractive index 1.39, density 1.76 gcm^{-3}) was found to have a novel tetrahedral framework enclosing a three-dimensional system of intersecting channels defined by 10-T-atom rings wide enough to absorb molecules up to 0.6 nm in diameter. The material was prepared by hydrothermal synthesis using alkylammonium (for example TPA) cations. In fact, the material was (nominally) Al-free ZSM-5, and the ensuing legal battle over definitions, ownership, and patent rights was most regrettable in that it dissipated the resources of two major companies and imposed a great strain upon many sincere and hard-working scientists and their colleagues. However, the concept of silicalite was very significant in that it brought about a number of important realisations, namely: 1. High-silica zeolites are essentially impure silica polymorphs and bear at least as much relationship to silicas as they do to Al-rich zeolites, feldspars and similar aluminosilicates. 2. High-silica zeolites are intrinsically hydrophobic and organophilic, a trend which reverses only with increasing aluminum content as their surface polarity and cation content increases. 3. For a given structure, there is usually a smooth transition in properties as the aluminum content is varied from zero to a limiting value, thus generating families of isostructural materials. 4. Traces of aluminium are likely to be incorporated into the lattice in tetrahedral positions, as may be confirmed by Si and Al MAS NMR spectroscopy. 5. Proposals for the mechanism of synthesis of highly siliceous zeolites must cover the whole family of compositions since it is very unlikely that the presence or absence of a small quantity of aluminum will radically alter the manner in which the structure comes together (Cundy & Cox, 2003).

shape having a 5.3 Å × 5.6 Å cross section while the zigzag channels have a 5.1 Å × 5.5 Å cross section.

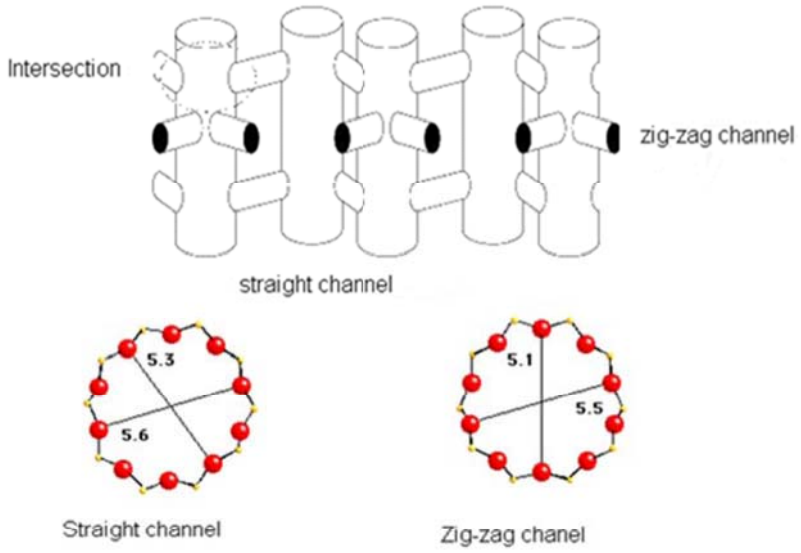

Figure 1-3 Schematic of structure of silicalite (Krishna & Paschek, 2001c). Dimensions are in Angstrom.

The unique properties of zeolites, such as high internal surface area, thermal stability and the presence of acid sites, have made zeolites important catalytic materials, adsorbents and molecular sieves. Adsorption in zeolites is of great scientific interest due to the application of adsorption in separation and catalysis. For instance, the separation of p-xylene from C_8 aromatic mixtures was performed on an industrial scale by using selective adsorption in synthetic faujasite type zeolite (Lachet et al., 1997). In another case, a zeolite adsorbent was used to increase the overall yield of natural gas to C_2 components significantly (Makri et al., 1996). In this case, the selective adsorption of ethylene and ethane on zeolites allowed the unreacted methane to be recycled. Adsorptive separation of gas mixtures using zeolites has several advantages over conventional separation methods, such as distillation. It has much higher selectivity and is less energy intensive due to

the unique structure of zeolites. Selective adsorption of molecules in the micropores forms the basis of the application of zeolites as catalysts in refining and for other applications in the petrochemical industry (Maxwell & Stork, 2001;Rabo, 1976).

Table 1-2 shows the details on silicalite structures used in this study.

Table 1-2 Silicalite lattice parameters used in alkane adsorption simulation

Silicalite	No. unit cells	No. Oxygen atoms	*a*(Å)	*b*(Å)	*c*(Å)
Silicalite	16	3072	40.14	39.84	53.68

a, *b* and *c* are the sizes of simulation box.

1.4 Traditional methods for adsorption studies

The theoretical modelling of adsorption has a long history. It commenced with the work of Von Saussure (von Saussure, 1814). The most famous and simplest analytical model of monolayer adsorption was derived by Langmuir (Langmuir, 1913;Langmuir, 1915;Langmuir, 1918). In his model, it is assumed that all the adsorption sites are indistinguishable and there are no interactions between the adsorbed molecules. Langmuir's model is an idealised model. It can be useful approximation but it does not fully embrace the experimental situation as it ignores these two effects. Since then, there have been many modifications to this model. Toth's (Toth, 1962) model in which different adsorption sites are considered; Temkin's model (Temkin & Pyzhez, 1940) where the effects of interactions between the adsorbates on adsorption isotherms included. The most widely used equation for describing

multilayer adsorption is the BET isotherm, which is named after Brunauer, Emmett and Teller and given by (Brunauer *et al.*, 1938)

$$\frac{[A]}{S_0} = \frac{C_B x_B}{(1-x_B)[1+(C_B-1)x_B]} \tag{1-1}$$

Where $[A]$ is the total number of molecules on the surface, S_0 is total number of sites on the surface and C_B is the equilibrium constant. The BET model is widely used industrially for the determination of surface areas.

Another widely used isotherm is that due to Freundlich and given by

$$\theta_A = \alpha_F P^{C_F} \tag{1-2}$$

Where α_F and C_F are fitting parameters. Deviations from isotherms are almost always due to strong intermolecular interactions or unusual molecular behaviour. None of these analytical models includes disorder and intermolecular interactions at the same time. Therefore, the practical applications of these models are limited.

In 1935, Fowler (Fowler, 1935) proposed a lattice gas model for describing adsorption. Hill (Hill, 1949) extended the results further. In Fowler's lattice model, each possible arrangement of the adsorbates is considered and the effects of the local interactions between adjacent adsorbates on isotherms are also taken into account. Accurate theoretical treatments of lattice gas model of adsorption tend to be difficult so approximate treatments are required. Recently, the development of fast computers makes it possible to do Monte Carlo treatments of lattice gas models but much remains to be

done. The main application of Monte Carlo methods has been for the simulation of adsorption of small molecules in realistic models of the adsorbent.

1.5 Molecular simulation of adsorption

Molecular simulation techniques are playing important roles in the computation of adsorption. There are two basic molecular simulation techniques , namely Molecular Dynamics (Allen & Tildesley, 1987;Frenkel & Smit, 2002;Ryckaert & Bellemans, 1978;Vanderploeg & Berendsen, 1982;Wang *et al.*, 1993c) and Monte Carlo methods (Allen & Tildesley, 1987;Frenkel & Smit, 2002;Metropolis *et al.*, 1953;Panagiotopoulos, 1992;Smit, 1995a;Vanmegen & Snook, 1980;Vuong & Monson, 1996a;Whitehouse *et al.*, 1983).

Molecular dynamics methods can be used to determine static or dynamic properties of an adsorbed system. It is in many ways similar to real experiments. During the simulation, the Newton's equations of motion are set up for the interested system and solved numerically by advancing in small time steps. The equilibration times of a system may be reflected in a molecular dynamics simulation. A minute of real experiment time would take of the order of 10^9 seconds in a computer simulation. Therefore, the application of molecular dynamics is limited (June *et al.*, 1992a).

With Monte Carlo simulations, the implementation of the techniques is rather straightforward. The basic task of the simulation is to randomly generate configuration of a system and to average the properties of the

system appropriate to a given statistical ensemble. In order to ensure that a proper average is achieved, an effective sampling is needed. Efficient importance sampling is the one in which the Metropolis algorithm is used (Metropolis et al., 1953). In such a sampling, a new configuration is acceptable immediately if the energy of the system is lowered, or with a probability of $\exp(-\Delta E / kT)$ if the energy is raised. More relevantly Stroud (Stroud et al., 1976) reported one of the first studies of the thermodynamic properties of adsorbed molecules in zeolites by Monte Carlo simulations. They studied methane in zeolite 5A and calculated thermodynamic properties such as the isosteric heat of adsorption and heat capacity. Kretschmer and Fiedler (Kretschmer et al., 1977) also performed some early Monte Carlo work for simulating of alkanes in zeolites. The early work was restricted to one molecule per cavity and therefore corresponds to the ideal gas limit. Since these pioneering works, many studies of the behaviour of adsorbed molecules in zeolites have been carried out by using Monte Carlo techniques (Catlow *et al.*, 1991a;Delara *et al.*, 1989a;Demontis *et al.*, 1992a;June *et al.*, 1990;Nicholas *et al.*, 1993b;Smit & Siepmann, 1994). Soto and Meyers (Soto & Myers, 1981) were the first persons to use the Grand Canonical Monte Carlo method to study adsorption in zeolite but they did not achieve good agreement with experiments. Somewhat late, Woods and Rowlinson (Woods & Rowlinson, 1989) successfully carried out Grand Canonical Monte Carlo simulations for xenon and methane adsorption in zeolite X and Y.

In chapter 4- Monte Carlo simulation will be discussed in more detail.

1.6 Other theoretical methods for adsorption studies

There is no doubt that Monte Carlo simulation is powerful for accurate computation of adsorption isotherms of short molecules. However, calculation can be time consuming, especially for long chain molecules. In some situations there is a need to circumvent these problems and find reliable models for description of the adsorption of longer molecules. The calculation of adsorption isotherms by using such models needs to be cheap and quick to use. A central part of the development of such practically models of adsorption of large molecules is the testing of these models against more accurate theories, such as Monte Carlo method. In this thesis several lattice models have been successfully put forward to try to provide an inexpensive route to the prediction of adsorption isotherms for hydrocarbon in zeolites.

1.7 Aim of this study

Adsorption of hydrocarbon in zeolites occurs in many processes in modern industries, such as heterogeneous catalytic reactions, gas purification and adsorptive separation processes etc. The use of adsorption in these areas is expanding. The design and optimisation of new adsorption processes and prediction as well as improvement of existing processes require detailed understanding of the adsorbed phase at the molecular level.

The goal of this study is to develop models for adsorption of hydrocarbon and CO_2 in silicalite based on the principles of statistical mechanics. Monte

Carlo simulation techniques are used to calculate the adsorption isotherms of methane/ethane and CO_2 binary mixture in silicalite at various temperatures over wide range of pressures. The technique also used to calculate the adsorption isotherm of binary and ternary mixture of propane, i-butane and n-butane at various temperatures over wide range of pressures. Furthermore, lattice model have been developed to calculate firstly for benzene adsorption on silicalite as well as for mixtures of small hydrocarbons/ CO_2 and propane/ butane isomers. The benzene adsorption lattice model reproduces successfully the double step structure of the isotherm. The mixture adsorption isotherms also able to reproduce satisfactorily the ones from Monte Carlo simulations. Exact matrix statistical mechanical method is employed for the lattice models.

1.8 Summary of the chapters

Following this introduction, a literature survey is given in chapter 2 where an introduction to Monte Carlo techniques and its applications are presented. A review of analytical models for adsorption is given along with the basis of the matrix method and some approximation theories.

Chapter 3 focuses on lattice model for adsorption of benzene in silicalite. In this chapter it is shown that the steps in adsorption isotherms could arise from re-orientational transitions amongst molecules in the adsorbed phase where there is energetic competition between open and closed-packed structures in a monomer-dimer model.

Chapter 4 focuses on Monte Carlo simulation of adsorption of CH_4, C_2H_6 and CO_2 binary as well as ternary mixtures in silicalite. The simulations are carried out at various temperatures and over wide range of pressure. In the second part of the chapter, simulations are carried out for binary and ternary mixtures of propane, i-butane and n-butane at various temperature and pressures.

In chapter 5 exact one dimensional lattice model is used to simulate the adsorption isotherms of methane, ethane and carbon dioxide binary mixtures in silicalite. The model is then extended to simulate ternary mixtures of the above components. In the final section, the model is used to find the adsorption isotherm of propane, i-butane and n-butane. The results then compared to the ones from Monte Carlo simulations.

In the final chapter, the most important conclusions from the preceding chapters are summarised and some suggestion for future work are proposed.

2- LITERATURE STUDY

2.1 Brief history and general review of adsorption studies

The phenomenon of adsorption[2] was discovered more than two centuries ago. Fontana (Fontana, 1777) had noted that freshly calcined charcoal, cooled under mercury, was able to take up several times its own volume of various gases; and in the same year Scheele (Scheele C.W., 1780) records that "air" expelled from charcoal on heating is taken up again on cooling. He describes the effect in the following words: *"I filled a retort half-full with very dry pounded charcoal and tied it to a bladder, emptied of air. As soon as the retort became red-hot at the bottom, the bladder would no longer expand. I left the retort to cool and the air returned from the bladder into the coals. I again heated the retort, and the air was again expelled; and when it was cool the air was again adsorbed by the coals. This air filled 8 times the space occupied by the coals."*

[2] The term adsorption appears to have been introduced by Kayser (Kayser, 1881) to connote the condensation of gases on free surfaces, in contradistinction to gaseous absorption where the molecules of gas penetrate into the mass of the absorbing solid.

In the early days, there were many arguments about the nature of adsorption. Faraday (Faraday, 1834) thought that adsorption was due to the electrical forces between the gas molecules and the solid surface and Berzelius (Berzelius, 1836) proposed that adsorption was a process where surface tension or some other force caused gas to be condensed on a surface. The idea that most adsorption processes were really just pore condensations was actively debated in the literature from 1850 to 1920. However, other researchers dissented from this view. Langmuir (Langmuir, 1918) and Sabatier (sabatier-Reid, 1922) were among those who believed that adsorption was a surface phenomenon as opposed to a pore phenomenon. Using Langmuir's model, Bancroft (Bancroft, 1918) examined most of the existing adsorption data and he concluded that when a gas molecule is adsorbed on a solid surface, there is a physical or chemical interaction between them.

Today, it is generally thought that the process of gas adsorption on a surface is a combination of direct adsorbate/surface binding and pore condensation. Firstly, gas directly contacts with the solid to form the first layer and then possibly a number of layers of gas condense onto the first layer (illustrated in Figure 2-1)

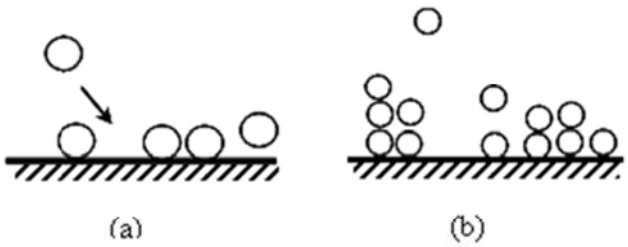

Figure 2-1 An illustration monolayer (a) and multilayer adsorption (b)

In the literature, there are tens of thousands of measurements of adsorption isotherms on a wide range of solids. Morozzo (Morozzo, 1783) and later Rouppe (Rouppe & Norden, 1799) made the earliest quantitative measurements of adsorption. They found that a number of common gases adsorbed on charcoal and the adsorbed amount of gas depended on the gas composition. Von Saussure (von Saussure, 1814) examined the adsorption process in more detail and discovered that the amount of gas adsorbed not only depended on the composition of the gas but also the temperature and pressure. He made a number of plots of the amount of gas adsorbed as a function of the pressure thereby obtaining the earliest adsorption isotherm.

During the nineteenth century and the early years of twentieth century, studies of adsorption were widespread and over the years, many adsorption isotherms were measured. Brunauer (Brunauer, 1945) and Valenzuela (Valenzuela & Meyers, 1989) presented good reviews for much of the earlier data.

Several classifications have been developed to characterise the shape of adsorption isotherms. The first systematic attempt to interpret adsorption isotherms for gas adsorption on solid was made by Brunaure, Deming, Deming and Teller (BDDT) (Brunauer et al., 1940).

They classified isotherms into five types, which are shown in Figure 2-2. This classification became the standard for modern classification of adsorption isotherms.

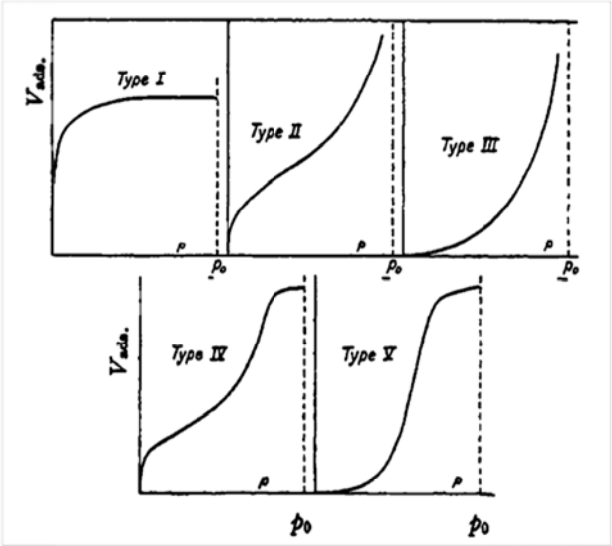

Figure 2-2 Five types of Van der Waals adsorption isotherms (Brunauer et al., 1940).

Isotherm **I** typifies monolayer adsorption. The adsorbed amount of gas increases with pressure and then reaches saturation at about monolayer coverage.

In type II the adsorbed amount firstly increases with pressure then keeps constant and finally starts to rise again at higher pressures. Type **II** is the typical isotherm for multilayer adsorption. Both isotherms are observed in adsorption on a flat surface. For type **III** (which is quite rare), there is only little adsorption at low pressure, but adsorption increases due to the strong adsorbate-adsorbate interactions at high pressures. The adsorption isotherm of ammonia on graphitized carbon is an example. Type **IV** and type **V** isotherms usually occur for multilayer adsorption of gas on the surface of the pores. Initially, the adsorption resembles a type II or type III adsorption, but eventually the adsorbed layer becomes so thick that fill the pores up. As a consequence, no more gas can be adsorbed and the isotherm saturates.

The BDDT classification of adsorption isotherms became the core of the modern IUPAC classification of adsorption isotherms, (Ter-Minassian-Saraga,

1985) as illustrated in Figure 2-3. Type I isotherms are characteristic of microporous[3] adsorbents. Types II and III describe adsorption on macroporous adsorbents with strong and weak adsorbate–adsorbent interactions respectively. Types IV and V represent adsorption isotherms with hysteresis. In addition to the five types of isotherms identified by BDDT, the IUPAC classification includes a sixth isotherm (Type VI) which has steps. All of these types of isotherms have been observed in numerous experiments (Gregg & Sing, 1982) and have been analyzed theoretically (Bruno *et al.*, 1987;Champion & Halsey, 1953;Nicholson, 1975;Nicholson, 1976;Nicholson & Silvester, 1977)

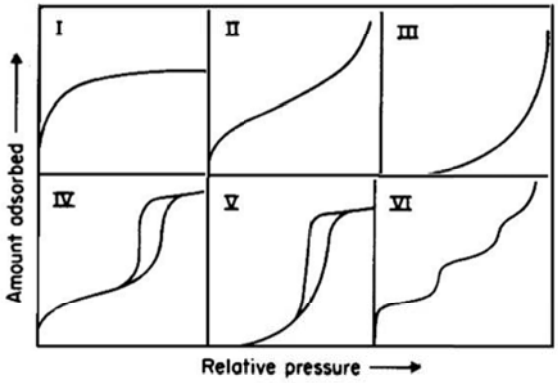

Figure 2-3 IUPAC classification of adsorption

Though the IUPAC classification is considered by many to be the ''Bible'' concerning adsorption behaviour, it should be emphasized that the IUPAC classification is applicable only to ''condensable vapours'' (Aranovich & Donohue, 1998a). In other words, the IUPAC classification should not be used for many important adsorptives, such as nitrogen, oxygen, inert gases, carbon dioxide and monoxide, methane, and ethylene at room temperature

[3] pores with widths exceeding about 50 nm are called *macropores*, pores of widths between 2 nm and 50 nm are called *mesopores*, pores with widths not exceeding about 2 nm are called *micropores* (Sing, 1985)

since they all are supercritical. The IUPAC classification has two deficiencies: it is incomplete and it gives the incorrect impression adsorption isotherms are always monotonic functions of pressure (Aranovich & Donohue, 1998b). The IUPAC manual (Sing, 1985) mentions that the differences between standard types of isotherms are due to different porous structures of adsorbents and adsorbate–adsorbent interactions. Also the adsorbate–adsorbate play an important role (Sing, 1985) and the specific surface area of the adsorbent is a key characteristic of adsorption behaviour. However, until recently there was no model capable of predicting the change in an adsorption isotherm as a function of geometry of adsorbent or energies of intermolecular interactions. Of course, methods of statistical mechanics and molecular simulations are able to do this.

It is pertinent to remark briefly on chemical bond formation at a surface. Figure 2-4 shows the typical adsorption isotherms of a gas on a clean metal surface (CO on Pd). In this case, the adsorbate and the surface form a strong bond characteristic of chemisorption. It can be electrified seen from the figure that at 295 K CO adsorption is significant even at low pressures. At higher temperatures such as 493 K, however, much higher pressures are needed to obtain significant adsorbed amount.

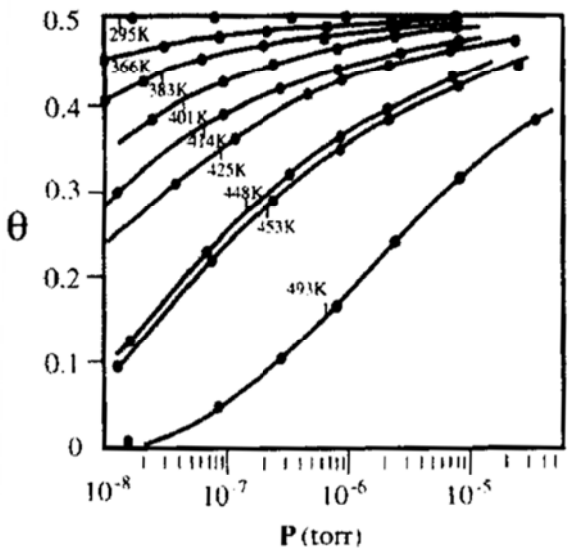

Figure 2-4 Adsorption isotherms for CO on Pd (Ertl & Koch, 1970)

The adsorption isotherms of gases on highly porous materials are different to that on other materials due to the effect of capillary condensation. Figure 2-5 gives a series of adsorption isotherms for krypton, argon and ammonia adsorption on graphitized carbon black (Bassett *et al.*, 1968b;Bomchil *et al.*, 1979;Putnam & Fort, 1975;Ross & Winkler, 1955) and these are typical for porous materials. Each of them shows different behaviour. For example, at 94.72K (the boiling point of krypton at 1 atm pressure) krypton condenses to form a single monolayer at 0.1 torr[4]. The adsorbed amount is almost constant at a pressure range of 0.1 torr to 2.0 torr. Then the adsorbed amount rises gradually due to the gas forming a second monolayer. At pressures of about 22 torr, a second plateau starts and at this point second monolayer fills up. When the pressure is above 30 torr, the amount of adsorption increases continuously until a bulk liquid is formed.

[4] 1 torr =133.3224 pascal = 0.001315789 atm

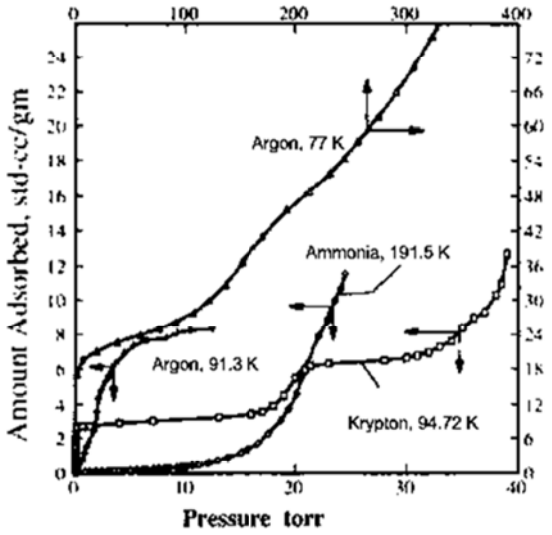

Figure 2-5 Adsorption Isotherms of krypton at 94.72K, argon at 77K and 91.3K, ammonia at 191.5K, on graphitized carbon black (Bassett *et al.*, 1968a;Bomchil *et al.*, 1979;Putnam & Fort, 1975;Ross & Winkler, 1955).

Experiment plays a key role in providing basic adsorption data. However, experimental studies of adsorption are sometimes difficult and are limited by equipment available and the rapidly increasing inaccuracy and uncertainty of measurements with pressure. Furthermore, experimental measurements require long equilibration times and under some extreme conditions, the experimental measurement of adsorption may be unfeasible. Therefore, there is a need to find other ways to obtain adsorption information. In fact, theoretical modelling has played a central role in adsorption studies. Langmuir (Langmuir, 1913;1915;1918) derived the most famous and simplest analytical model of monolayer adsorption. Although his model is an idealised model, it can be a useful approximation. Since then, many modifications to this model have been made. For example, Toth's model (Toth, 1962), Temkin's model (Temkin & Pyzhez, 1940), etc. However, none of these analytical models takes all significant molecular interactions into account at the same time. In the modern times, with the rapidly development of

techniques, it has been recognised that computer simulation could be of immense importance in exploring adsorption phenomena. Computer simulations of adsorption have been performed widely on various adsorbents (Catlow, 1992a;Nicholson & Parsonage, 1982a;Okayama *et al.*, 1995).

In general, isotherm and kinetics, together with heat of adsorption are basic information needed to classify adsorption. Both experimental measurements and theoretical calculations have been widely used to obtain such information. The main experimental methods for the determination of the adsorbed amount are volumetric (Richardson, 1917;Titov, 1911) and gravimetric (McBain & Britton, 1930). Other early approaches were the optical method (Rayleigh, 1903), and the accommodation coefficients technique (Roberts, 1930). For the determination of heats of adsorption both isothermal (Favre, 1874)[5] and adiabatic (Beebe & Taylor, 1924) calorimeter have been used alongside adsorption isotherms. Indeed, in past decades much valuable adsorption information has been obtained by such experiments. However, in many cases it is difficult to carry out experimental measurements of adsorption since they are prohibitively time consuming. For example, the measurement of each point on an isotherm for decane in silicalite requires at least two weeks of equilibration (Stach et al., 1984). Such measurements are even more difficult for mixtures since they involve not only measuring the weight increase of the zeolites as a function of

[5] Favre, using a Mercury calorimeter, was the first to make a quantitative measurement of the heats of adsorption of a number of gases on charcoal and of hydrogen on platinum.

pressure but also the change in composition of the gas mixture. Furthermore, experiments may be unfeasible at some extreme conditions of high temperature and pressure and consequently related experimental data for such adsorption phenomena are often lacking.

2.2 Adsorption forces

As indicated before, the adsorption of gas molecules on a solid surface is the outcome of the forces between the individual molecules from the gas phase and the ions or atoms composing the solid. Intermolecular forces have been studied theoretically over a number of decades. Boscovich (Maitland et al., 1987) was the first person who proposed the concept of intermolecular force. He thought that molecules must repel each other at a small distance and attract as the separation distance increased.

2.2.1 Dispertion-Repulsion Energy

The repulsive force is due to the overlap of the electron clouds of two molecules whereas when the overlap of the electron clouds is small the long-range attractive force becomes more significant. There are three possible types of long-range forces according to the nature of the interacting molecules, which are electrostatic forces, induced forces and dispersion forces. Some molecules (like HCL) possessing permanent dipole moments due to the electric charge distribution in the molecule which can induce an electric dipole in another polarisable molecule. The induced force is mainly due to an interaction between a charged or polar molecule with an induced dipole and thereby a molecule with permanent moment can interact with a

non-polar molecule. The induced contribution also exists in the case of the interaction of two polar molecules. The dispersion force then arises from the instantaneous electric dipoles producing an attractive dispersion force.

The dispersion force always exists in all molecular interactions. For simple non-polar molecules, the dispersion force is always the greatest contribution to the intermolecular interaction at long-range. Studies of dispersion forces began with London (1930a,b) and Lennard-Jones (1932) in the 1930s and then followed by many others, e.g. (Lifshitz, 1956;Mclachlan, 1964).

The most important representation of intermolecular force between two molecules is the potential energy function. Van der Waals first proposed the general formation of the intermolecular potential energy function U(r) for spherically symmetric atoms. Generally, intermolecular energy between two molecules with non-spherical symmetry not only depends on the distance of the two molecules but also on the relative orientation for example in the interaction of two N_2 molecules. For such molecules, rotational and vibrational energies make extra contributions to the total energy, which comes from internal energy of the molecules themselves. The earliest and simplest representation of an intermolecular potential energy is the hard sphere potential model

$$\begin{aligned} U(r) &= \infty & r \le r_0 \\ U(r) &= 0 & r > r_0 \end{aligned} \qquad (2\text{-}1)$$

Where U is the intermolecular potential energy and r_0 is the diameter of a hard sphere. This potential model only has one parameter r_0 but in view of

the nature of interaction forces, this model is evidently unrealistic. The most frequently used potential model is the Lennard-Jones potential (Lennard-Jones, 1925), which is sometimes referred to as the n-6 potential

$$U(r)=\varepsilon\left\{\frac{6}{n-6}\left(\frac{r_m}{r}\right)^n-\frac{6}{n-6}\left(\frac{r_m}{r}\right)^6\right\} \tag{2-2}$$

Where r_m is the Van der Waals radius and $r_m=2^{1/6}\sigma$. This model possesses the general features of the true intermolecular potential energy in which it has a repulsive short-range region joined a long-range attractive region. The attractive component of this function is theoretically based on the dispersion energy contribution, but the repulsive term has no theoretical justification. The most common form of this model is the 12-6 function.

$$U(r)=4\varepsilon\left\{\left(\frac{\sigma}{r}\right)^{12}-\left(\frac{\sigma}{r}\right)^6\right\} \tag{2-3}$$

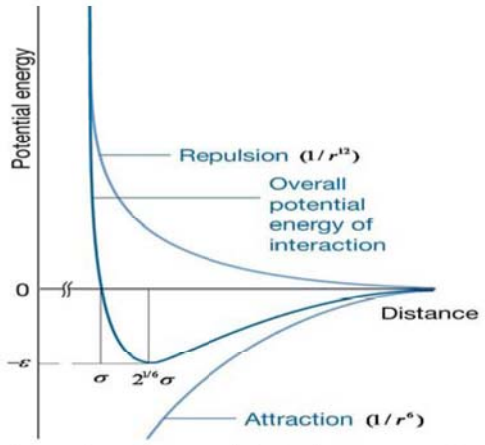

Figure 2-6 The Lennard-Jones (12, 6)-potential. At long range the interaction is attractive, but at close range the repulsion is dominate. (Atkins, 1998)

where σ is the intermolecular separation for which the energy is zero. The parameters of the Lennard-Jones function can be determined by fitting experimental data to a model, which uses the potential.

The force constant ε and σ are characteristics of the particular molecular species and tabulated values for many common molecules are available e.g. (Cuadros et al., 1996).

The interaction parameters between two different united atoms i and j are given by geometric mean (Jorgensen et al., 1984):

$$\sigma_{ij} = \sqrt{\sigma_i \sigma_j} \qquad \varepsilon_{ij} = \sqrt{\varepsilon_i \varepsilon_j} \tag{2-4}$$

Setting $\frac{d(U(r))}{dr} = 0$ in equation (2-3) gives, for the equilibrium separation between centres of an isolated pair of molecules:

$$r_m = 2^{1/6}\sigma \tag{2-5}$$

Another pair potential function occasionally employed is a modified form of the Buckingham potential (Buckingham, 1938)

$$U(r) = \varepsilon \left\{ \frac{6}{\alpha - 6} e^{-\alpha\left(\frac{r}{r_m} - 1\right)} - \frac{\alpha}{\alpha - 6}\left(\frac{r_m}{r}\right)^6 \right\} \tag{2-6}$$

This model potential also contains the term of the dispersion energy contribution at long range, but the repulsive contribution has the physically more realistic exponential form. There are many more simple function forms for the intermolecular pair potential energy (Aziz & Chen, 1977;Barker & Henderson, 1971;Guggenheim & Mcglashan, 1960;Maitland & Smith, 1973).

2.2.2 Electrostatic energies

In ionic adsorbents such as zeolites where there is a significant electric field in the region of the surface, additional contributions to the energy of

adsorption may arise from polarisation U_P, field-dipole U_μ, and field gradient U_Q quadrupole interactions. These are given by the following expressions:

$$\begin{aligned} U_P &= -\frac{1}{2}\alpha E^2 \\ U_\mu &= -\mu E \\ U_Q &= \frac{1}{2}Q\frac{\partial E}{\partial r} \end{aligned} \tag{2-7}$$

Where E is the electric field, α the polarisability, μ the dipole, and Q the quadrupole moment, defined by

$$Q = \frac{1}{2}\int q(\rho,\theta)(3\cos^2\theta - 1)\rho^2 dV \tag{2-8}$$

$q(\rho,\theta)$ is the local charge density at the point (ρ,θ) with the origin at the centre of molecule, and the integration is carried out over the entire volume of molecule. Thus, for an ionic adsorbent the overall potential is given by the sum of six terms:

$$U = U_D + U_R + U_P + U_\mu + U_Q + U_S \tag{2-9}$$

Where U_S represents the contribution from sorbate-sorbate interaction.

2.3 Analytical models for adsorption

The most important analytical model of monolayer adsorption came from the work of Langmuir (Langmuir, 1913;Langmuir, 1915;Langmuir, 1918). In Langmuir's adsorption models, the adsorption process is treated as a reaction, in which a gas molecule A_g reacts with an empty site, S, to create

an adsorbed complex A_{ad}. The basic assumptions Langmuir's adsorption models are:

Surface is homogeneous, that is adsorption energy is constant over all sites.

Adsorption on surface is localised, that is adsorbed molecules are adsorbed at definite, localised sites.

Each site can accommodate only one molecule.

There are no interactions between the adsorbed molecules.

The Langmuir theory is based on a kinetic principle, that is the rate of adsorption is equal to the rate of desorption from the surface.(Do, 1998)

The key results of Langmuir's adsorption model are as following

$$\theta_A = \frac{K^A_{equ} P_A}{1 + K^A_{equ} P_A} \tag{2-10}$$

$$\theta_A = \frac{K^A_{equ} P_A}{1 + K^A_{equ} P_A + K^B_{equ} P_B} \tag{2-11}$$

$$\theta_B = \frac{K^B_{equ} P_B}{1 + K^A_{equ} P_A + K^B_{equ} P_B} \tag{2-12}$$

Where P_A and P_B are the partial pressures of species A and B. K^A_{equ} and K^B_{equ} are adsorption equilibrium constants. Here equation (2-10) is the expression for the adsorption isotherm for pure component without dissociation and equations (2-11)-(2-12) are forms for a mixture adsorption without dissociation. It has been found that Langmuir's models can fit a number of adsorption systems. However, in some cases, the Langmuir's theory cannot explain the experimental data due to inequivalent sites and interactions

between the adsorbed molecules. Therefore, there is a need to correct the Langmuir's adsorption models and take the multiple inequivalent sites and significant interactions of adsorbate-adsorbate into account.

2.3.1 The Freundlich model

Over the years, there have been many attempts to modify Langmuir's adsorption isotherms. The simplest deviations from the Langmuir's adsorption isotherms come for the adsorption on rough inhomogeneous surfaces. On a rough surface, there are multiple sites available for adsorption and the heat of adsorption may vary from site to site. Modifications to Langmuir's model are needed for such systems. Much work in these aspects has been done (Jaroniec & Madey, 1988).

The most important multi-site adsorption isotherm for rough surfaces is the Freundlich adsorption isotherm:

$$\theta_A = \alpha_F P^{C_F} \tag{2-13}$$

where α_F and C_F are fitting parameters. Freundlich equation is an empirical equation, which works better than Langmuir's for adsorption on rough surfaces. However, it has been found that a Freundlich model usually only fits adsorption data over a small pressure range and it has little predictive value. Consequently, this model is now rarely used.

2.3.2 The Temkin model

In real adsorption systems, when the systems reach saturation the adsorbed phase has a liquid-like density. Therefore, there are strong interactions

between adsorbed molecules. However, in both the Langmuir and Freundlich model, such strong interactions are ignored. Temkin (Temkin & Pyzhez, 1940) put forward an adsorption model which considered the effects of indirect adsorbate/adsorbate interactions on adsorption isotherms given by

$$\ln\left(K_{equ}^{A,0}P_A\right)=\frac{\Delta H_{ad}^{0}\alpha_T\theta}{kT} \tag{2-14}$$

where ΔH_{ad}^{0} is the heat of adsorption at zero coverage. θ and P_A are the coverage and pressure respectively. Temkin's model assumed that the heat of adsorption of all molecules in the layer would decrease linearly with coverage due to adsorbate/adsorbate interactions. The problem with Temkin's model is that ordering of the adsorbent layer is not taken into account.

2.3.3 The Fowler model

Instead of indirect adsorbate/adsorbate interactions, the direct adsorbate/adsorbate interactions were considered in Fowler's model (Fowler, 1935). It assumed that the heat of adsorption on an adjacent site of an occupied site would be reduced by an amount $\Delta H_{ad}\alpha/2$, where α is positive for repulsive interactions and negative for attractive interactions. Since there are attractive and repulsive interactions between molecules on adjacent sites, the probability of filling a given site should depend on whether the sites adjacent to the given site are filled or empty. However, this gives a poor description of experimental data.

2.3.4 The BET adsorption isotherm

The analytical models mentioned above are only applicable for monolayer adsorption. For most reaction systems, the reaction is based on a single monolayer. However, in some other systems, multilayer adsorption may be important. Basically, multilayer adsorption is different from monolayer adsorption. In monolayer adsorption, adsorbate/surface interactions dominate the adsorption whereas for multilayer adsorption the adsorbate/adsorbate interactions control the adsorption. The first multilayer adsorption isotherm was derived by Brunauer, Emmett and Teller (Brunauer *et al.*, 1938), which is called the BET equation. They treated the surface as several different types of sites, which are either empty or covered by one monolayer or by two monolayer and so on. Then they assumed that the various types of sites are in a random distribution. The formula for the BET equation is

$$\frac{[A]}{S_0} = \frac{C_B x_B}{(1-x_B)[1+(C_B-1)x_B]} \tag{2-15}$$

Where $[A]$ is the total number of molecules on the surface, S_0 is total number of sites on the surface, C_B is equal to K_1/K_m. K_1 is the equilibrium constant between the gas phase and the first adsorbed layer. Km is the equilibrium constant between the gas phase and m^{th} adsorbed layer. $x_B = P_A K_m$. It is clear that when $x_B = 1$ the coverage goes to infinity therefore, the gas begins to condense and as C_B increases the BET equation changes from type III behaviour to type I. Hence, the BET equation can qualitatively

reproduce the isotherms shown in Figure 2-2. It only contains two parameters, which is an important advantage. Unfortunately, the BET equation does not fit the experimental data of multilayer adsorption well since it ignores the surface tension. The BET equation does fit the experimental data at coverage near to a full monolayer. Therefore, the BET equation is a useful way to estimate how much gas adsorbs in a monolayer. One of the main applications of the BET equation is in measurement of surface areas. The BET isotherm is the most widely used equation for describing adsorption (Brunauer *et al.*, 1938) and is of high practical value.

The limitation of the proposed models of adsorption is that none of them takes into consideration both surface heterogeneity and the adsorbate-adsorbate interactions (Soto & Myers, 1981). Therefore, the applications are limited.

2.4 Lattice gas models for adsorption

A lattice gas is a collection of atoms in which the position of the atoms can take on only discrete values. Each lattice site cannot be occupied by more than one atom. Figure 2-7 illustrates a configuration of a two-dimensional lattice gas, where solid circles stand for the atoms and the open cycles refer to the empty lattice sites. Using the lattice gas model to simulate the behaviour of the adsorbed phase, it is often applied to systems in which the adsorbed molecules are localized at discrete adsorption sites with only infrequent movement of the molecules between sites. It is assumed that there are a series of sites on a solid surface that are available to adsorb gas.

In this sense, the adsorption process can be treated as a reaction that is when a gas molecule Ag reacts with an empty site S, adsorption occurs and an adsorbed complex is created

$$A_g + S \Leftrightarrow A_{ad} \tag{2-16}$$

In the lattice gas model, the possible arrangement of the adsorbates on the surface as well as the interactions between the nearest neighbours was taken into account. The lattice gas model considers the fact that even at a given coverage, different arrangements of surface atoms have different numbers of nearest neighbour interactions, and therefore different energies. This allows the lattice gas model to consider the influence of the adsorbate arrangement on the adsorption isotherm. In fact, the Langmuir isotherm, the BET isotherm as well as other analytic models mentioned above were based on some elements of the lattice gas model, but missing some of them. It is therefore shown that lattice gas models are better able to predict the behaviour of adsorbed molecules than the analytical adsorption models.

Fawler (1935) derived the first description of a lattice gas model for adsorption. The further extension was made by (Hill, 1949). In a long series of papers, Hill (Hill, 1960) discussed many of the statistical mechanical aspects of the theory and attempted to introduce various refinements.

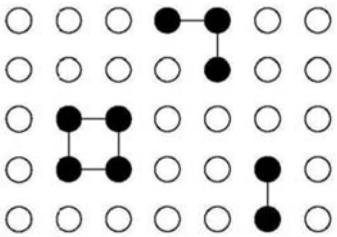

Figure 2-7 A configuration of a lattice gas. Solid circles represent atoms and open circles empty sites. Lines show bonds between nearest–neighbouring atoms.

Later developments of the model were to try to improve the treatment of intermolecular interaction (Champion & Halsey, 1953). However, only limited calculations were possible until modern computing facilities became readily available. Several workers have shown that lattice models can be quite useful for discussion of multilayer adsorption (Deoliveira & Griffiths, 1978;Ebner, 1980;Nicholson, 1975). Besides, renormalization group theory has contributed a lot to the understanding of phase diagrams in lattice systems.

In 1952, Lee and Yang (Lee & Yang, 1952) proved that the problems of an Ising model (Ising, 1925) in a magnetic field and of a lattice gas are mathematically equivalent. In other words, an occupied site of the lattice gas identifies with an Ising spin in the `up' state and an empty site corresponds to an Ising spin in the `down' state. The significance of this confirmation is that the solution of the Ising model can be transformed for use in the lattice gas model. Some related details are given in the next section.

The starting point of the lattice gas model is the partition function of the system that is all possible arrangements of all molecules in the system. The solution methods for lattice models usually are a Monte Carlo simulation, a matrix method and some approximation methods. Pan and Mersmann (Pan

& Mersmann, 1990) used the statistical mechanical lattice gas model for explaining steps within adsorption isotherms in zeolites. Van Tassel (Vantassel et al., 1994) introduced a lattice model for adsorption of small molecules in zeolites. This model is an improvement over many thermodynamic models in common use because it provides a realistic way to treat the interactions between the adsorbates.

2.5 Matrix method

Kramers and Wannier (Kramers & Wannier, 1941) first introduced the matrix method to solve the problem of the statistics of an Ising model. The Ising model is a simple famous statistical model, which is often used in the study of ferromagnetism, anti-ferromagnetism and other problems. Ising who was a student of Wilhelm Lenz in the early 1920s first proposed it. Initially, the Ising model was used to explain ferromagnetism, which results from the interaction among electron spins of the atoms comprising the ferromagnetic material. The Ising model consists of a regular lattice of sites in one, two, or three dimensions. When the molecule occupied a site with two states and the potential energy of interaction between nearest neighbour pairs of sites are considered. The next nearest neighbour pair interactions are ignored. It has been found that the one-dimensional Ising problems can be solved exactly. A solution for the two-dimensional square lattice model was first obtained by (Onsager, 1944) and in magnetic field by Yang (Yang, 1952). The three-dimensional Ising model can be used for a description of the phase transition in liquids, anisotropic magnets and binary alloys. However, so far,

for the three-dimensional Ising model, there is no widely accepted exact solution. In general for two or three-dimensional models, approximation methods are almost always required.

Matrix methods are widely used in statistical mechanics in which the partition function of the system is often expressed as a trace of a matrix. The basic idea of the matrix method is that it is assumed that the lattice consists of m layers each of which has M/m sites. M is the total number of the molecules in the system and m is the number of the layers. For one dimension, a layer is a single molecule; for two dimensions, a layer is a row of molecules; and for three dimensions, a layer is a conventional layer of molecules. The total number of the configurations of a layer is $2^{M/m}$ and the configuration of the whole lattice is presented by a set of number $S_1, S_2, ..., S_m$.

The partition function for such system is given by

$$Q = \sum_{S_1, S_2, \ldots, S_m = 1}^{2^{M/m}} \exp(-\beta E) \tag{2-17}$$

Where $E = \sum_{k=1}^{m} \left(E_{S_k S_{K+1}} + E_{S_K} \right)$ then

$$\begin{aligned} Q &= \sum_{S_1, S_2, \ldots, S_m = 1}^{2^{M/m}} \exp\left(-\beta \sum_{k=1}^{m} \left(E_{S_k S_{K+1}} + E_{S_K} \right) \right) \\ &= \sum_{S_1, S_2, \ldots, S_m = 1}^{2^{M/m}} A_{S_1 S_2} A_{S_2 S_3} \ldots A_{S_{m-1} S_m} A_{S_m S_{m+1}} \end{aligned} \tag{2-18}$$

Where,

$$A_{S_k S_{K+1}} = \exp\left\{ -\beta \left(E_{S_k S_{K+1}} + E_{S_K} \right) \right\} \tag{2-19}$$

Using the inter-product rule of multiplying matrices, that is

$$\sum_{S_2=1}^{2^{M/m}} A_{S_1S_2} A_{S_2S_3} = A^2_{S_1S_3} \tag{2-20}$$

$$\sum_{S_2,S_3=1}^{2^{M/m}} A_{S_1S_2} A_{S_2S_3} A_{S_3S_4} = A^3_{S_1S_4} \tag{2-21}$$

.....

$$\sum_{S_2,S_3,\ldots,S_m=1}^{2^{M/m}} A_{S_1S_2} A_{S_2S_3} \ldots A_{S_{m-1}S_m} A_{S_mS_{m+1}} = A^m_{S_1S_{m+1}} \tag{2-22}$$

Since the layers are in a ring, $S_{m+1} = S_1$. Therefore, the partition function of the system can be rewritten as

$$Q = \sum_{S_1=1}^{2^{M/m}} A^m_{S_1S1} = traceA^m = \lambda_1^m + \lambda_2^m + \ldots + \lambda^m_{2^{M/m}} \tag{2-23}$$

where $\lambda_1, \lambda_2, \ldots \lambda_m$ are the eigenvalues of the matrix $\mathrm{A} = \|A_{ij}\|$. In the thermodynamic limit $M \to \infty$, only the largest eigenvalue makes significant contributions to the partition function, then

$$Q \approx \lambda^M_{\max} \tag{2-24}$$

$\lambda_{\max}$ is the largest eigenvalue of the matrix. Therefore the evaluation of Q can be transformed into the problem of finding the largest eigenvalue of a matrix. For more dimensions and two states problem, it is easy to obtain the largest eigenvalue,

$$\begin{vmatrix} A_{11} - \lambda & A_{12} \\ A_{21} & A_{22} - \lambda \end{vmatrix} = 0 \tag{2-25}$$

$$\lambda_{\max} = \frac{A_{11} + A_{22} + \sqrt{(A_{11} - A_{22})^2 + 4A_{12}}}{2} \tag{2-26}$$

then the partition function of the system can be calculated exactly.

In fact, the solution of the Ising model by the matrix method described above can be transformed for use in the lattice gas model. The occupied sites in the lattice gas model correspond to the spin up state in the Ising model and empty sites to spin down. In the Ising model a set of numbers $\{S_1, S_2, ..., S_m\}$ defines one configuration, whereas in the lattice gas model the number of the occupied sites determines a number of configurations, which is $Na!$ (Na is the number of molecules). The difference caused is due to the fact that the molecules are allowed to move from site to site in the lattice gas model. This difference can be removed by adoption of "correct Boltzmann counting". Therefore, the solution described above for the Ising model can be immediately transcribed to be a solution of the lattice gas model. Lee and Yang (Lee & Yang, 1952) proved that the problems of an Ising model in a magnetic field is mathematically equal to a lattice gas model. For the Ising model they considered a lattice of a pair of interacting spins with two possible orientations, $\uparrow$ and $\downarrow$. For the lattice gas, they considered a corresponding lattice with each lattice point either vacant or occupied by an atom. To each configuration of the lattice of spins there is a corresponding configuration of the lattice gas in which a lattice point is vacant or occupied according to whether the corresponding spin is $\uparrow$ and $\downarrow$. They used this equivalence for a two-dimensional lattice gas and obtained an exact calculation of the phase transition regions in the P-V diagram.

Several workers (Bell, 1969;Bell & Salt, 1973;Flory, 1969) have discussed it extensively for one dimensional lattice model. Bell and Dunne (Bell & Dunne, 1978) developed the basic formalism in a way to suit to the constant pressure partition function for that problem. See Chapter 5 for details

In this study, the matrix method is developed and used to predict the steps in the adsorption isotherms of benzene in zeolites. In this case, approximate treatments such as mean-field descriptions may be unreliable since they are well known to erroneously predict phase transition in one dimensional problem, which may show as artifactual steps in adsorption isotherms. The Monte Carlo simulations are expensive and time consuming. Therefore, the matrix method, as an accurate statistical treatment, is appreciated on several counts.

2.6 Approximation methods

The difficulty with Monte Carlo methods is that for a general type of interaction the analytical expressions for adsorption isotherm cannot be obtained. Therefore, it takes a considerable amount of computer time to model experimental data. Practically, one would like to have an analytical expression of adsorption isotherms and an approximation method can help one to work it out. Here, the features of the main approximation methods are reviewed. They are the mean-field approximations and the Bethe-Peierls method.

2.6.1 Mean-Field approximation

The mean-field method is the simplest approximation for the partition function, which was proposed by Bragg and Williams (1934). Initially, this approximation was used to calculate the structure of an alloy and then Fowler (1935) extended it to use on the surface. The basic idea of this approximation for the adsorption study is to take an average for the adsorbate/adsorbate interactions. This approximation neglects the fact that an adsorbate on the site affects the probability of the occupancy of an adjacent site that is the local ordering of the atoms on the surface. In this case, only the interactions of the nearest neighbour sites are considered. The results of the mean-field approximation do not exactly fit the phase behaviour of a two-dimensional lattice gas, but it indeed can reproduce the adsorbed phases qualitatively. If they are effective for a particular model, it is in giving an approximate description of the system. Since the random mixing approximation and mean-values are used in the mean-field theory, there is a serious deficiency at low temperatures. However, it may be less problematic to use the mean-field theory for `hot' supercritical systems. In this study, the mean-field approximation is used for investigation of supercritical methane adsorption in silicalite.

2.6.2 Bethe-Peierls method

The reason that the mean-field approximation does not fit the phase behaviour exactly is that the local ordering of the atoms on the surface is ignored. The fact is the molecules often order on surfaces. Therefore, the

probability of one site being occupied is dependent on the probability of an adjacent site being occupied, which affects the isotherms.

Bethe (1935) and Peierls (1936) developed an approximation independently, in which a cluster of a few atoms was considered and then the interactions within the cluster was calculated exactly and others were calculated by using the mean field approximation. It has been found that this approximation makes a considerable error in the co-existence region.

2.7 Molecular simulation

Molecular simulation is a computational 'experiment' conducted on a molecular model. Molecular model is built on the given sufficient information about the intermolecular interactions. Clearly, it would be very nice if we could obtain essentially exact results for a given model system, without having to rely on approximate theories. However, we can compare the calculated properties of a model system with those of an experimental system: if the two disagree, our model is inadequate, i.e. we have to improve on our estimate of the intermolecular interactions. Rephrasing, the validity of any simulation will rest on the suitability and accuracy of the equations used for the intermolecular potentials. Molecular mechanics deal with that subject and many forms have been developed for describing the interparticle potentials known as force fields.

There are two basic molecular simulation techniques , namely Molecular Dynamics (Allen & Tildesley, 1987;Frenkel & Smit, 2002;Ryckaert & Bellemans, 1978;Vanderploeg & Berendsen, 1982;Wang *et al.*, 1993a) and

Monte Carlo methods (Allen & Tildesley, 1987;Frenkel & Smit, 2002;Metropolis *et al.*, 1953;Panagiotopoulos, 1992;Smit, 1995a;Vanmegen & Snook, 1980;Vuong & Monson, 1996b;Whitehouse *et al.*, 1983).

Molecular dynamics methods can be used to determine static or dynamic properties of an adsorbed system. It is in many ways similar to real experiments. During the simulation, the Newton's equations of motion are set up for the interested system and solved numerically by advancing in small time steps. The equilibration times of a system may be reflected in a molecular dynamics simulation. A minute of real experiment time would take of the order of 10^9 seconds in a computer simulation. Therefore, the application of molecular dynamics is limited (June *et al.*, 1992b).

With Monte Carlo simulations, the implementation of the techniques is rather straightforward. The basic task of the simulation is to randomly generate configuration of a system and to average the properties of the system appropriate to a given statistical ensemble. In order to ensure that a proper average is achieved, an effective sampling is needed. Efficient important sampling is the one in which the Metropolis algorithm is used (Metropolis et al., 1953). In such a sampling, a new configuration is acceptable immediately if the energy of the system is lowered, or with a probability of $\exp(-\Delta E / k_B T)$ if the energy is raised.

More relevantly Stroud (Stroud et al., 1976) reported one of the first studies of the thermodynamic properties of adsorbed molecules in zeolites by Monte Carlo simulations. They studied methane in zeolite 5A and calculated thermodynamic properties such as the isosteric heat of adsorption and heat

capacity. Kretschmer and Fiedler (Kretschmer et al., 1977) also performed some early Monte Carlo work for simulating of alkanes in zeolites. The early work was restricted to one molecule per cavity and therefore corresponds to the ideal gas limit. Since these pioneering works, many studies of the behaviour of adsorbed molecules in zeolites have been carried out by using Monte Carlo techniques (Catlow *et al.*, 1991b;Delara *et al.*, 1989b;Demontis *et al.*, 1992b;June *et al.*, 1990;Nicholas *et al.*, 1993a;Smit & Siepmann, 1994).

2.8 Molecular mechanics

The goal of molecular mechanics is to predict the detailed structure and physical properties of molecules. Examples of physical properties that can be calculated include enthalpies of formation, entropies, dipole moments, and strain energies. Molecular mechanics calculates the energy of a molecule and then adjusts the energy changes in bond lengths and angles to obtain the minimum energy structure.

2.8.1 Interparticle interactions

The most fundamental approach is to attempt to calculate the interparticle interactions from first principles by solving the electronic Schrödinger equation

$$\hat{H}\Psi = E\Psi \tag{2-27}$$

for the electronic energy at each nuclear configuration. Many methods for doing this are available but three of the more commonly used types are passed upon density functional theory, molecular orbital theory and valence

bond theory. All three are first principles or ab initio methods in the sense that they attempt to solve Schrödinger equation with as few assumptions as possible. Although these methods can give very accurate results in many circumstances they are expensive and hence cheaper alternatives have been developed.

One way of making progress is to drop the restriction of performing first-principles calculations and seek ways of simplifying the ab initio methods outlined above. These so called semi-empirical methods have the same overall formalism as that of the ab initio but they approximate various time-consuming parts of the calculation with simpler approaches. Of course, because approximations have been introduced the methods must be calibrated to ensure that the results they produce are meaningful. This often means that the values of various empirical parameters in the methods have to be chosen so that the results of the calculations agree with the results of accurate ab initio quantum mechanical calculations. Semi-empirical versions of all the ab initio methods mentioned above exist.

A second and even cheaper approach is to employ an entirely empirical potential energy function. This consists of choosing an analytic form for the function, which is to represent the potential energy surface for the system and then parameterizing the function so that the energies that it produces agree with experimental data or with the results of accurate ab initio quantum mechanical calculations.

2.8.2 Force fields

Many of the problems that we would like to tackle in molecular modelling are too large to be considered by quantum mechanics. Quantum mechanics methods deal with the electrons in a system, so that even if some of the electrons are ignored (as in the semiempirical methods) a large number of particles must still be considered, and the calculations are time-consuming. Force field methods, otherwise known as molecular mechanics, ignore the electronic motions and calculate the energy of a system as a function of the nuclear positions only. Force field is thus invariably used to perform calculations on systems containing significant numbers of atoms.

Many of the molecular modelling force fields in use today for molecular systems can be interpreted in terms of a relatively simple four-component picture of the intra- and inter-molecular forces within the system.

$$E_{potential} = \sum_{bonds} E_{stretch} + \sum_{angles} E_{bend} + \sum_{dihedrals} E_{torsions} + \sum_{pairs} E_{nonbond} \qquad (2\text{-}28)$$

The first term refers to the interaction between pairs of bonded atoms. The second term is the summation over all valence angles[6] in the molecule. The third term is a torsional potential which refers to the energy changes as a bond rotates. The fourth contribution is the non-bonded term. This is calculated between all pairs of atoms that are in different molecules.

Energetic penalties are associated with the deviation of bonds and angles away from their 'reference' or 'equilibrium' values, there is a function that describes how the energy changes as bonds are rotated, and finally the force

[6] A valence angle is the angle formed between three atoms A-B-C in which A and C are both bonded to B

field contains terms that describe the interaction between non-bonded parts of the system. The various contributions are schematically represented in Figure 2-8.

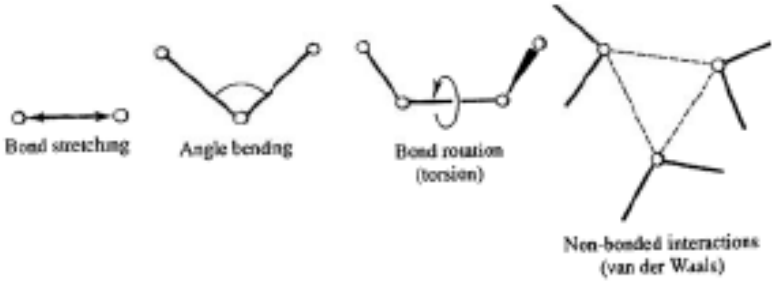

Figure 2-8 Schematic representation of the four key contributions to a molecular mechanics force field (Leach, 2001)

2.9 Statistical mechanics

A macroscopic system is, typically, composed of the order of 10^{23} particles. It is impossible to know, investigate, or describe the exact microscopic behaviour of each individual particle in such a system. We must limit our knowledge to the average properties, thermodynamic quantities like the temperature or pressure and correlation functions.

Statistical mechanics is the bridge between the microscopic and macroscopic world, it provides methods of calculating the macroscopic properties, like the specific heat, from the microscopic information, like the interaction energy between the particles. The essential ingredient of statistical mechanics is the probability distribution, i.e., the collection of occupancies of different configurations (microscopic states).

Table 3 shows examples of microscopic and macroscopic variables for 1/6th mole[7] of an n-component monoatomic gas (approx. 10^{23} molecules) obeying classical mechanics.

Table 3 Microscopic and macroscopic variables examples

Microscopic variables	Macroscopic variables
3×10^{23} positions (x,y,z) 3×10^{23} velocities (x,y,z)	$n+2$ independent thermodynamic variables e.g. for $n=1$, N,V,E

Let's consider as an example the ideal gas of N particles in a three dimensional space (see Figure 2-9). The Hamiltonian is

$$H(p_i,r_i)=\sum_{i=1}^{N}\frac{1}{2m_i}p_i^2+V(r_i)=K+U=E \tag{2-29}$$

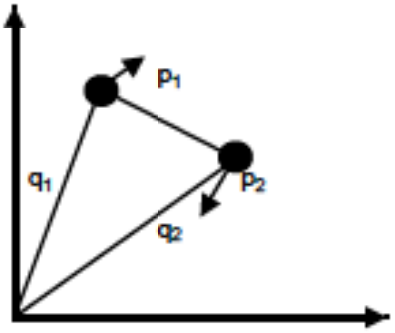

Figure 2-9 diatomic molecule in phase space. The position and motion of the particle are presented by the point with coordinates $(q_{1x}, q_{1y}, q_{1z}, q_{2x}, q_{2y}, q_{2z}, p_{1x}, p_{1y}, p_{1z}, p_{2x}, p_{2y}, p_{2z})$ in a 2-dimensional phase space. For clarity, the z-components are not indicated

(p_i is the component of the momentum, m_i is the particle mass, and $V(r_{ij})$ the interaction between particles. The interaction term is necessary for the system of particles to reach thermal equilibrium, but it can be neglected compared to the kinetic energy.). The $3N$ coordinates and $3N$ momenta from

[7] A mole is 6.02×10^{23}

$6N$ dimensional phase space. Each point in the phase space represents a microscopic state of the system. The microscopic state changes in time according to the canonical equation of motion:

$$\dot{q}_i = \frac{\partial \mathcal{H}}{\partial p_i} \quad \text{and} \quad \dot{p}_i = \frac{\partial \mathcal{H}}{\partial q_i} \tag{2-30}$$

and trace a trajectory (see Figure 2-10) in the phase space.

Figure 2-10 Trajectory in two-dimensional phase space representing the time development of the system.

The system is completely described if we know the coordinates and momenta of all particles ($6N$ 6N variables - a terrible task). To get an average of a physical quantity, say A, one should make the time average over a long segment of the trajectory (a collection of consecutive configurations) of such a system in the phase space,

$$\langle A \rangle = \frac{1}{t}\int_0^t A[q_i(t), p_i(t)]dt \tag{2-31}$$

However, usually we know neither the exact microscopic state, i.e., the location of the system in the phase space, nor the trajectory. What we can know, is the macroscopic state (temperature, pressure, volume, ...). Instead of studying a particular microscopic state and the trajectory over the phase

space, we investigate an ensemble of systems, i.e., a collection of all possible microscopic systems, all belonging to the same macroscopic state.

To calculate the average of a physical quantity, we substitute the time average over one system by an average over an ensemble of equivalent systems at fixed time:

$$\langle A \rangle = \int_W A(\{q_i, p_i\}) \rho(\{q_i, p_i\}) d^{3N} q d^{3N} p \tag{2-32}$$

The integral is over the whole phase space W and ρ is the probability density in the phase space; it is the probability that a unit volume of the phase space is occupied. Therefore, instead of the time average, we make an ensemble average at fixed time. When the time and the ensemble averages are equal, we say that the system is ergodic. In an alternative but equivalent definition we say that a system is ergodic if it evolves in such a way that it visits with equal probability all points of the phase space which are accessible from the initial configuration subject to the constraint of energy conservation. In other words, the trajectory in the phase space of an ergodic system will spend equal time intervals in all regions of the constant energy surface. Most of the physical systems of interest in statistical mechanics are ergodic, so in most of the cases time averages is replace by the corresponding ensemble averages.

2.9.1 Ensembles is statistical mechanics

An ensemble is a collection of many configurations of a system, all describing the same thermodynamic state. Ensembles are classified according to the constraints imposed on the corresponding thermodynamic system. The four

most important types are the *microcanonical ensemble* NVE, the *canonical ensemble* NVT, *isothermal- isobaric* NPT and the *grand canonical ensemble* μVT.

A microcanonical ensemble represents a collection of configurations of isolated systems that have reached thermal equilibrium. A system is isolated from its environment if it exchanges neither particles nor energy with its surrounding. The volume V, internal energy E and number of particles N of such a system are constant and are the same for all configurations that are part of the same microcanonical ensemble.

A canonical ensemble is a collection of closed systems at constant temperature. Closed systems have fixed number of particles and volume but can exchange energy with their surroundings. The energy of a closed system is therefore not constant. As an example we can imagine a gas of particles (air molecules, e.g.) in a closed container at constant temperature.

In the isothermal-isobaric or NPT ensemble, pressure is imposed instead of volume of the system is used to predict fluid density. This ensemble is used for instance, when the properties of a fluid are to be determined at known pressure and temperature. The grand canonical ensemble is defined as the assembly off all states that has a fixed value of μ, V and T, where μ is the chemical potential. The Grand canonical ensemble is the ensemble that is most adapted to adsorption in microporous solids, where the temperature, the volume, and the chemical of each species are the imposed variables.

Table 2-4 Types of Ensembles

Ensemble	Constraints
Microcanonical	N,V,E
Canonical	N,V,T
Grand Canonical	μ,V,T
Isothermal – Isobaric	N,P,T

The ensembles summarised in Table 2-4 occur in two broad categories. The microcanonical, canonical and isothermal–isobaric ensembles describe closed systems for which there is no change in the number of particles. In contrast, the grand canonical ensemble is an open system in which the number of particles can change.

Beside common average properties like density, pressure or energy, the analysis of fluctuations allows to determine thermo physical properties like the heat capacity, the compressibility, the thermal expansion coefficient or the Joule-Thomson coefficient.

2.10 Basic of Monte Carlo techniques

In general, Monte Carlo methods are statistical simulation techniques. Monte Carlo methods can be used to calculate the thermodynamic average of the properties of a system by generating a new configuration of a system using certain moves from an old configuration. If the potential energy of a new configuration is lower than that of the old one, the new configuration is accepted unconditionally. Otherwise, the new configuration is accepted by a

probability $\exp(-\Delta U / k_B T)$. By averaging over the properties of the accepted configurations, the desired information can be obtained.

2.10.1 Major components of a Monte Carlo algorithm

The major components of a Monte Carlo algorithm are:

- Probability distribution density function, which can describe the physical or chemical systems.
- Random number generators providing a source of random numbers uniformly distributed over an interval.
- Sampling rules that gives a statement for sampling from a specified probability distribution function.
- Accumulation of quantities of interest over all configurations accepted.
- Error estimation in which the statistical error has been calculated.
- Variance reduction techniques that is the methods for reducing the variance in the estimated solution to reduce the computational time.
- Parallelisation and vectorisation. These are the algorithms to allow Monte Carlo simulations to be carried out efficiently on parallel computers.

Example: Estimating the function $f(x)=\int_0^{\pi/2} Cos(x)$ using Monte Carlo technique.

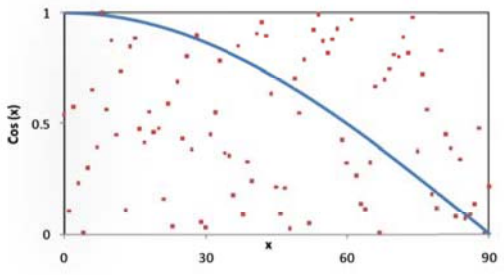

Figure 2-11 random points generated for the intervals of $x=0$ to $x=\pi/2$

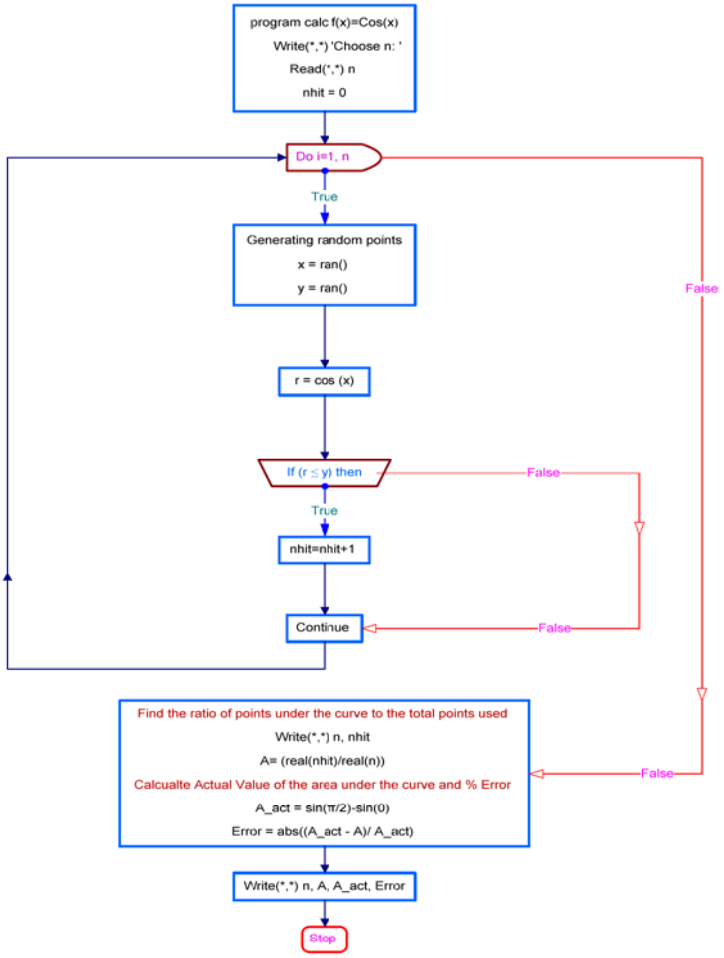

Figure 2-12 Simple Monte Carlo algorithm estimating the integral of $f(x)=Cos(x)$ for the intervals of $x=0$ to $x=\pi/2$

2.10.2 The principle of Monte Carlo integration

The simplest non-trivial example of the Monte Carlo method is multidimensional integration, for which traditional numerical quadrature,

such as Simpson's rule, is almost useless for a high dimensional system. Suppose that N points $X_1 \ldots X_N$ area selected at random and which are uniformly distributed in a multidimensional volume V. Then according to the basic theorem of Monte Carlo method, the integral of a function f over the multidimensional volume can be estimated. It is given by (Press & Flannery, 1994)

$$\int f dV \approx V\langle f\rangle \pm V\sqrt{\frac{\langle f^2\rangle - \langle f\rangle^2}{N}} \tag{2-33}$$

The angular brackets stand for the arithmetic mean over the N sample points, that is,

$$\langle f\rangle \equiv \frac{1}{N}\sum_{i=1}^{N} f(x_i) \qquad \langle f^2\rangle \equiv \frac{1}{N}\sum_{i=1}^{N} f^2(x_i) \tag{2-34}$$

The "plus-or-minus" term in (2-33) is a one standard deviation error estimate for the integral. As it can be seen this standard deviation error estimate is proportion to the reciprocal of square root of the number of sampled points, but it is independent of the dimensionality of sampling space. This is the reason why the Monte Carlo method is especially useful for multidimensional integration. In statistical mechanical problems there are many classical expressions that involve multidimensional integration, such as the partition function and a variety of ensemble averages. Only in a few exceptional cases can the integral over multidimensional volume be computed analytically and in all other cases the traditional numerical integration methods are unfeasible. Therefore, Monte Carlo integration is a

powerful tool to evaluate such integrals. In practice, this simplest Monte Carlo integration is highly inefficient for molecular simulation, because each state needs to be generated at random and then $3N$ random numbers have to be calculated to determine the coordinates of each molecule. A large portion of the states created in this way would give a small contribution to the average of macroscopic properties of system. Furthermore, the accuracy of this Monte Carlo integration (as shown in equation (2-33) increases with the square root of the number of sampled points, N. This means if one wants to increase the accuracy 10 times, the number of sampled points must be increased by 100. Therefore, for molecular applications of the Monte Carlo method it is important to find a solution which lead to faster convergence.

2.10.3 Importance sampling

Important sampling techniques (Metropolis et al., 1953) make Monte Carlo evaluation efficient and which can lead to high efficiency as well as faster convergence. The basic idea behind importance sampling is to sample points at random from a distribution function $\rho(x)$, which is weighted to allow more sample points to be concentrated in the region which make significant contribution to the function evaluation. In practice, for evaluation of an integral this just amounts to a change of an integral variable.

Thus, suppose that integral of a function f can be presented as the product of a function h times another function g. Then the integral over a multidimensional volume V can be described as follows:

$$\int sdV = \int (f/g)gdV = \int hgdV \tag{2-35}$$

Here, a change of variable can be made, that is $gdV = dG$. Then equation (2-35) can be rewritten as

$$\int sdV = \int (f/g)gdV = \int hdG \tag{2-36}$$

Furthermore, suppose that points x_i are selected within the volume V with a sampling density g satisfying

$$\int gdV = 1 \tag{2-37}$$

Then the basic theorem of Monte Carlo integration is applied to equation (2-36) to give

$$\int fdV = \int \frac{f}{g} dG \approx \langle \frac{f}{g} \rangle \pm \sqrt{\frac{\langle f^2/g^2 \rangle - \langle f/g \rangle^2}{N}} \tag{2-38}$$

Where angular brackets denote arithmetic means over N points which is exactly same as in equation (2-34). the "plus-or-minus" term is a standard deviation error estimate. As can be seen, the estimated value of integration remains unchanged, but the magnitude of variance can be reduced greatly by choosing an appropriate function $g(x)$. It is widely stated (see (Press & Flannery, 1994) that the best choice for the probability sampling density is given by

$$g = \frac{|f|}{\int |f| dV} \tag{2-39}$$

In fact, importance sampling described above cannot be used in practice. The reason is that one does not know how to construct such an optimal

probability sampling density. However Metropolis and co-workers gave an elegant alternative efficient solution(Metropolis et al., 1953).

2.10.4 Metropolis sampling

Suppose that the following multidimensional integral needs to be evaluated:

$$Q = \int \exp\left[-\beta U\left(r^M\right)\right] dr^M = \int f dr^M \tag{2-40}$$

As described in previous section, when distribution of the sampled points satisfy the probability density,

$$\rho(r^M) = \frac{|f|}{\int |f| dr^M} = \frac{\exp[-\beta U(r^M)}{\int \exp[-\beta U(r^M)] dr^M} \tag{2-41}$$

Then the standard deviation error estimate is minimum, as described by Press et al (Press & Flannery, 1994). The equation is then how to create points in phase space with such a distribution.

In the Metropolis sampling scheme, a Markov chain is constructed to create a sequence of random states of the system where at the end of the simulation each state has occurred with the appropriate probability. A Markov chain is a sequence of trials that satisfies two conditions:

The configuration generated by each trial must belong to a finite number of configurations, which is called the state space, $\{\Gamma_1, \Gamma_2, \ldots \Gamma_n, \Gamma_o, \ldots\}$.

Each configuration depends on the configuration that immediately precedes it.

In a Markov chain, any two states Γ_o and Γ_n are connected with a transition probability $\pi(o \to n)$. $\pi(o \to n)$ is the probability of transition from state o to

state n. If $\rho^{(1)}$ is the initial probability distribution then after one step transition the probability distribution is changed to $\rho^{(2)} = \rho^{(1)}\pi(o \to n)$. As long as the Markov chain is long enough, then the probability distribution is close to a limiting one, which is given by

$$\rho = \lim_{\tau \to \infty} \rho^{(1)} \pi^{\tau} \tag{2-42}$$

The matrix elements $\pi(o \to n)$ have to satisfy one condition, which is that they do not destroy an equilibrium distribution once it is reached. This implies that the average number of accepted trial from old state to new state must be exactly equal to the reverse one. The detailed balance condition is as following:

$$\rho(o)\pi(o \to n) = \rho(n)\pi(n \to o) \tag{2-43}$$

This is called "microscopic reversibility". Meanwhile since the transition matrix π is a stochastic matrix, it should satisfy the following equation as well

$$\sum_{n} \pi(o \to n) = 1 \tag{2-44}$$

In fact there are many possible forms of the transition matrix $\pi(o \to n)$ which satisfy equations (2-43) and (2-44). There are a number of suitable transition matrices. There are a number of suitable transition matrices. It is therefore important to choose one particular transition matrix, which minimises the variance in the estimate of a function evaluation. It is essential that the Markov chain select a representative portion of state space in a reasonable

number of moves. The Metropolis solution appears to lead to a faster convergence of the chain.

In the Metropolis sampling method, a symmetric underlying matrix α is introduced, which is the probability of performing a trial move from state o to n,

$$\pi(o \to n) = \alpha(o \to n) \times acc(o \to n) \tag{2-45}$$

Where $acc(o \to n)$ is the probability of accepting a trial move from o to n.

Because $\alpha(o \to n)$ is a symmetric matrix, then equation (2-43) can be rewritten in terms of the $acc(o \to n)$:

$$\rho(o) \times acc(o \to n) = \rho(n) \times acc(n \to o) \tag{2-46}$$

Again, there are many choices of $acc(o \to n)$ which, satisfy this condition. The choice of Metropolis scheme is

$$\begin{aligned} acc(o \to n) &= 1 && \rho(n) \geq \rho(o) \\ &\text{or} && \\ &= \rho(n) / \rho(o) && \rho(n) < \rho(o) \end{aligned} \tag{2-47}$$

Therefore, if the state o and n are distinct, the choice of transition probability in Metropolis scheme is as follows:

$$\begin{aligned} &\pi(o \to n) = \alpha(o \to n) && \text{if } \rho(n) \geq \rho(o) \quad o \neq n \\ &\pi(o \to n) = \alpha(o \to n)\{\rho(n) / \rho(o)\} && \text{if } \rho(n) < \rho(o) \quad o \neq n \\ &\pi(o \to o) = 1 - \sum_{o \neq n} \pi(o \to n) && \end{aligned} \tag{2-48}$$

It is clear that this solution only involves the ratio $\rho(n)/\rho(o)$. The transition probability defined by the above equation satisfies the microscopic reversibility condition.

There is considerable freedom in choosing the underlying stochastic matrix α and the only constraint is the symmetric property, namely $\pi(o \to n) = \alpha(o \to n)$. Metropolis et al. used the following steps to perform the sampling:

Randomly select a particle and then calculate its energy $U(o)$.

Make a trial move for this particle, that gives the particle a random displacement as well as rotation, the co-ordination of the particle would be changed to

$$x' = x + \delta_1 \xi_1 \qquad y' = y + \delta_1 \xi_2 \qquad z' = z + \delta_1 \xi_3$$
$$\theta' = \theta + \delta_2 \xi_4 \qquad \varphi' = \varphi + \delta_2 \xi_5 \qquad \phi' = \phi + \delta_2 \xi_6$$

Here x, y and z are the coordinates of a molecular centre of mass, θ, φ and ϕ are the Euler angles of a particle in the phase space. δ_1, δ_2 are the maximum displacement and rotation angle respectively. $\xi_1 \ldots \xi_6$ are random numbers uniform in range of $[-1,1]$.

Calculate the energy of new configuration $U(n)$.

Acceptance test. If $U(n) \le U(o)$, then $\rho(n) \ge \rho(o)$, the trial is accepted unconditionally. That means a new point in phase space generated. If $U(n) > U(o)$, then $\rho(n) < \rho(o)$ therefore the trial is accepted conditionally. That is, if $\exp\{-\beta[U(n) - U(o)]\}$ is greater than a random number then the trial is accepted; otherwise it is rejected. In the latter case, the system remains in

the original state, which is a new state of the Markov chain again. The reason for such a condition is that rejection of all trial states with less probability would cause the simulation to grind to a halt at some low energy configuration. This would not be representative of a real system where entropic effects cause the macroscopic thermodynamic properties continually to vary around the equilibrium value.

δ_1 and δ_2 adjustable parameters, which govern the size of the trial move and control the convergence of the Markov chain. If they are too small, of course the acceptance of trial moves is high but it may lead to inefficient sampling of state space and the convergence of the chain is slower. In contrast, if they are too large nearly all the trial moves are rejected and the points sampled may not be a representative portion of state space.

Reasonable parameters should lead to an optimum acceptance and result in the most efficient sampling of phase space. In practice, one has to adjust the parameters during the simulations according to the probability of acceptance and therefore make sure the probability of acceptance is around 50%. However, there are still some arguments about the optimal acceptance. In general, an acceptance of approximately 30-50% is widely considered as close to optimum.

2.11 Statistical mechanic basis of adsorption in zeolites

The probability distribution density function is the key component in Monte Carlo simulation of a physical process. To find the probability density function, the understanding of the statistical mechanical basis for the

ensemble selected is essential. The basic postulate of statistical mechanics is to use an ensemble average to replace the time average, which is over the microstates. Therefore, the value of a macroscopic property B, which is located in a particular state Γ in phase space, then can be written as

$$B_{abs} = \langle B \rangle_{time} = \sum_{microstates} B_i \rho_{ens\,i} \tag{2-49}$$

B_{abs} is the experimentally observable macroscopic property. $\langle B \rangle_{time}$ is the time average of B. $\langle B \rangle_{ens}$ is the average value of B over the ensemble. B_i is the value of B in microstate i and $\rho_{ens\,i}$ is the probability of finding an arbitrary system in microstate i in the ensemble. To calculate $\rho_{ens\,i}$, an assumption has been made that the probability of a microstate depends only on its energy, i.e. all microstates with the same energy occur with equal probability. The classical equivalent of a microstate is a point in phase space. Thus the summation over all microstates can be replaced by an integral over phase space and furthermore the energy of the system can be divided into two parts, namely a kinetic part and a potential part. As the kinetic part is a quadratic function of the momenta, the integration over momenta can be calculated analytically. Hence, the integral over phase space only involves the potential energy.

For an adsorption experiment, the adsorbent is placed in a container of fixed volume, which then is immersed in an isothermal bath to keep the temperature constant during the experiment. For a specified bulk pressure, once the equilibrium is reached, the amount adsorbed can be measured. For

a multicomponent adsorption experiment, the gas phase components are specified and the composition of the adsorbed phase is measured. At a macroscopic thermodynamic level, this means setting the chemical potential of each component in the reservoir, the pore volume and the temperature. In statistical mechanics, this corresponds to the *Grand Canonical ensemble*. Using Grand Canonical ensemble (μVT) Monte Carlo simulation for study of adsorption in zeolites, it mimics a zeolites in contact with a reservoir (bulk gas) (as shown in Figure 2-13). The reservoir keeps constant temperature and chemical potential of each component whereas the number of particles is allowed to fluctuate during the simulations. In the experimental set-up, the adsorbed gas (inside the zeolites) is in equilibrium with the gas in the reservoir. The equilibrium conditions are that the temperature and chemical potential of each component of gas inside and outside the absorbent must be equal.

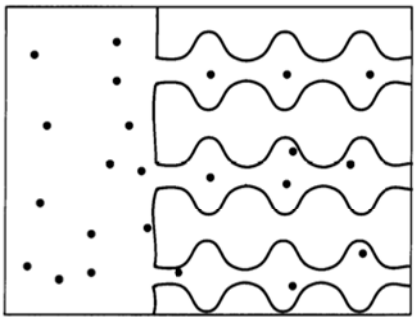

Figure 2-13 zeolite in contact with a reservoir that imposes constant chemical potential and temperature by exchanging particles and energy (Frenkel & Smit, 2002)

When the temperature and chemical potential of the reservoir are known, the equilibrium concentration inside the adsorbent (or say inside the pores) can be obtained. The expression for the classical partition function of adsorption in the Grand Canonical ensemble can be given by

$$\Xi = \sum_{M=0}^{\infty} \frac{\exp(\beta\mu M)V^M}{\Lambda^{3M} M!} \int \exp[-\beta U(r^M)] d(r^M) \tag{2-50}$$

Where $\Lambda = \sqrt{h^2/(2\pi m k_B T)}$ is the thermal de Broglie wavelength. β is reciprocal temperature $(1/k_B T)$. h and k_B are Planck's and Boltzmann's constant. m is a particle mass. μ is the chemical potential and r^M is a vector denoting the coordinates of all molecules in the system. Here is assumed that the volume of the reservoir must be much larger than the volume inside each pore and then the bulk phase is treated as an ideal gas. From the partition function above the corresponding probability density can be expressed as follows:

$$\rho_{ens}(r^M) = \frac{1}{\Xi} \frac{V^M \exp(\beta\mu M)}{\Lambda^{3M} M!} \exp[-\beta U(r^M)] \tag{2-51}$$

The macroscopic quantity B is given by

$$\langle B \rangle_{\mu,V,T} = \frac{1}{\Xi} \sum_M \frac{1}{\Lambda^{3M} M!} V^M \exp(\beta\mu M) \int B(r^M) \exp[-\beta U(r^M)] dr^M \tag{2-52}$$

Equations (2-50) and (2-51) are the basis equations for Monte Carlo simulations of adsorption in the Grand Canonical ensemble.

2.12 Conventional grand canonical Monte Carlo

In this scheme, the ordinary Metropolis Monte Carlo method is used[8]. The probability of generating a particular configuration is equal to that of all configurations, and therefore the probability of generating configuration n is equal to the probability of generating configuration o:

$$\alpha(o \to n) = \alpha(n \to o) \tag{2-53}$$

Therefore, the acceptance rule should obey following equation:

$$\frac{acc(o \to n)}{acc(n \to o)} = \frac{\rho(n)}{\rho(o)} \tag{2-54}$$

[8] Basic Grand Canonical Ensemble simulation algorithm (ran is the random number, npav is the number of attempts to displace particles, nexc is number attempts to exchange particles with the reservoir and npart is total number of particles.

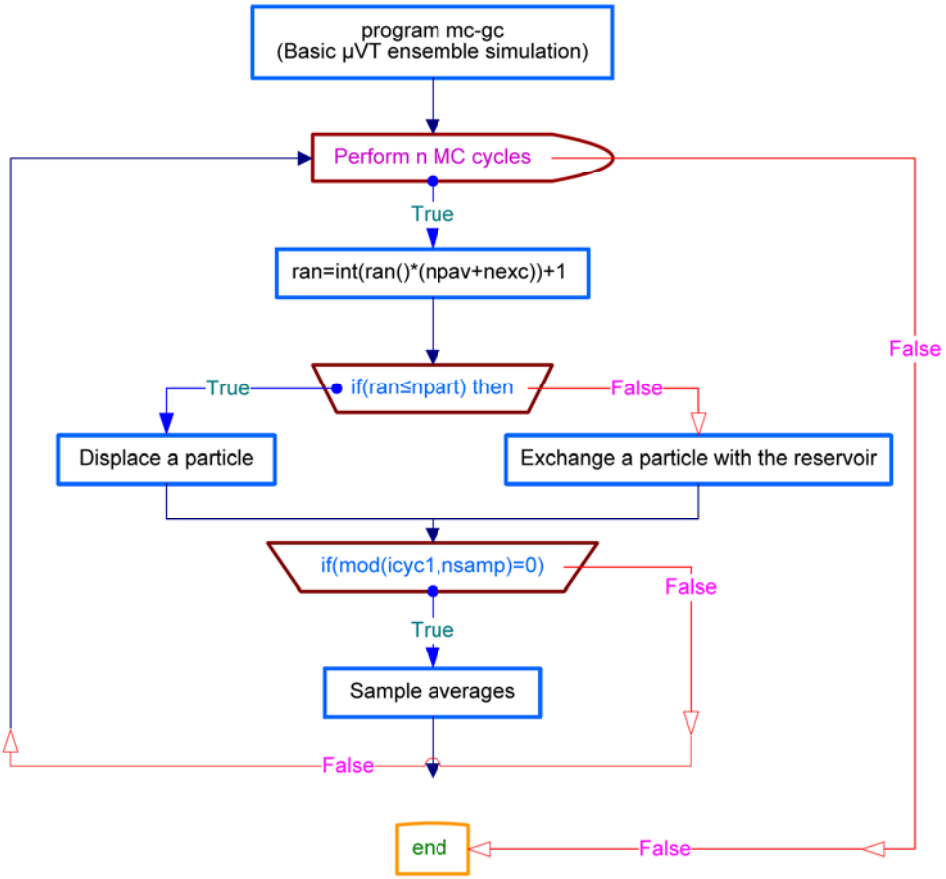

Here $\rho(n)$ and $\rho(o)$ are the probability of being in state n and o respectively. There are many possible rules for $acc(o \to n)$ which satisfy this condition. One of them is the Metropolis acceptance rule:

$$acc(o \to n) = \begin{cases} \dfrac{\rho(n)}{\rho(o)} & \text{if } \rho(n) < \rho(o) \\ 1 & \text{if } \rho(n) \geq \rho(o) \end{cases} \tag{2-55}$$

There are three trial moves involved in this scheme. In addition to particle displacement, attempts of adding or removing particles from the simulation box are also involved. For a particle insertion step, the whole particle is inserted at a random position at once. The details of trial moves involve in this scheme are presented below (Frenkel & Smit, 2002):

Displacement of particles: randomly chose one particle at each time and give a randomly selected displacement. During the simulation, the maximum displacement is adjusted according to the acceptance ratio to achieve an overall acceptance of 50%. From the description of probability density of adsorption in the Grand Canonical ensemble equation (2-51), the acceptance rule of this trial move is

$$acc(o \to n) = \min[1, \exp\{-\beta[U(n) - U(o)]\}] \tag{2-56}$$

Insertion/removal of a particle: randomly decided whether an attempt is made to insert a particle at a random position or to remove a particle randomly chosen. Consider the probability density of the ensemble and the Metropolis acceptance rule, the acceptance rules of above moves are:

For particle insertion:

$$acc(o \to n) = \min\left[1, \frac{V}{\Lambda^3 (M+1)} \exp\left\{\beta\left[\mu - U(n) + U(o)\right]\right\}\right] \quad (2\text{-}57)$$

For particle removal:

$$acc(o \to n) = \min\left[1, \frac{\Lambda^3 M}{V} \exp\left\{-\beta\left[\mu + U(n) - U(o)\right]\right\}\right] \quad (2\text{-}58)$$

Complete re-growing: a particle chosen randomly is re-grown at a random position in the simulation.

A sufficient number of accepted insertions in the pressure range of interest can be achieved. However, due to steric overlap, for longer chain molecules (such propane and butane) this method is not efficient so instead a special technique, which is called Configurational-Bias Monte Carlo, is used for additions of a longer chain molecules.

2.13 Configurational-Bias Monte Carlo

Due to steric overlap, the conventional Grand Canonical Monte Carlo method becomes impractical for insertion of longer chain molecules. To solve the problem, a novel Monte Carlo technique has been developed (Depablo *et al.*, 1992;Mooij *et al.*, 1992), known as the Configurational-Bias Monte Carlo method. In contrast to the conventional Grand Canonical Monte Carlo, the trial movements of swapping a particle are no longer random and the probability of generating a particular configuration is different from others. The basic idea of this method originally came from Rosenbluth and Rosenbluth (Rosenbluth & Rosenbluth, 1955), which relied on the smart insertion, namely, insert one segment of the molecule at a time. In contrast

to the conventional Monte Carlo technique, the insertion of a molecule is performed with growing atom by atom in a favourable direction instead of a completely random insertion. This growing process introduces a bias that is removed by adjusting the acceptance rules. In this scheme overlap between the molecules can be avoided.

The Configurational-Bias Monte Carlo scheme follows a special route. The insertion of a chain molecule by using such a scheme is described as follows (also shown in Figure 2-14)

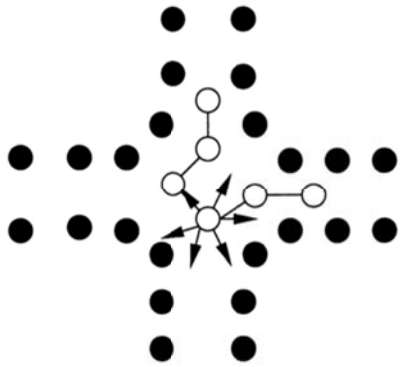

Figure 2-14 schematic drawing of the growth a chain molecule in a zeolite (Smit, Siepmann, 1994) by using the Configurational-Bias Monet Carlo algorithm. The solid black circles represent the atom of zeolites, and the white circles are the ones of a chain molecules. The set of arrows indicates a set of k trial orientations.

1. Randomly insert the first bead of the chain molecule.

The first united atom is inserted at a random position in the zeolites and the potential energy of this atom is calculated, which is denoted by $U^{n,ext}$ (it includes the potential energy between this atom and all other alkane molecules as well as the energy between this atom and the zeolites). According to the energy, a rejection test is made. If overlap occurs (according to the potential energy) then repeat the above procedure until there is no overlap remaining. Then, the randomly chosen position gives the coordinates of the first atom.

2. For the rest of the chain molecule

A set of possible trial orientation is generated according to the internal energy (bond bending and torsion energy). One of them is selected according to the external energy (intermolecular energy as well as non-bonded intramolecular energy). The detailed procedure is:

For these united atoms, indicate with index I, according to the internal energy k possible trial directions are generated. These trial positions can be denoted by $\{b\}=(b_1,b_2,...,b_k)$. They are a set of random vectors distributed on the surface of a sphere, which is centred on the previously inserted united atom of the molecule and has radius equal to the bond length. In the simulations it assumed that the alkane molecules have fixed bond length so that for second united atom there is no internal energy existing due to the constrains of the bond length. The trial positions for this atom are randomly distributed on a sphere. From the third atom on, an intramolecular energy is involved. In this case firstly a random vector on a unit sphere is created and then the bond bending and bond torsion angle θ,φ are determined. Finally, according to θ,φ, the internal energy (bond bending and bond torsion) is calculated and a rejection test is made. If rejected, the procedure will be repeated all over again until a value of θ,φ has been accepted. In this study k equals 6. Hence, the calculation is repeated six times. Then, six possible vectors are created. Each vector is accepted with a probability $\exp\left[-\beta(U^{bend}(\theta))+U^{tors}(\varphi)\right]$.

For each of these trial positions the external energy is calculated, which includes this united atom with the atom of other molecules (zeolites and other alkanes) and with the atoms of the same molecule that are already grown. This energy is denoted by $U_l^{n,ext}(b_j)$. One of these positions is selected with a probability

$$p_l^{ext}(b_j) = \frac{\exp\left[-\beta U_l^{n,ext}(b_j)\right]}{w^{n,ext}(l)} \tag{2-59}$$

where

$$w^{n,ext}(l) = \sum_{j=1}^{k} \exp\left[-\beta U_l^{n,ext}(b_j)\right] \tag{2-60}$$

Repeat the previous step until the whole length of the molecule has been grown and then the Rosenbluth factor of configuration n is determined by

$$W^n = \exp\left[-\beta U^{n,ext}(1)\right] \prod_{l=2}^{M} \frac{w^{n,ext}(l)}{k} \tag{2-61}$$

The new molecule is accepted with a probability:

$$acc(M \to M+1) = \min\left(1, \frac{\exp(\beta\mu^B)V}{\Lambda^3(M+1)}\right) W^n \tag{2-62}$$

Where μ^B is the chemical potential of the reservoir.

Compared to the conventional Grand Canonical Monte Carlo method, there are two additional trial moves included in this scheme, which are:

Rotation of a molecule: a chain molecule selected randomly is given a random rotation around its centre of mass. During the simulation the maximum rotation angle is adjusted according to the acceptance ratio to

achieve an overall acceptance of 50%. The acceptance rule of this trial move is given by

$$acc(o \to n) = \min\left[1, \exp\left\{-\beta\left[U(n) - U(o)\right]\right\}\right] \tag{2-63}$$

Partial re-growth: a chain molecule is selected at random and is partially re-grown by using the Configurational-Bias Monte Carlo algorithm in a randomly chosen direction starting at a randomly chosen segment.

Using the Configurational-Bias Monte Carlo scheme, is then performed insertion/removal of a chain molecule. In this study, the Configurational-Bias Monte Carlo technique has been used for simulation of methane, ethane, propane, normal butane, isobutene and CO_2.

2.14 Monte Carlo simulation in Gibbs ensemble

The Gibbs ensemble Monte Carlo simulation methodology was put forward originally by Panagiotopoulos (Panagiotopoulos, 1987a). The purpose of this method is to directly obtain phase coexistence properties of pure components and mixtures from a single simulation, without the need for determining the chemical potential. The essence of the technique is to perform a simulation simultaneously in two distinct physical regions, in which the densities and compositions are different and each region represents a small homogeneous phase with periodic boundary conditions (Allen & Tildesley, 1987). There are no physical contacts between the two regions and no interface. The equilibrium conditions for coexistence of two or more phases are that each region should be in internal equilibrium,

temperature, pressure and the chemical potentials of all components should be the same in the two regions (see Figure 2-15).

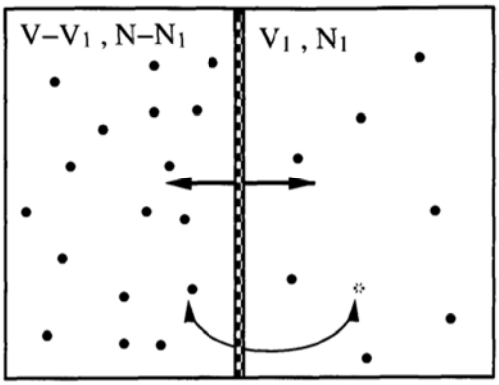

Figure 2-15 Schematic sketch of the "Gibbs ensemble" in which two systems can exchange both volume and particles in such a way that total volume V and the total number of particles N are fixed.

To satisfy equilibrium conditions for coexisting phases, there are three types of Monte Carlo moves to be conducted in Gibbs ensemble:

- **Particle displacement.** A random displacement of molecules in each region, which ensures equilibrium within each region.
- **Volume change.** An equal and opposite change in the volume of the two regions that leads to equality of pressures.
- **Particle exchange.** Randomly transfer molecules between the two regions that enable the chemical potential of each component in the two regions to be equal.

The details of the trial moves are shown in the following figure.

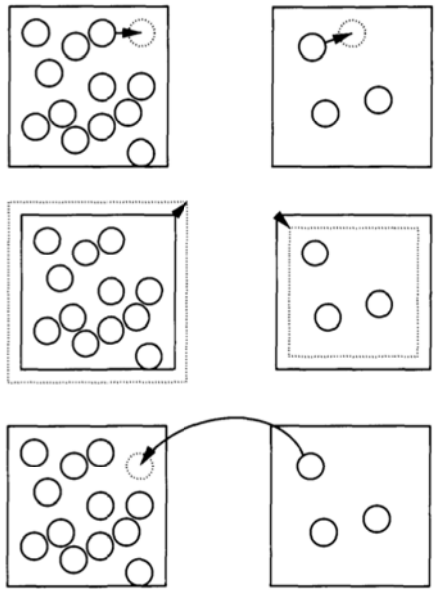

Figure 2-16 Monte Carlo steps in the Gibbs ensemble method: particle displacement, volume change, and exchange of particles (Frenkel & Smit, 2002).

As other simulation techniques, the aim of Gibbs Monte Carlo simulations can be either to obtain accurate results for well-defined simple model fluids in order to test statistical mechanics theories or to simulate the behaviour of real system for which relatively complicated intermolecular potentials can be used and these potential models possess parameters fitted to experimental data. Monte Carlo simulation of phase equilibrium in the Gibbs ensemble does not require any previous knowledge or calculation of the chemical potentials of components in a system (Panagiotopoulos, 1992). From the point of programming, the Gibbs ensemble is indeed more complicated than constant ensemble, due to three different types of steps to be performed.

The Gibbs technique has been used to predict vapour-liquid, liquid-liquid and osmotic equilibrium for binary Lennard-Jones mixtures (Panagiotopoulos et al., 1988), phase transitions for fluids in pores (Panagiotopoulos, 1987b)

and calculations of phase diagrams for diatomic Lennard-Jones molecules (Galassi & Tildesley, 1994).

Similar to all other simulation methods, the Gibbs ensemble Monte Carlo technique is not perfect simulation method. There are some difficulties. A main issue for the Gibbs Monte Carlo method is the size dependence of the results.

2.15 Recoil growth method

The recoil growth (RG) scheme is a dynamic Monte Carlo algorithm that was developed with the dead-alley problem in mind (Consta *et al.*, 1998;Consta *et al.*, 1999). The algorithm is related to earlier static MC schemes due to Meirovitch (Meirovitch, 1988) and Alexandrowicz and Wilding (Alexandrowicz, 1998). The basic strategy of the method is that it allows escaping from a trap by "recoiling back" a few monomers and retrying the growth process using another trial orientation. In contrast, the Configurational bias Monte Carlo scheme looks only one step ahead. Once a trial orientation has been selected, we cannot "deselect" it, even if it turns out to lead into a dead alley. The recoil growth scheme looks several monomers ahead to see whether traps are to be expected before a monomer is irrevocably added to the trial conformation (see Figure 2-17).

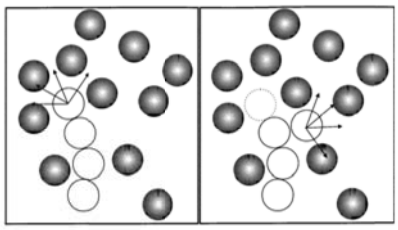

Figure 2-17 The conformational-bias Monte Carlo scheme fails if the molecule is trapped in a dead alley (left); irrespective of the number of trial orientations the CBMC scheme will never generate an acceptable conformation. In the recoil growth scheme (right) the algorithm "recoils" back to a previous monomer and attempts to regrow from there (Frenkel & Smit, 2002).

In this way, we can alleviate (but not remove) the dead-alley problem.

3- LATTICE MODEL - BENZENE ADSORPTION IN SILICALITE

3.1 Introduction

The theoretical prediction of the shape of adsorption isotherms for hydrocarbons in zeolites has a number of challenging features. Among them, there is the rationalisation of the well-known steps in the adsorption isotherms of benzene in silicalite[9] reproduced in Figure 3-1.

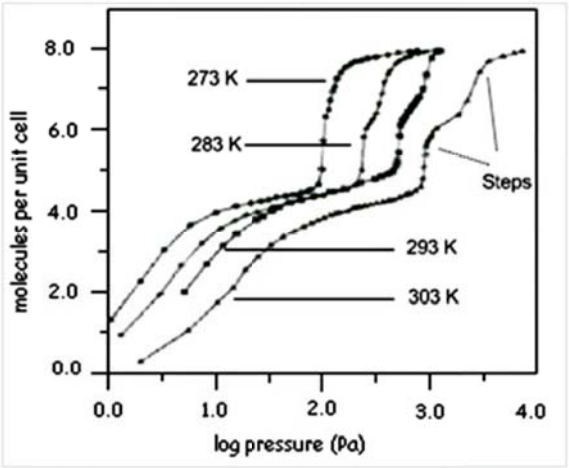

Figure 3-1 Experimental adsorption isotherms for benzene adsorption in the silicalite zeolites at 273 K (•••), 283 K (◆◆◆), 293 K (▪▪▪) and 303 K (▲▲▲) (Chiang et al., 1997)

[9] Silicalite is a zeolite with a well-known pore structure composed of zigzag and straight pores and intersections (Olson et al., 1981). It is commonly assumed that these pores house the adsorption sites. The pores in the three-dimensional structure are made up of well-separated layers. It is believed that for benzene adsorption there are three types of adsorption sites: I (intersections), S (in straight channels) and Z (in zigzag pores)(Du *et al.*, 2000).

The appearance of the steps may have different causes such as capillary condensation, structure changes in zeolites, commensurate freezing in the assembly of adsorbed molecules (Dunne & Reuben, 1995a;Maris *et al.*, 1998;Snurr *et al.*, 1993;Vlugt *et al.*, 1999) or sharp rise in heat of adsorption at some intermediate loading (Pope, 1986). Whatever the reason is, one common conclusion is that at higher loading molecules can seek residence in sites, which are energetically more demanding, and this can result steps in adsorption isotherms.

X-ray diffraction studies (Lee *et al.*, 1992;Mentzen & Lefebvre, 1997) show the behaviour of benzene in silicalite to be extremely complex. At low loading it is thought from the available experimental evidence that the intersections (I sites) are predominantly occupied with at least two distinct orientations for the benzene molecule. For higher loading, six benzene molecules per unit cell are found in the intersection sites and zigzag pores (I and Z sites occupied). At still higher loading (eight molecules per unit cell) the inter-sections and straight pores are predominantly occupied (I and S sites).

In this chapter, using a lattice model following the theme above, it will be shown that the steps in adsorption isotherms can also arise from re-orientational transitions amongst molecules in the adsorbed phase where there is energetic competition between open and closed-packed structures in a monomer-dimer model. An exact calculation of the statistical mechanics of a generic lattice model is presented, where to obtain higher-loading

molecules must seek residence in sites, which are energetically more demanding, and this can lead to steps in the adsorption isotherms.

The lattice model has a *dimer state* to represent molecules lying in extended state denoted by symbol ___, *monomer state* to represent molecules forced into higher energy smaller volume residence denoted by symbol | and vacant sites or holes allow for incomplete filling of the lattice sites. (see Figure 3-2)

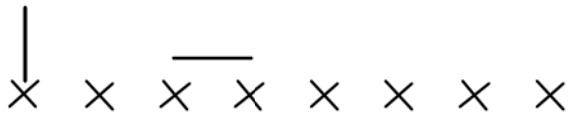

Figure 3-2 Benzene Molecule position on silicalite based on lattice model. | monomer, ___ dimer and × adsorption site.

Du and Dunne (Du et al., 2000) developed a lattice model with monomer states to represent erect conformation of the molecules, a dimer state to represent conformations parallel to the interface and vacant sites or "*holes*".

It was possible to extend the model developed by Du and Dunne, for benzene adsorption in silicalite zeolites to produce the adsorption isotherms for benzene in several temperatures over a wide range of pressures.

Later in the chapter, a modified one-dimensional lattice model with characteristic features of distinct adsorption sites in each channel system is introduced.

The benzene vapour phase is treated as an ideal gas in equilibrium with the adsorbed phase. In order to have confidence in the calculated results of this model, an accurate statistical treatment of the adsorbed phase is essential.

3.2 The model

In the model, each molecule is attached to one of the N_s sites of a quadratic lattice. The area per site is denoted by a_0 and hence the area a per molecule is given by

$$a = N_s a_0 / M \tag{3-1}$$

where M is the number of molecules. Here a_0 is regarded as constant but the area per molecule depends on the ratio M / N_s.

In the erect conformation, each molecule occupies single lattice site and such molecules are said to be in "*monomer*" states. It is assumed that nearest-neighbour pairs of monomers will tend to diminish their interaction energy by adopting the most advantageous relative orientation.

To represent this behaviour it is assumed that there are two monomer orientational states, labelled 1 and 2, and that 1-1 and 2-2 nearest-neighbour pairs have interaction energy $-(\varepsilon_{mm} + J)$ while 1-2 pairs have interaction energy $-(\varepsilon_{mm} - J)$ where negative sign means attraction.

There is also an extended or "*dimer*" state in which the molecule occupies two lattice sites with $-U(T)$ the free energy of transition.

The introduction of the extended state involves two more interaction energy parameters, $-\varepsilon_{md}$ for a nearest-neighbour pair consisting of a monomer and a dimer segment and $-\varepsilon_{dd}$ for a nearest-neighbour pair of segments of two different dimers.

In addition to occupation by a molecule in monomer states 1 or 2 or by a segment of a molecule in the dimer state, a site may be vacant. We denote the number of molecules in states 1 and 2 by N_1 and N_2, respectively, the number of molecules in the dimer state by N_d and the number of vacant sites or "*holes*" by N_h.

These numbers are related to the total number of sites N_s and the number of molecules M by the equations

$$N_1 + N_2 + N_d = M \tag{3-2}$$

$$N_1 + N_2 + 2N_d + N_h = M + N_d + N_h = N_s \tag{3-3}$$

A number density ρ is defined by

$$\rho = M / N_s \tag{3-4}$$

The upper bound of ρ is 1 and is only attained for perfect "*close-packing*" with all molecules in monomer states and no sites vacant ($N_d = N_h = 0$).

For any temperature above absolute zero, $\rho = 1$ implies infinite surface pressure. We use the term "*open structure*" when all molecules are in dimer state and no sites are vacant.

Since the coordination number of quadratic lattice is four, each dimer in open structure forms six nearest-neighbour pairs with segments of other dimers. Hence the total interaction energy is ($-3\varepsilon_{dd}M$) for a lattice occupied by M molecules and, since the total area for the open structure is $2Ma_0$, the enthalpy is

$$H_0 = -3\varepsilon_{dd}M - UM + 2Ma_0P \tag{3-5}$$

where P is the pressure.

An alternative state is a "*closed-packed structure*" with each site occupied by a molecule in a monomer state. To minimise the interaction energy all monomers must be in the same orientation state.

Hence on the quadratic lattice the total interaction energy is $-2M(\varepsilon_{mm} + J)$ and, since the total area for the closed-packed structure is Ma_0, the enthalpy is

$$H_c = -2M(\varepsilon_{mm} + J) + Ma_0P \tag{3-6}$$

3.2.1 Equilibrium states and thermodynamic relations

We employ the Flory-Huggins[10] (Bell & Dunne, 1978) or randomised approximation for the number Ω of configurations possible with given numbers of dimers and monomers in their two orientational states on a given number of lattice sites.

Bell and Dunne (Bell & Dunne, 1978) have shown that in this approximation the configuration number for M molecules, with N_d in the dimer and $M - N_d$ in a single monomer state, on a quadratic lattice of N_s sites, is

$$\left(\frac{2}{N_s}\right)^{N_d} \frac{N_s!}{(M-N_d)!N_d!(N_s-M-N_d)!} \tag{3-7}$$

[10] The Flory-Huggins theory defines the volume of a polymer system as a lattice which is divided into microscopic subspaces (called sites) of the same volume. In the case of polymer solutions, the solvent molecules are assumed to occupy single sites, while a polymer chain of a given type, i, occupies ni sites. The repulsive forces in the system are modelled by requiring each lattice site to be occupied by only a single segment. Attractive interactions between non-bonded sites are included at the lattice neighbour level.

It was found that results derived from this expression were quite close to those obtained by an accurate series method, indicating that the Flory-Huggins approximation is reasonably accurate for the derivation of isotherms from monomer-dimer models.

To allow for the existence of two monomer orientational species this expression must be multiplied by $(M-N_d)!/(N_1!N_2!)$

to give

$$\Omega=\left(\frac{2}{N_s}\right)^{N_d}\frac{N_s!}{N_1!N_2!N_d!N_h!} \tag{3-8}$$

where $N_h=N_s-M-N_d$ is the number of vacant sites or holes.

Randomised approximation (mean field) expressions for mean numbers of various types of nearest-neighbour pair are required for the calculation of E_c , the configurational interaction energy.

As an example, we consider the number of nearest-neighbour pairs formed by segments of two different dimers.

Since each dimer has six nearest-neighbours on the quadratic lattice and each monomer has four, the probability of a nearest-neighbour site to a given site being occupied by a dimer segment, with the other segment of the same dimer not occupying the given site, is

$$\frac{6N_d}{4N_1+4N_2+6N_d+4N_h}=\frac{6N_d}{2N_b} \tag{3-9}$$

Here N_b is the total number of nearest-neighbour pairs not formed by segments of the same dimer which, using equation (3-3), is given by

$$N_b = 2N_s - N_d = 2N_1 + 2N_2 + 3N_d + 2N_h \tag{3-10}$$

Hence, disregarding short-range ordering, the number of nearest-neighbour pairs formed by segments of two different dimer is

$$\frac{1}{2}6N_d(6N_d / 2N_b) = 9N_d^2 / N_b \tag{3-11}$$

where the factor $\frac{1}{2}$ prevents double counting of symmetrical pairs. Deriving the numbers of other types of pair in a similar way, the configurational interaction energy is given by

$$\begin{aligned} E_c = -[&4(\varepsilon_{mm} + J)(N_1^2 + N_2^2) + 8(\varepsilon_{mm} - J)N_1N_2 + \\ &12\varepsilon_{md}(N_1 + N_2)N_d + 9\varepsilon_{dd}N_d^2] / N_b \end{aligned} \tag{3-12}$$

The configurational *Helmholtz* free energy can now be expressed as

$$F_c = E_c - kT\ln\Omega - N_dU \tag{3-13}$$

In the canonical ensemble the values of N_s and M are given while the values of the internal variables N_1, N_2 and N_d are those, which minimise F_c subject to the relation (3-2). k is the Boltzmann's constant[11].

It is helpful to introduce independent parameters s and σ defined by

$$s = (N_1 + N_2) / M, \quad \sigma = (N_1 - N_2) / (N_1 + N_2) \tag{3-14}$$

Here s denotes the fraction of molecules in the monomer states while σ is a parameter expressing the degree of orientational ordering among the monomers and is equal to zero when orientational ordering is absent.

Using equation (3-3) for N_h and equation (3-10) for N_b, we can write

[11] Boltzmann constant = $1.3806503 \times 10^{-23}$ m^2 kg s^{-2} K^{-1}

$$N_1 = \frac{1}{2}N_s\rho s(1+\sigma),\quad N_2 = \frac{1}{2}N_s\rho s(1-\sigma),\quad N_d = N_s\rho(1-s)$$
$$N_h = N_s(1-2\rho+\rho s),\qquad N_b = N_s(2-\rho+\rho s) \tag{3-15}$$

Where the number density ρ is defined by equation (3-4).

Using Stirling's approximation[12] for the logarithm of the configuration number given by equation (3-7), we can now express the configurational free energy per site f_c in the form

$$\begin{aligned} f_c = \frac{F_c}{N_s} = kT[&\rho s(\frac{1+\sigma}{2}\ln(\frac{1+\sigma}{2}) + \frac{1-\sigma}{2}\ln(\frac{1-\sigma}{2})) + \\ &\rho\{s\ln s + (1-s)\ln(\frac{1-s}{2})\} + \rho\ln\rho + \\ &(1-2\rho+\rho s)\ln(1-2\rho+\rho s) + \rho(1-s)] - \\ &\rho(1-s)U - \rho^2\phi(\sigma,s)/(2-\rho+\rho s) \end{aligned} \tag{3-16}$$

Where

$$\phi(\sigma,s) = 4(\varepsilon_{mm} + J\sigma^2)s^2 + 12\varepsilon_{md}s(1-s) + 9\varepsilon_{dd}(1-s)^2 \tag{3-17}$$

Equilibrium conditions are achieved by minimising the Helmholtz free energy per site, thus

$$\frac{\partial f_c}{\partial \sigma} = 0 \tag{3-18}$$

$$\frac{\partial f_c}{\partial s} = 0 \tag{3-19}$$

3.2.2 Chemical potentials and Isotherms

The configurational chemical potential μ_c is given by

[12] Stirling's approximation (or Stirling's formula) is an approximation for large factorials. It is named after James Stirling. $\ln n! \approx n\ln n - n$

$$\mu_c = \left(\frac{\partial F_c}{\partial M}\right)_{N_s,T} = \frac{\partial f_c}{\partial \rho} \tag{3-20}$$

Solving equation (3-18) and (3-19) for s and σ, we can find out the chemical potential μ_c for a range of ρ changing from 0 to 1.

By plotting s versus ρ, Figure 3-3 shows that at low density about half the molecules are in the monomer state while molecules re-orient as density increases. Increasing pressure forces molecules to choose their monomer state.

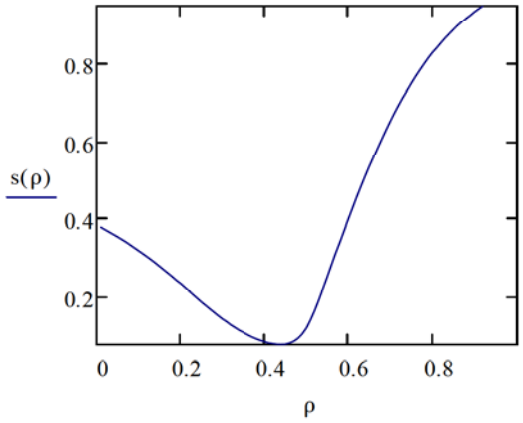

Figure 3-3 Fraction of molecules in the monomer states against the degree of orientational ordering among the monomers. T=293 K

The chemical potential in the ideal gas phase (Hill, 1960) is described by

$$\mu_g = \mu^0 + kT\ln\left(\frac{P}{P_0}\right) \tag{3-21}$$

Considering benzene in vapour phase as ideal gas, μ_0 the standard chemical potential (Atkins, 1998) is as follows

$$\mu^0 = \left[\frac{2\pi mkT}{h^2}\right]^{\frac{3}{2}} kT \tag{3-22}$$

h is the Planck's constant[13], m the molecular mass of the adsorbate and T the temperature

At equilibrium the chemical potential of the adsorbed phase μ_c and the gas phase μ_g are equal

$$\mu_g = \mu_c \tag{3-23}$$

Therefore

$$\mu_c = \mu^0 + kT\ln(\frac{P}{P_0}) \tag{3-24}$$

Now it would be possible to construct the adsorption isotherm by enabling the gas phase pressure to be determined.

3.2.3 Calculation procedure

Mathcad® is used to solve the equation (3-24) and calculation procedures are as follows:

- Define the free energy of transition $U(T)$.
- Define monomer dimer interaction energies, ε_{mm}, ε_{md}, ε_{dd}.
- Set the temperature T.
- Derive the configurational interaction energy E_c, equation (3-12).
- Express the configurational Helmholtz free energy F_c, equation (3-13).
- Express configurational free energy per site f_c, equation (3-16).
- Define the equilibrium conditions, equations (3-18) and (3-19)
- Solve the equilibrium condition equations for s and ρ.

[13] Planck's constant = 6.626068 × 10-34 m2 kg / s

- Derive the configurational chemical potential μ_c, for the adsorbed phase, equation (3-20).
- Calculate using equation (3-24).
- Plot the adsorption isotherm

3.2.4 Results and discussion

Adsorption isotherms are calculated for three different temperatures (T = 273 K, 283 K and 293 K) and plotted against experimental data available. The results are presented in Figure 3-4, Figure 3-5 and Figure 3-6. The agreement between experimental data and simulation is exceptional.

It is interesting to note that the isotherm in all cases experimental and theoretical shows a step. The cause of this is that dimer state molecules do not compress into a close packed arrangement until the chemical potential is sufficiently high.

The same effect could be seen in Figure 3-3 where the graph shows the fraction of molecules in the monomer states against the fractional filling.

To solve the equation (3-24) one needs to have the value of μ_c, the chemical potential of the adsorbed phase and this involved four unknown parameters namely the free energy of transition from a monomer to a dimer state for an isolated molecule $U(T)$, and interaction energy for a nearest neighbour pair consisting of a monomer and a dimer, two monomers and two dimers ε_{md}, ε_{mm} and ε_{dd} respectively.

The effect of the free energy of transition $U(T)$ was on the step. For higher energy of transition a wider step is observed, which means higher pressure is

required for re-orientational transitions amongst molecules in the adsorbed phase and vice versa.

The effects of the interaction energies were very different. Increasing the monomer-monomer interaction energy ε_{mm}, increases the slope of the isotherm at higher pressure and increasing the monomer-dimer interaction energy ε_{md}, decreases the slope of the isotherm at higher pressure. The effect of the dimer-dimer interaction energy ε_{dd} is rather interesting. By reducing this, the step nearly disappears and the isotherm nearly loses its step, which means the isotherm changes its category according to adsorption isotherms classification by Brunauer in Figure 2-2.

In conclusion it could be said that at lower pressures the dimer-dimer interaction energy ε_{dd}, plays a key role in the isotherm and at higher pressures it is the monomer-monomer interaction energy ε_{mm} which have the biggest effect and reflects the importance of the three different interaction energies and the free energy of the transition from a monomer state to a dimer state.

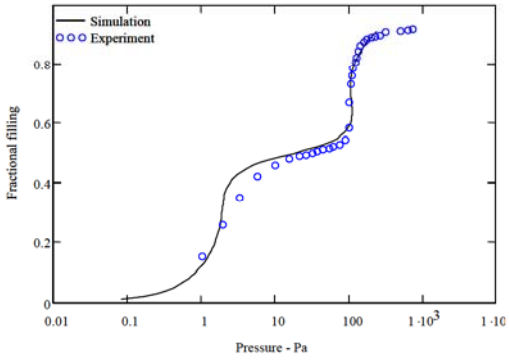

Figure 3-4 theoretical adsorption isotherm of benzene on zeolites comparing to the experimental data (Chiang et al., 1997) at T=273 K

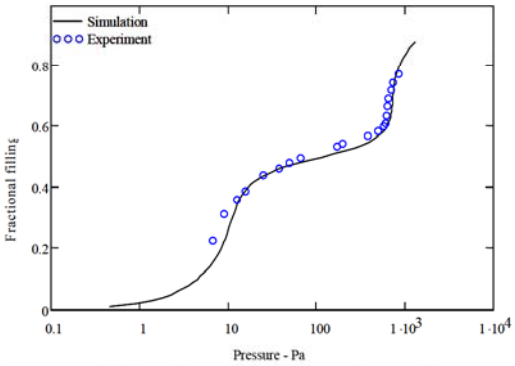

Figure 3-6 theoretical adsorption isotherm of benzene comparing to the experimental data at T=293 K

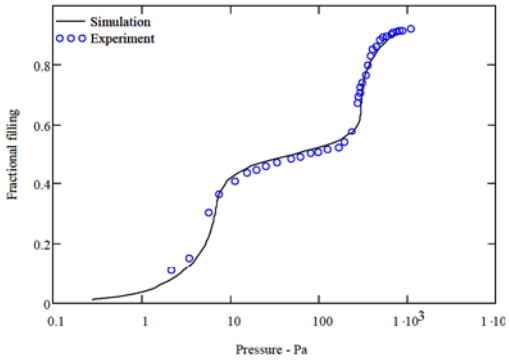

Figure 3-5 theoretical adsorption isotherm of benzene comparing to the experimental data at T=283 K

The one-dimensional model does not reproduce a double step phenomena at 303 K (see Figure 3-1) so in this section, two-dimensional statistical mechanical model of benzene adsorption in the pores of silicalite is presented which although is successful simulation but it fails to produce the double step. This model also used a dimer state to represent molecules lying flat at the wall of the pore, and a monomer state to represent molecules standing perpendicular to the pore wall and vacant sites or holes. It was treated using the Flory-Huggins approximation and over a range of interaction energies predicts steps in adsorption isotherms similar to those observed experimentally for benzene adsorption in silicalite (Chiang et al.,

1997). One-dimensional models of benzene adsorption (Du et al., 2000) have shown that the very unusual double step in the isotherm at higher temperature (303 K) is due to different adsorption energies of benzene molecules in the two different silicalite channels, straight and zigzag. Although the dimensions of the two channel systems differ only slightly, even these small differences result to significantly different values of adsorption energies as these channels are comparable to molecular scale. The additional intermediate step arises from an earlier conversion of dimers in the energetically favourable channels compared with the dimers in the second channel system where the energy penalty of conversion of dimers into monomer is higher.

3.3 Two dimensional lattice model of benzene adsorption in silicalite of inter-convertible monomer-dimer mixtures

When different adsorption energies were introduced for each pore system in the two dimensional model, it was not possible to predict the double step. Two model extensions have been considered, one with two energetically different dimer configurations in the two sets of silicalite pores, another one with two energetically different monomer configurations. However, a further improvement allows development of a double layer model reproducing the additional step.

3.3.1 Two energetically different monomers and one dimer

For a system with N_s sites, Bell and Dunne (Dunne & Bell, 1980) have shown that the canonical partition function of N_d molecules in dimer state and N_{m1}, N_{m2} molecules in the straight channels and zigzag channels respectively in monomer state is

$$\Omega = \left(\frac{2}{N_s}\right)^{N_d} \frac{N_s!}{N_{m1}!N_{m2}!N_d!N_h!} \tag{3-25}$$

where N_h is the number of the vacant sites. Using (3-25) the canonical partition function can be evaluated in a mean-field approximation (Bell et al., 1978).

Benzene molecules arranged on the lattice may have two possible ground states, which are with molecules lying down or standing up. It transpires that the steps in the isotherms are due to energetic competition between these two arrangements. Thus, we assume that the potential energy of an adsorbed monomer 1 is $-U_{01}$, while that of an adsorbed monomer 2 is $-U_{02}$, the corresponding energy of a dimer is U_d:

$$U_d = U_{01} + U_1 = U_{02} + U_2 \tag{3-26}$$

Where U_1 and U_2 are the corresponding energy penalties to convert a dimer to monomers 1 and 2 respectively.

The model assumes that although the monomer adsorption energies are different ($U_{01} \neq U_{02}$), dimers resulting through conversion from either type are

energetically the same, i.e. the penalties U_1 and U_2 are adjusted in such a way that

$$U_{01} + U_1 = U_{02} + U_2 \tag{3-27}$$

The parameter U_d includes also the cost in energy to cause a local structure or ro-vibrational energy change to enable the molecule to fit into the crystal and in this sense has some relation to the model discussed in (Jalili et al., 2003). We write the configurational Helmholtz free energy as

$$F_c = E_c - kT\ln(\Omega) - N_{m1}U_{01} - N_{m2}U_{02} - N_d U_d \tag{3-28}$$

$$F_c = E_c - kT\ln(\Omega) - N_{m1}U_{01} - N_{m2}U_{02} - (M - N_{m1} - N_{m2})U_d \tag{3-29}$$

$$\begin{aligned} F_c = E_c - kT\ln(\Omega) - N_{m1}U_{01} - N_{m2}U_{02} - \\ MU_d + N_{m1}(U_{01} + U_1) + N_{m2}(U_{02} + U_2) \end{aligned} \tag{3-30}$$

$$F_c = E_c - kT\ln(\Omega) - MU_d + N_{m1}U_1 + N_{m2}U_2 \tag{3-31}$$

where E_c is the configurational interaction energy given by

$$E_c = -\left[\begin{array}{c} 4(\varepsilon_{mm} + J)(N_{m1} + N_{m2}) + 8(\varepsilon_{mm} - J)N_{m1}N_{m2} \\ +12\varepsilon_{md}(N_{m1} + N_{m2})N_d + 9\varepsilon_{dd}N_d^2 \end{array}\right] / N_b \tag{3-32}$$

ε_{mm}, ε_{md} and ε_{dd} are the interactions between benzene molecules in monomer-monomer, monomer-dimer and dimer-dimer states respectively.

Here N_b is the total number of nearest-neighbour pairs not formed by segments of the same dimer given by

$$N_b = 2N_s - N_d \tag{3-33}$$

In the canonical ensemble the value of N_s and M are given while the value of the internal variables N_{m1}, N_{m2} and N_d are those, which minimise F_c, subject to the relation

$$N_{m1} + N_{m2} + N_d = M \tag{3-34}$$

Introducing mole fractions for monomers/dimer we have

$$\frac{M}{N_s} = \frac{N_{m1}}{N_s} + \frac{N_{m2}}{N_s} + \frac{N_d}{N_s} \Rightarrow \rho = X_{m1} + X_{m2} + X_d \tag{3-35}$$

Rearranging (3-31) using (3-34) and (3-35) and introducing order parameters

$$\begin{aligned} \sigma &= \frac{X_{m1} - X_{m2}}{X_{m1} + X_{m2}} \\ s &= \frac{X_{m1} + X_{m2}}{X_{m1} + X_{m2} + X_d} \end{aligned} \tag{3-36}$$

The configurational free energy per site f_c could be expressed a

$$\begin{aligned} f_c &= \frac{F_c}{N_s} \\ &= \frac{\rho 2\phi(\sigma, s)}{2 - \rho - \rho s} - kT\{-\rho \ln(\rho) - \rho[s\ln(s) + (1-s)\ln(1-s)] \\ &- (1 - 2\rho + \rho s)\ln(1 - 2\rho + \rho s) - \rho s\left[\left(\frac{1+\sigma}{2}\right)\ln\left(\frac{1+\sigma}{2}\right) + \left(\frac{1-\sigma}{2}\right)\ln\left(\frac{1-\sigma}{2}\right)\right] \\ &- \rho(1-s)\} - \rho U_0 - \rho s\left(\frac{1+\sigma}{2}\right)U_1 - \rho s\left(\frac{1-\sigma}{2}\right)U_2 \end{aligned} \tag{3-37}$$

where

$$\begin{aligned} \phi(\sigma, s) &= 4(\varepsilon_{mm} + J\sigma^2)s^2 + 12\varepsilon_{md}s(1-s) \\ &+ 9\varepsilon_{dd}(1-s)s^2 \end{aligned} \tag{3-38}$$

The configurational chemical potential μ_C, then is given by

$$\mu_c = \left(\frac{\partial F_c}{\partial M}\right)_{N_s,T} = \frac{\partial f_c}{\partial \rho} \tag{3-39}$$

At equilibrium the chemical potential of the adsorbed phase is equal to that of the gas phase which we assume to be ideal (Atkins, 1998) and hence in the standard way defines the external benzene vapour phase pressure

$$P = \exp((\mu_c - \mu^0)/kT) \tag{3-40}$$

3.3.2 Two energetically different dimers and one monomer

The mathematical treatment of this model is similar to the previous model. Having two different dimer molecules in this model, the potential energy of an adsorbed dimer type 1 is $-(U_0 + U_1)$ and that of the adsorbed dimer type 2, $-(U_0 + U_2)$ while that of the monomer is $-U_0$. U_1, U_2 being the energy penalties for converting dimers type 1 and 2 into monomers respectively.

The equation for the configurational Helmholtz free energy is

$$F_c = E_c - kT\ln(\Omega) - N_{d1}(U_0 + U_1) - N_{d2}(U_0 + U_2) - N_m U_0 \tag{3-41}$$

$$F_c = E_c - kT\ln(\Omega) - MU_0 - N_{d1}U_1 - N_{d2}U_2 \tag{3-42}$$

Where N_{d1}, N_{d2} are the number of molecules for dimer 1 and 2 respectively. The methodology for solving the equation system and calculate the gas phase pressure is the same as above.

3.3.3 Numerical results

Although the new model accounts explicitly for different adsorption energy levels in the silicalite structure, surprisingly it does not reproduce the additional step in the isotherm observed experimentally at 303K. For a wide

range of parameters, the model is unable to predict the additional step. The reason becomes clear when the individual mole fractions of both types of monomers are plotted (Figure 3-7). Benzene dimers prefer to convert to only one type of monomers, the one with the lower imposed penalty. The geometry of our model does not sufficiently differentiate between monomers. Since monomers are positioned in the intersections (i.e. the same dimer is able to convert to either monomer), all dimers prefer by far to convert through the easiest transformation. This causes both monomer type curves to rise at the same filling fraction resulting in a smooth overall adsorption isotherm (see Figure 3-8).

The explanation for the model 3.3.2 to predict the additional step is similar. The silicalite structure is filled only with dimers having the highest adsorption energy. The geometry of the model allows these dimers to occupy all sites. The result is a lattice full of dimers having the same orientation. No sites are free in order for any dimers to be adsorbed with different orientation (see Figure 3-9).

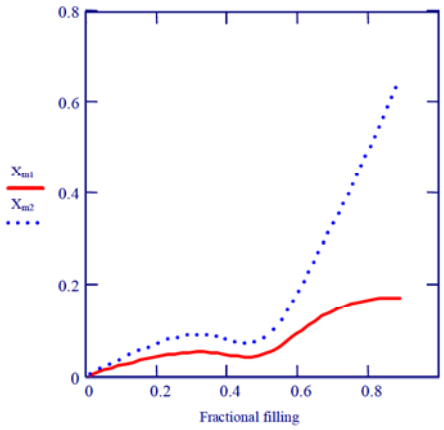

Figure 3-7 Monomers fraction adsorbed in zeolites calculated by model 2.1

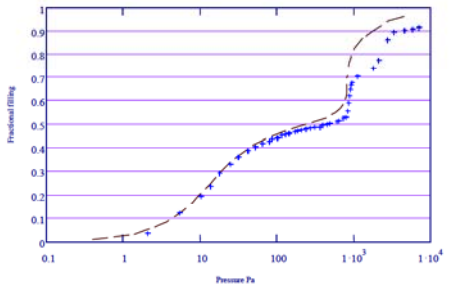

Figure 3-8 Experimental and theoretical adsorption isotherms for benzene in silicalite at T=303 K calculated by model 3.3.1

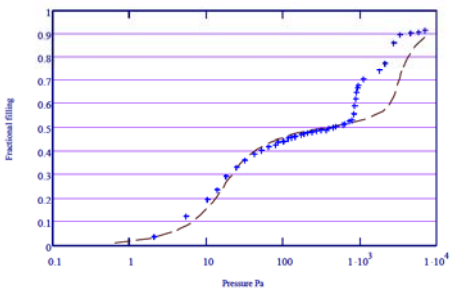

Figure 3-9 Experimental and theoretical adsorption isotherms for benzene in silicalite at T=303 K calculated by model 3.3.2

3.3.4 Average or double layer model

The double layer model actually is based on two independent two dimensional lattice fluid model of inter-convertible monomer-dimer mixtures each on different pore system; one based on the straight channels and the second one on the zigzag silicalite channels. The model uses different adsorption energies for monomer benzene molecules in the different pore systems of silicalite namely straight and zigzag channels. The overall fractional filling is calculated as the average of the fillings resulted by each set of pores.

Dimers in each lattice, i.e. each pore system, straight or zigzag, convert into monomers at a different filling, i.e. pressure, as the energies needed to convert them are different. This results into the intermediate step in the isotherm (see Figure 3-10).

In conclusion, the inherent difficulty of two-dimensional models to predict the extra isotherm step lies with the lattice geometry. It does not differentiate sufficiently between two types of dimers or monomers leading in preferential full adsorption of only one type. The double layer model of two different energetically but independent lattice overcomes this problem.

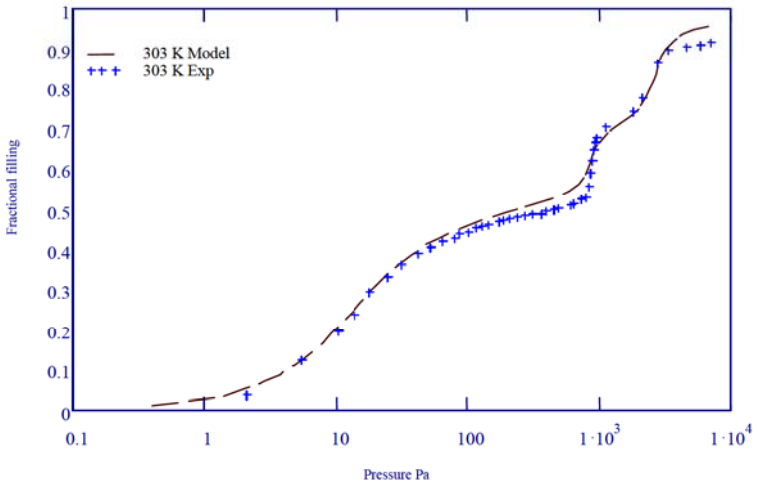

Figure 3-10 Experimental and theoretical adsorption isotherms for benzene in silicalite at T=303 K calculated by model 3.3.4

3.4 Matrix model - One dimensional lattice model of benzene in silicalite

To account for the two-dimensional character of the silicalite structure, we introduce a modified one-dimensional lattice model that possesses the characteristic features of distinct adsorption sites in each channel system.

The basis of this lattice can be symbolised by,  where the vertical line represents two sites in the straight silicalite pores positioned just at the intersection and the horizontal line represents adsorption sites in the zigzag pores. This basis with four adsorption sites corresponds to one-half of the adsorption sites per unit cell of silicalite.

Figure 3-11 positions the adsorption sites in the silicalite structure, where the plausibility of the suggested lattice model can be justified. Since the distance between inter-sections along the straight pores is considerably shorter than the equivalent distance along the zigzag channels, the position

of sites in straight pores is nearer to the intersection than the equivalent position of sites in the zigzag pores.

To model orientational and positional transitions benzene molecules are assumed to adopt the various configurations shown in Figure 3-12.

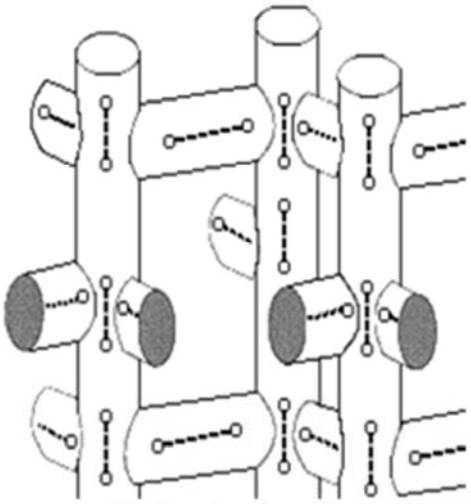

Figure 3-11 Pore structure of silicalite showing the various considered positions for adsorbed benzene molecules in extended configurations.

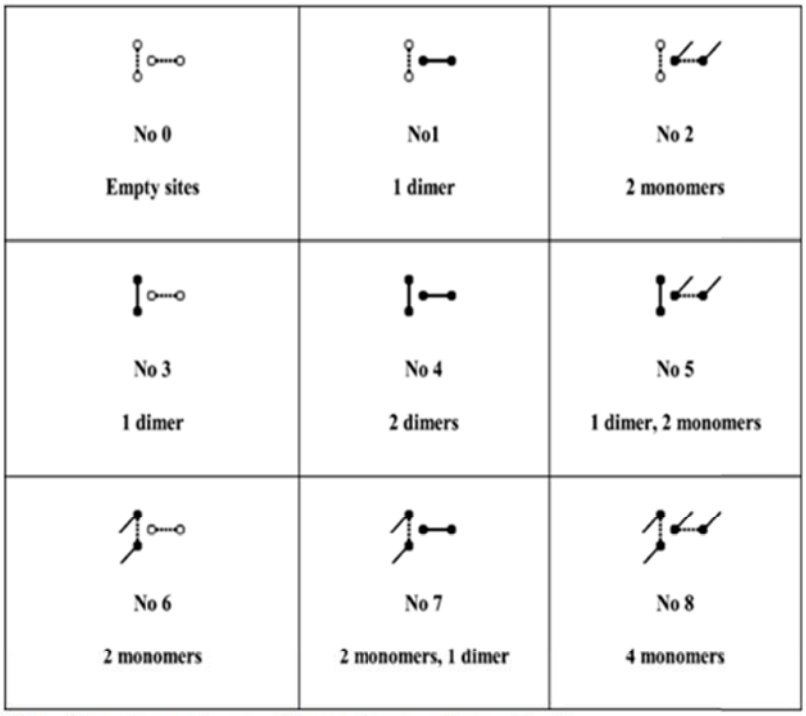

Figure 3-12 Possible adsorption configuration on the unit cell.

3.4.1 Matrix method for grand partition function

An ideal benzene vapour phase at ambient pressure and temperature P, T in equilibrium with an adsorbed phase of molecules in zeolites pores is considered. Matrix method for one-dimensional lattice fluid problem have been discussed by Dunne and Manos (Dunne & Manos, 2004) previously. Here a chain of N groups of four sites (see Figure 3-12), each pair of neighbouring groups of n sites being separated by a spacing, which is a constant independent of pressure and temperature, is considered. Each group is either vacant or occupied by a cluster of molecules. M is the total number of adsorbed molecules. The internal degrees of freedom of a benzene molecule contribute a factor q_{int} to the partition function, which is assumed independent of whether the molecule is in the vapour or adsorbed in the Zeolites pore. Accordingly, for each molecule there is a factor q_{int} in the total partition function, which can be omitted without any effect on the equilibrium distribution of the molecules or on the adsorption isotherms.

The grand partition function Ξ for the adsorbed phase is given by

$$\Xi = \sum_{M=0}^{\infty} \exp\left[\frac{\mu M}{kT}\right] Q(M, nN, T) \tag{3-43}$$

Where μ is the chemical potential, $Q(M,nN,T)$ is the canonical partition function for M interacting molecules absorbed over nN sites in Zeolites channel and k is Boltzmann's constant. In this model $n=4$. It is assumed that occupation of sites by pairs of molecules is energetically forbidden so that we have

$$\Xi = \sum_{M=0}^{nN} \exp\left[\frac{\mu M}{kT}\right] Q(M, nN, T) \tag{3-44}$$

There are now at most nN species on the lattice. It is assumed cyclic boundary condition and consider the possible configurations of clusters $0,1,2,...,8$ on a chain of N cells. By inspection, it can be seen that Ξ may be written as the sum of the products of N factors given by

$$\Xi = \sum_{(\alpha=0,1,...,8)} \sum_{(\beta=0,1,...,8)} \cdots \sum_{(\omega=0,1,...,8)} A_{\alpha\beta} A_{\beta\gamma} A_{\gamma\delta} \ldots A_{\omega\alpha} \tag{3-45}$$

The factor above are given by

$$A_{\mu\upsilon} = (\phi_\mu \phi_\upsilon)^2 \phi_{\mu\upsilon} \tag{3-46}$$

$$\phi_0 = 1 \tag{3-47}$$

$$\phi_i = \exp\left[\frac{\upsilon_i(\mu - \lambda\rho^2) - B_i}{kT}\right] \tag{3-48}$$

$$\phi_{\mu\upsilon} = \exp\left[\frac{-J_{\mu\upsilon}}{kT}\right] \tag{3-49}$$

Where υ_i is the number of molecules in clusters i, B_i is the energy of the cluster i, which includes the internal interactions, and adsorption energy. $J_{\mu\upsilon}$ is the interaction energy between clusters μ and υ. The term $\lambda\rho^2$ attempts to account for long-range interaction between molecules distant clusters ($\lambda = 0.27kT$) and is added in a similar way to that routinely used in Monte-Carlo simulations of adsorption (Catlow, 1992b;Frenkel & Smit, 2002;Nicholson & Parsonage, 1982b). To implement this, a good

approximation that ρ is proportional to the logarithm of the pressure is used.

Using the inner product rule

$$D_{ij} = \sum_{k} B_{ik} C_{kj} \tag{3-50}$$

For matrix multiplication of a pair of matrices **B** and **C** the Grand Partition function can be expresses as

$$\begin{aligned} \Xi &= \sum_{(\alpha=0,1,2,\ldots,8)} (A^N)_{\alpha\alpha} = Trace(A^N) \\ &= (\lambda_1)^N + (\lambda_2)^N + \ldots + (\lambda_9)^N \end{aligned} \tag{3-51}$$

Where $\lambda_1, \lambda_2, \ldots, \lambda_9$ are the eigenvalues of the matrix **A**.

For macroscopically large N we then obtain

$$\Xi = \left(\lambda_{\max}\right)^N \tag{3-52}$$

Where $\lambda_{\max}$ is the largest eigenvalue of the above matrix, which can be obtained numerically and analytically. It was observed numerically that even with weak inter-cluster interactions one of the eigenvalues is an order of magnitude larger than any other and whose logarithm of the trace of matrix. The validity of this was checked and isotherms calculated by this procedure for weak interactions were found to be practically indistinguishable to those obtained by numerical differentiation of the maximum eigenvalue. Some insight into the dominant eigenvalue can be obtained as follows for the case when interactions between groups are zero. Using the notation $\chi_\mu = \phi_\mu^{1/2}$ the secular equation for the matrix **A** above for the case when inter-group

interactions are zero is obtained by equating the determinant of the matrix to zero.

The characteristic polynomial is very simple and is given by

$$-\lambda^9+[(\chi_0)^2+(\chi_1)^2+(\chi_2)^2+(\chi_3)^2+(\chi_4)^2 \\ +(\chi_5)^2+(\chi_6)^2+(\chi_7)^2+(\chi_8)^2]\lambda^8 \tag{3-53}$$

The roots λ_i of the characteristic polynomial are

$$(\chi_0)^2+(\chi_1)^2+(\chi_2)^2+(\chi_3)^2+(\chi_4)^2 \\ +(\chi_5)^2+(\chi_6)^2+(\chi_7)^2+(\chi_8)^2 \tag{3-54}$$

And 0 which is eightfold degenerate. The non-zero root is dominant and splits off from the eightfold degenerate 0 manifold. Then in such a case, only one of the eigenvalues is finite and hence we have an exact evaluation of the Grand Partition function for the case defined above. This is also a good approximation for weak inter-group interactions where some of the elements of the set $\{J_{\mu\nu}\}$ are finite.

The mean number of adsorbed molecules ρ for zero inter-cluster interactions is then given by the relation

$$\rho=\frac{kT}{n}\frac{\partial}{\partial\mu}\ln\left(\sum_{i=0}^{8}\phi_i\right) \tag{3-55}$$

Giving

$$\rho=\frac{1}{n}\frac{\sum_{i=0}^{8}i\phi_i}{\sum_{i=0}^{8}\phi_i} \tag{3-56}$$

Even with weak interactions, we obtain virtually exact adsorption isotherms from straightforward evaluation of

$$\rho = \frac{kT}{n}\frac{\partial}{\partial \mu}\ln\left(\sum_{i=0}^{8} A_{ii}\right) \tag{3-57}$$

The chemical potential of a component in an ideal gas is given by equation (3-21).

Changes in ro-vibrational free energies for adsorption into the Zeolites are implicitly accounted for in the B_i parameters, so the chemical potential only includes the translational component of the reference chemical potential.

3.4.2 Numerical results and discussion

Adsorption isotherms were calculated for a wide range of interaction parameters. Overall, the shape of the adsorption isotherms, which are shown in Figure 3-13, calculated by the matrix method are very similar to those obtained experimentally, Figure 3-1. The steps in the theoretical isotherms are not due to a phase transition in the absorbed system but simply arise from co-operative re-orientational and positional transitions. When the chemical potential is sufficiently high, dimer state molecules compress into a close packed arrangement of monomers. Firstly, the adsorption of benzene molecules give rise to configurations 1, 3 and 4 containing dimerically adsorbed molecules. As the adsorption energy of dimerically adsorbed benzene molecules is the same in all above configurations, a gradual increase is observed in the isotherm to a plateau at fractional coverage 50% that corresponds to all sites being occupied by

dimers. Further pressure increase results in dimer molecules standing up and freeing sites that can be occupied by additionally adsorbed benzene molecules in the monomer configuration. This results in a step in the isotherm.

The model uses different adsorption energies for benzene molecules in the different pore systems of silicalite. When the temperature is sufficiently high this differentiation results in the process of converting dimer into monomers preferentially occurring in one set of pores, the ones with the lower energy penalty standing up first. This shows as an additional intermediate step in the isotherm at fractional coverage of 75%.

The presence of such an intermediate step depends critically on the relative magnitude of parameters $B_7/3$ and $B_8/4$ which are the adsorption free energies per molecule for cluster 7 and 8.

With increasing temperature, lattice vibrational mode amplitudes increase and confined molecules may be expected to lose free energy such that $B_7/3$ and $B_8/4$ may cross over in magnitude with rising temperature. Configuration 8, with 4 tightly packed molecules per cluster is expected to loose configurational freedom with rising temperature more readily than those in configuration 7 with three molecules per cluster. This re-ordering may then give rise to the novel temperature dependence of the isotherm steps shown in Figure 3-1 and Figure 3-13. More specifically $B_7/3 = -8.1\times10^{-20} J$ over the entire temperature while $B_8/4$ changes from -8.325×10^{-20} to $-6.75\times10^{-20} J$ over the temperature range $273-303\,K$. Crudely

speaking the four molecules in configuration 8 are more readily squeezed together by the increasing amplitude of the zeolite wall vibrational modes with rising temperature than the three molecules of configuration 7. This increase in amplitude follows from the equipartition theorem (Atkins, 1998;Hill, 1960;Huang, 1988) An alternative explanation might be found in a loss of configurational entropy with rising temperature for configuration 8 along the lines suggested some time ago by Cracknell and Nicholson (Cracknell & Nicholson, 1994).

In summary, this model reproduces the experimentally found steps in benzene isotherms on silicalite and satisfactory reproduces also the essential features of the very unusual temperature dependence of the isotherms, namely this double step at higher temperatures.

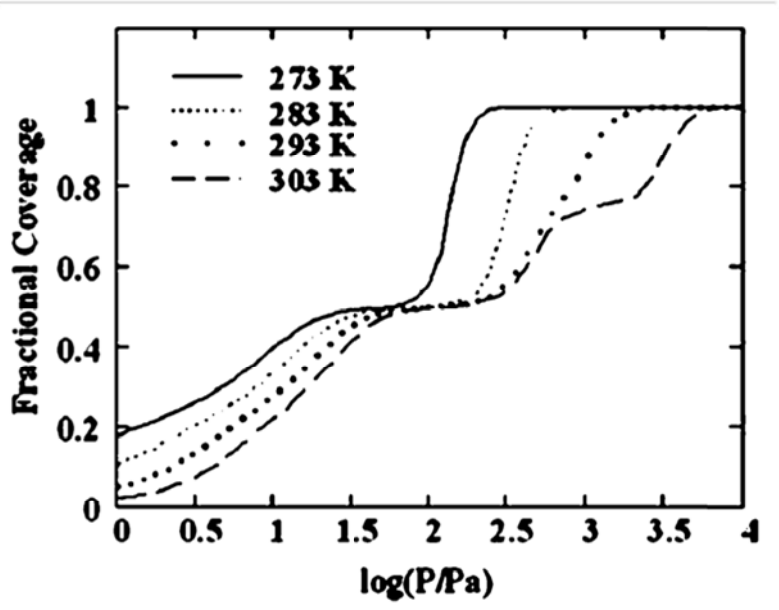

Figure 3-13 Adsorption isotherm calculated for a wide range of interaction parameters using the Matrix model. ($J_{11}=-0.1\times10^{-20}$ J, $J_{22}=-0.2\times10^{-20}$ J, $J_{33}=-0.8\times10^{-20}$ J, $J_{44}=-0.2\times10^{-20}$ J, $J_{55}=-0.3\times10^{-20}$ J, $J_{66}=-1.1\times10^{-20}$ J, $J_{77}=-0.8\times10^{-20}$ J, $J_{88}=-1.1\times10^{-20}$ J, $J_{99}=-0.1\times10^{-20}$ J **and all other interactions equal to zero.)**

4- MONTE CARLO SIMULATION OF HYDROCARBON AND CO_2 ADSORPTION IN ZEOLITE

4.1 Simulation models

4.1.1 Interaction potential between alkane and alkane

In the simulations, the alkane atom groups, such as CH_4, $-CH_3$ and $-CH_2$ are considered as a single interaction centre, known as united atom model (Ryckaert & Bellemans, 1978). The interactions between these united atoms are described with Lennard-Jones potential (briefly discussed in section2.2.1)

$$U(r_{ij}) = \begin{cases} 4\varepsilon_{ij}\left[\left(\frac{\sigma_{ij}}{r_{ij}}\right)^{12} - \left(\frac{\sigma_{ij}}{r_{ij}}\right)^{6}\right] & r_{ij} \le r_c \\ 0 & r_{ij} > r_c \end{cases} \quad (4\text{-}1)$$

Where r_{ij} is the distance between united atom i and j. ε_{ij} and σ_{ij} are the energy and size parameters of the Lennard-Jones potential, respectively. r_c is the cut-off radius of the potential. In this study the cut-off radius of the potential is equal to 13.8 Å and usual tail correction are applied (Allen &

Tildesley, 1987). The average potential energy in three-dimensional of any given atom i can be presented by

$$U_i = \frac{1}{2}\int_0^\infty 4\pi r^2 \rho(r) U(r) dr \tag{4-2}$$

Where $\rho(r)$ denotes the average number density at a distance r from a given atom i. The factor of $\frac{1}{2}$ is for correcting the double counting of intermolecular interactions. Hence the tail contribution (Frenkel & Smit, 2002) is then

$$U^{tail} = \frac{1}{2}\int_{R_c}^\infty 4\pi r^2 \rho(r) U(r) dr \tag{4-3}$$

For the Lennard-Jones potential this tail correction can be expressed as

$$\begin{aligned} U^{tail} &= \frac{1}{2} 4\pi \int_{R_c}^\infty r^2 \rho(r) U(r) dr \\ &= \frac{8}{3}\pi\rho\varepsilon_{ij}\left[\frac{1}{3}\left(\frac{\sigma_{ij}}{r_c}\right)^9 - \left(\frac{\sigma_{ij}}{r_c}\right)^3\right] \end{aligned} \tag{4-4}$$

Jorgensen geometric mixing rules (see section 2.2.1) are used to determine the interaction parameters, ε_{ij} and σ_{ij}, between different united atoms i and j.

The intramolecular interactions between three successive united atoms of the same molecule are determined by a harmonic potential (Vanderploeg & Berendsen, 1982), known as a bond bending potential given by

$$U^{bend}(\theta) = \frac{1}{2} k_\theta (\theta - \theta_0)^2 \tag{4-5}$$

Where $U^{bend}(\theta)$ is the bond bending energy. k_θ is the force constant, which is equal to 62500 $krad^{-2}$. θ is the bond bending angle. θ_0 is the equilibrium angle and is equal to 113.0^o. The intramolecular interactions between four successive united atoms of the same molecule are modelled by dihedral potential(Wang *et al.*, 1993b), which is abond torsion potential by

$$U^{tors}(\varphi) = C_0 + C_1\cos(\varphi) + C_2\cos^2(\varphi) + C_3\cos^3(\varphi) \quad (4\text{-}6)$$

Where $U^{tors}(\varphi)$ is the bond torsion energy, φ is the bond torsion angle, where for straight chain alkanes $C_0/k_B = 1009.728K$, $C_1/k_B = 2018.446K$, $C_2/k_B = 136.341K$, $C_3/k_B = -3164.52K$. k_B is the Boltzmann's constant.

4.1.2 Interaction potential for adsorbate-zeolites and adsorbate-adsorbate

Following the work of Bezus and his colleagues (Bezus et al., 1978), the zeolites crystal is assumed to be a rigid lattice. In principle, simulation should be performed in a vibrating lattice. Indeed, it is important to take lattice vibrations into account for dynamical properties. For example, for diffusion the vibrating lattice may reduce barriers. However, in this work, only static properties are of interest and therefore the vibrations of the lattice do not make a great contribution to the ensemble average of equilibrium properties. The consideration of zeolites as a rigid structure is reasonable.

It assumes that dispersive forces dominate interactions between the alkane and zeolites molecules. It is described by Lennard-Jones potential (as shown in equation (2-3). The usual tail correction to the total energy is used for the contributions of the atom beyond the cut-off distance. Since the size and

polarisability of the silicon atoms in SiO_4 are much smaller than those of the oxygen atoms, it is assumed that silicon is effectively screened by oxygen and any short-range interaction between an adsorbate and silicon is negligible. The details of parameters for the various interactions are listed in Table 4-1. The interaction parameters of methane-methane are taken from the work of Verlet and Weis (Verlet & Weis, 1972). Other alkane interaction parameters come from the work of Siepmann and his colleagues (Siepmann et al., 1997). To determine the interaction parameters of alkane-zeolite, fitting the parameters with experimental data (Shen & Rees, 1991;Smit, 1995b) have been undertaken. In this fit, equal Lennard-Jones size parameters for all alkane-zeolite interaction have been used, so that all the alkane-zeolite interactions can be calculated using only one grid, which can save computer memory during the simulation especially for mixture simulations. The parameters for carbon dioxide used in this work are also determined through fitting to experimental data (Babarao *et al.*, 2006b;Garcia-Perez *et al.*, 2007) and will later be presented in Table 4-2 (Page 129).

Table 4-1 Lennard-Jones energy and size parameters

	ε / k_B [K]	σ [Å]
$CH_4 - CH_4$	148.0	3.73
$CH_3 - CH_3$	98.1	3.77
$CH_2 - CH_2$	47.0	3.93
$CH_4 - O$	96.5	3.6
$CH_3 - O$	80.0	3.6
$CH_2 - O$	58.0	3.6

4.2 Technical details of the simulation

4.2.1 Initialisation

To start the simulation all particles in the system should be assigned initial positions. Since the equilibrium properties of the system do not (or at least, should not) depend on the choice of initial conditions, theoretically, all reasonable initial configurations are in principle acceptable. It is reasonable that the particles should not be positioned at points that result in an appreciable overlap of the atomic or molecular cores. This can be achieved by initially placing the particles on a cubic lattice. Generally, almost any lattice is suitable, but the face-centred cubic structure with $4M^3$ (M=2, 3, 4.....) lattice points is the initial configuration which is used most frequently for simulation studies. In this work, the crystal structure of silicalite, which is a primitive cubic structure, was taken at the beginning of the simulation. The consequent simulations started from the end configuration of the previous simulation.

4.2.2 Periodic boundary conditions and minimum image convention

In the simulations carried out in this work the periodic boundary conditions (Allen & Tildesley, 1987) are used in the x, y, and z directions respectively. The reason is that most of computer simulation systems contain a few hundred to a few thousand particles. A large proportion of the molecules will lie in the system boundaries. In these systems the effect of the boundary conditions on the properties of the system cannot be ignored. In a three-dimensional N-particle system with free boundaries, the fraction of all molecules that is at the surface is proportional to $N^{-1/3}$. For example, in a simple cubic crystal of 1000 atoms, some 49% of all atoms are at the surface, and for 10^6 atoms this fraction has decreased to only 6% (Frenkel & Smit, 2002). This problem of molecules on the surface experience different forces to the ones in the bulk can be overcome by using periodical boundary condition. The volume containing the N particles is treated as the primitive cell of an infinite periodic lattice of identical cells. Any particle can interact with all other particles in this finite periodic system. The main idea of the periodical boundary condition technique is to replicate the cubic boxes surrounding the original box to form an infinite lattice. During the simulations, as the molecule moves in the original box, its periodic image in each of the neighbouring boxes moves in exactly the same way. Therefore, as a molecule leaves the central box, one of its images will enter through the opposite face. There are no walls at the boundary of the central box and no surface molecules. A two-dimensional periodic system is shown in Figure 4-1.

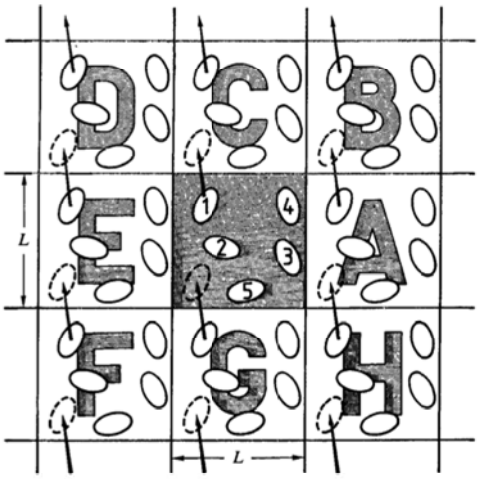

Figure 4-1 A two dimensional periodic system. Molecules can enter and leave each box across of four edges (Allen & Tildesley, 1987).

The most demanding task in the Monte Carlo simulations is to calculate the potential energy of a particular configuration since it takes into account all the interactions between molecules and other molecules in the simulation box and also include interactions between molecules and images. The number of calculations is impossible in practice; hence for a short range potential energy an approximation is made to limit the calculation, it is known as the 'minimum image convention'. Short range interactions in this case means that the total potential energy of a particle is dominated by interactions with neighbouring particles that are closer than some cut-off distance. However, for a system with large number of molecules, the calculation is still large. A further approximation is used to improve the simulation. That is to use a spherical cut-off distance. This means that the pair potential is equal to zero for $r \geq r_c$. The error that results when the interactions at larger distance are ignored can be made arbitrary small by choosing r_c sufficiently large. When periodic boundary conditions are used

the cut-off radius must be less than $L/2$ (half the diameter of the periodic box) for consistency in the minimum image convention.

4.2.3 Computer code for simulation

The program originally comes from a program called FLEXNEWN, which was written by Siepmann in FORTRAN 77 in 1991. The program is then developed to simulate flexible chain molecules and has been rewritten in FORTRAN 95. The program has been tested on different machines with F95 compiler and Intel Pentium 4 with windows XP with Compaq FORTRAN 95 compiler. The core task of the program is to calculate the potential energy of a particular configuration. The following are the main components of the program:

1. Random number generator and testing.
2. Input the data needed in the simulation, such as temperature, pressure, compositions and the Lennard-Jones parameters to describe the interactions between the molecules, etc.
3. Create a tabulated potential of the zeolite
4. Initialization of the simulation system.

5. Trial move performance[14]
   - Displacement
   - Rotation
   - Insertion
   - Remove
   - Regrow
   - Partial regrow
6. Calculation of potential energy between adsorbate and adsorbate.
7. Calculation of potential energy between adsorbate and adsorbent.
8. Configurational Bias Monte Carlo for the chain molecules insertion.
9. Calculate bond bending and torsion energy.

[14] Attempt to displace a particle

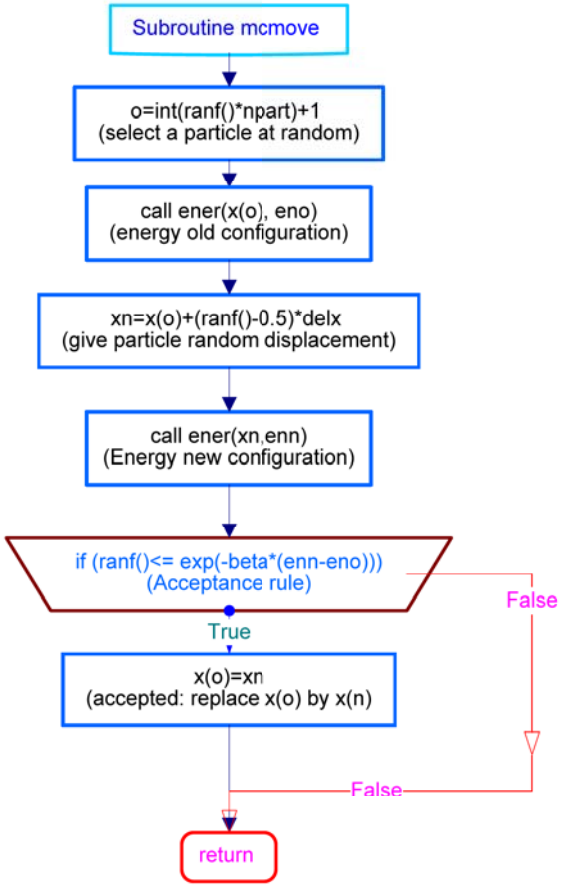

10. Application of periodic boundary conditions and minimum image convention.
11. Calculation of tail correction.
12. Calculation of the total energy of initial and final configuration.
13. Output.

4.2.4 Simulation procedure

Before running an adsorption simulation the total pressure of the gas or gas mixture, composition (introduced as partial pressure through Dalton's law), and temperature have to be specified. The number of Monte Carlo cycles used in a total simulation is up to 1×10^6 cycles. The number of trial moves in a cycle is equal to the number of molecules in the simulation box.

All simulations for pure, binary, and ternary mixtures of methane, ethane, and carbon dioxide are carried out at various temperatures ranging from 250K to 353K and pressures as low as 0.5 kPa and up to 200,000 kPa. The Grand Canonical Monte Carlo and the Configurational Bias Monte Carlo techniques are used in these simulations to obtain the adsorption isotherms. To speed up the simulations, a developed Dual cut-off Configurational Bias Monte Carlo has been used. In this scheme, a second interaction cut-off radius is used to bias the selection of a trial segment. In this method the trial moves can be significantly speeded up (Vlugt et al., 1998).

A flow chart representing the basic procedure of Monte Carlo algorithm followed for simulating adsorption isotherms is shown in Figure 4-2.

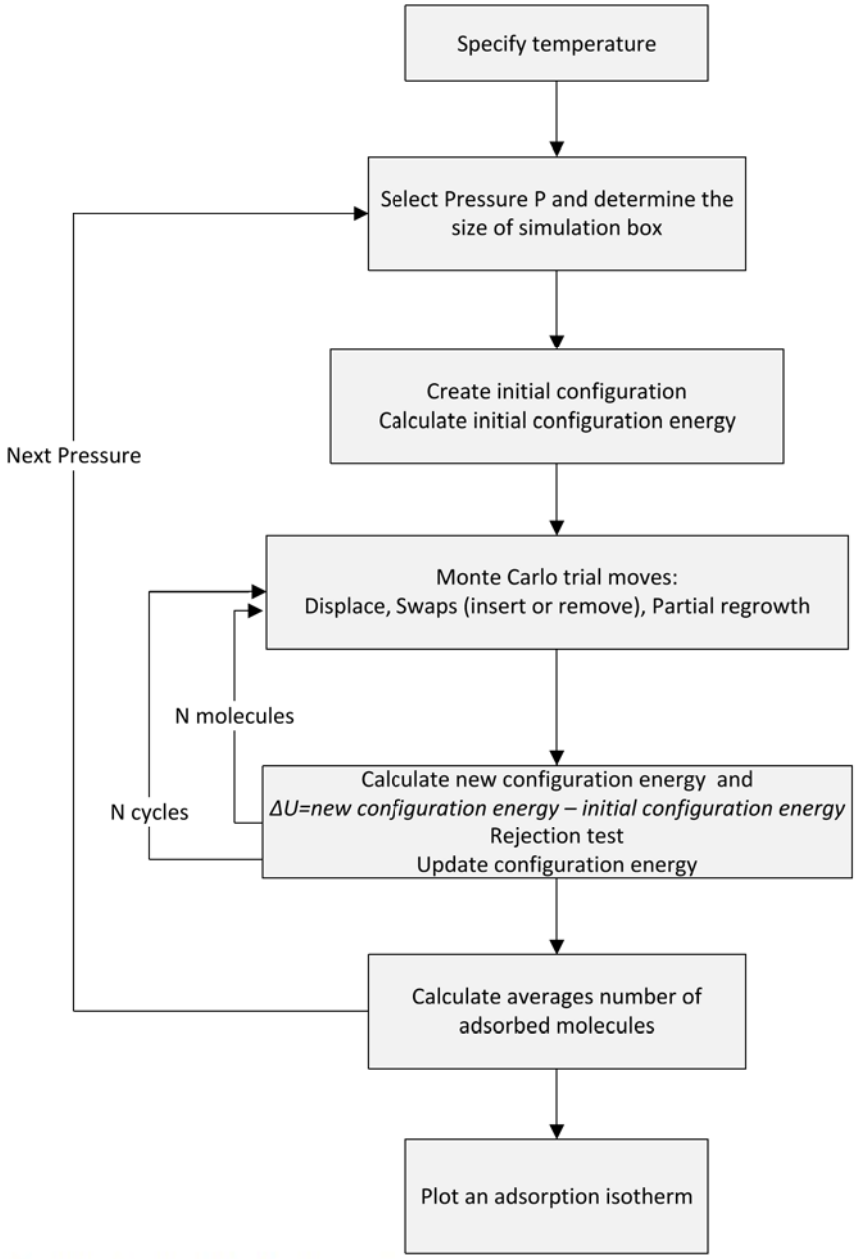

Figure 4-2 Flow chart of the basic procedure of Monte Carlo algorithm for simulating adsorption isotherms.

4.3 Results and discussion

The main aim of this study to simulate and investigate the adsorption of short alkane mixtures namely methane and ethane as well as carbon dioxide in silicalite. An attempt has also been made to simulate the adsorption of normal butane, iso butane and propane mixtures in silicalite at various temperatures.

Short alkane adsorption has already been studied (Du *et al.*, 1998;Dunne *et al.*, 1996a;Golden & Sircar, 1994b;Sun *et al.*, 1998e) but for testing our Monte Carlo programme, simulations were carried out on pure components against experimental data. The Lennard-Jones potential parameters values also needed to be justified by the agreement and close matching with the experimental data. The adsorption isotherms for pure carbon dioxide, methane, and ethane were obtained for various temperatures ranging from 277 K to 353 K and over a wide range of pressures. The result for pure methane and ethane simulations are presented in appendix A.

4.3.1 Lennard-Jones potential parameters for carbon dioxide

Before running a simulation one needs effective Lennard-Jones potential parameters (σ and ε) to be used in the Lennard-Jones potential model which describes the interactions of molecules. Different values have been used for carbon dioxide; some studies have modelled carbon dioxide molecule as a quadrupole triatomic molecule with three charged Lennard-Jones centres (Babarao *et al.*, 2006a;Nicholson & Gubbins, 1996), whereas in this work the united atom model was used to describe the carbon dioxide molecule. The challenging task in this study is to determine suitable Lennard-Jones parameters for carbon dioxide that fits the experimental data.

Many simulations were carried out in this work with different LJ parameters to observe the effect of changing each parameter on the adsorption isotherm trend in comparison with the experimental data. The sensitivity analysis was made for four sets of parameters; $\sigma_{CO_2-CO_2}$, $\varepsilon_{CO_2-CO_2}$, σ_{CO_2-O}, and

ε_{CO_2-O}, which are the size (σ) and energy (ε) parameters for the interactions of carbon dioxide-carbon dioxide and carbon dioxide-silicalite respectively.

In Figure 4-3 the parameter $\sigma_{CO_2-CO_2}$ (size parameter also known as collision diameter) was changed for different simulations, while the rest of the interaction parameters were kept constant. The Figure illustrates that the $\sigma_{CO_2-CO_2}$ has an effect on the upper region (right hand side of the graph) of the adsorption isotherm trend i.e. on the higher pressure region, while it has almost no effect on the lower pressure region (left hand side) as all simulation points match closely with each other at lower pressures. In addition, it is noted that as the value of $\sigma_{CO_2-CO_2}$ is decreased, the simulation results for the higher pressure region matches more closely to the experimental data.

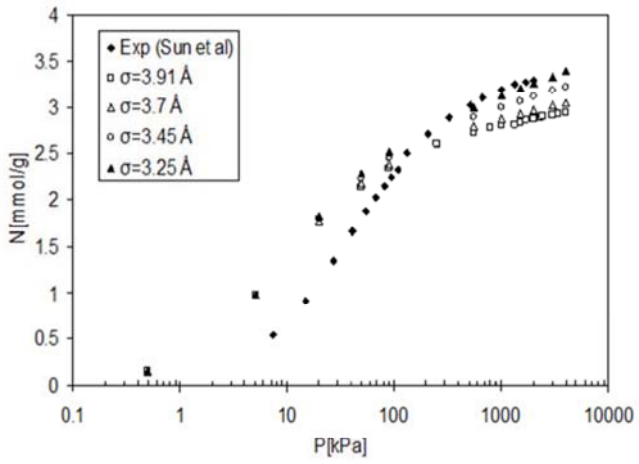

Figure 4-3 Effect of changing Lennard-Jones size parameter for the interaction of carbon dioxide-carbon dioxide $\sigma_{CO_2-CO_2}$ at 277 K in comparison with experimental data (Sun *et al.*, 1998f).

In Figure 4-4, the parameter ε_{CO_2-O} (energy parameter also known as the depth of the potential well) was changed and the other parameters were

kept constant. The graph demonstrates that the parameter has more effect on the lower pressure region. Also as the value of ε_{CO_2-O} is decreased, the simulation results for the lower pressure region match more closely to the experimental data.

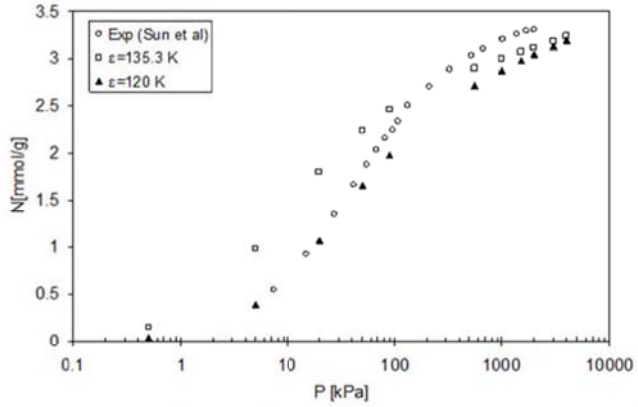

Figure 4-4 Effect of changing Lennard-Jones energy parameter for the interaction of carbon dioxide-silicalite ε_{CO_2-O} at 277 K in comparison with experimental data (Sun *et al.*, 1998g).

The effect of the other two parameters σ_{CO_2-O} and $\varepsilon_{CO_2-CO_2}$ have been found to have insignificant contribution for fitting the simulation results with the experimental data.

Table 4-2 shows Lennard-Jones potential parameters, which would fit the experimental results for carbon dioxide:

Table 4-2 Lennard-Jones parameters

	ε / k_B [K]	σ [Å]
$CO_2 - CO_2$	125.32	3.035
$CO_2 - O$	120.00	3.600

These values have been used in the Lennard-Jones potential to describe carbon dioxide interactions in the simulations in order to obtain the adsorption isotherms.

4.3.2 Adsorption isotherms of pure carbon dioxide

The adsorption isotherms for carbon dioxide in silicalite at various temperatures and over a wide range of pressures in comparison with the experimental data (Dunne *et al.*, 1996b;Golden & Sircar, 1994a;Sun *et al.*, 1998a) is shown in Figure 4-5.

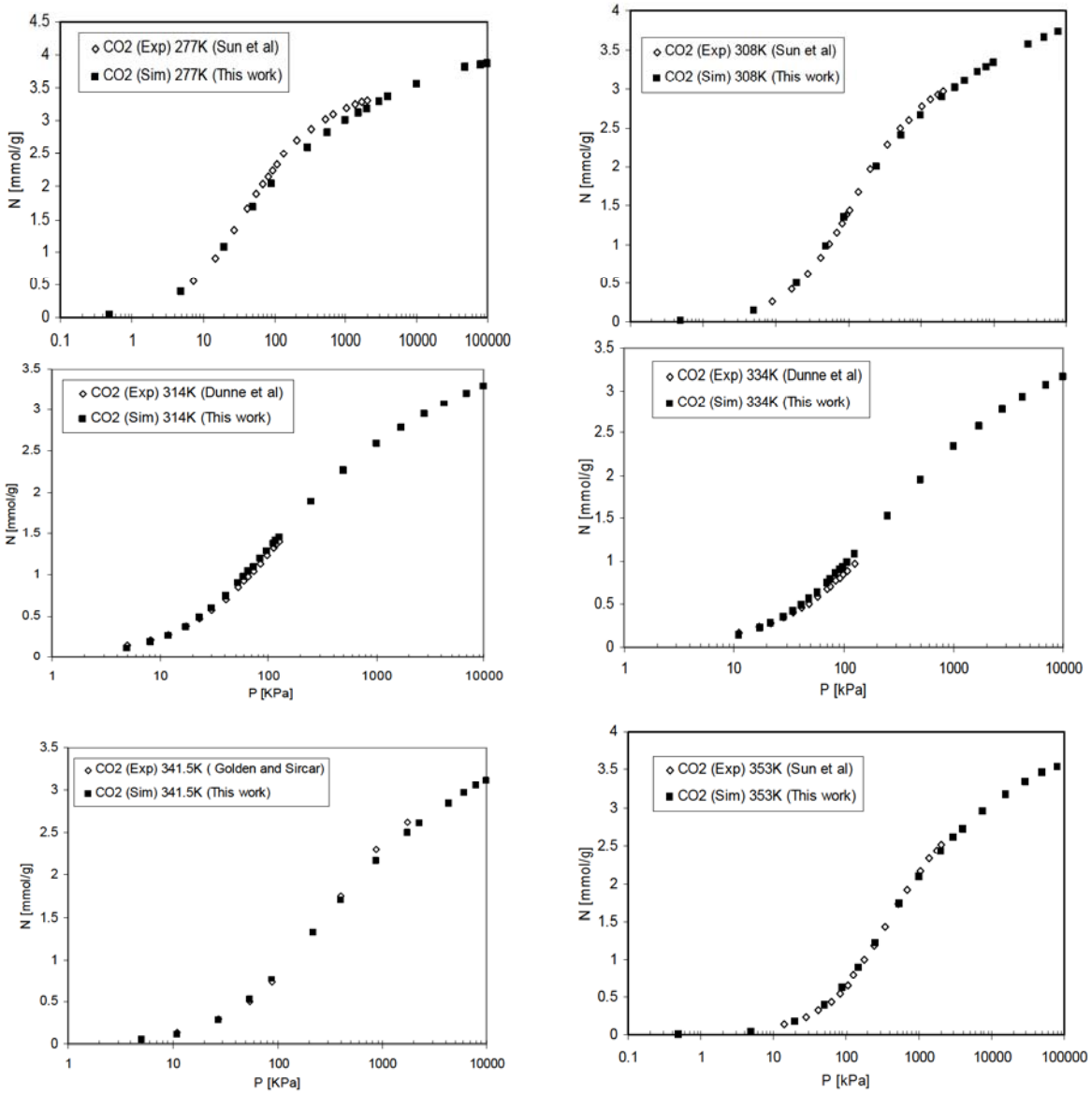

Figure 4-5 Computed simulations (Sim) and experimental (Exp) adsorption isotherms of pure carbon dioxide in silicalite at various temperatures.

The simulations were carried out for the following temperatures 277 K, 308 K, 314 K, 334 K, 341.5 K, and 353 K.

All the simulated isotherms show excellent agreement with the corresponding experiments which confirms that the determined Lennard-Jones potential parameters were accurate, reliable and mimic the real behaviour of carbon dioxide molecules.

4.3.3 Results of binary mixtures

Monte Carlo simulation was carried out for binary mixtures; carbon dioxide-methane, carbon dioxide-ethane, and methane-ethane. The carbon dioxide-methane mixture has been further studied by varying the gas phase compositions of the components. The simulations were carried for various temperatures ranging from 250 K to 353 K and over a wide range of pressures up to 200,000 kPa.

Carbon dioxide-methane mixtures

The adsorption isotherms for the carbon dioxide-methane mixture were calculated for the following compositions in the gas phase; 50% carbon dioxide-50% methane, 10% carbon dioxide-90% methane, and 80% carbon dioxide-20% methane.

Figure 4-6 shows the adsorption isotherms of equimolar (50% each) binary mixtures of carbon dioxide-methane as a function of total bulk pressure at various temperatures. At all temperatures carbon dioxide is more preferentially adsorbed than methane as expected because of the stronger interaction between carbon dioxide and the surface of the zeolite. Also as the temperature increases methane becomes less adsorbed and at the temperature of 353 K very small amounts of methane are adsorbed. This

shows that the use of adsorption on silicalite as means of separation of carbon dioxide-methane mixtures is an excellent method.

Figure 4-7 shows the adsorption isotherms of mixtures of 10% carbon dioxide-90% methane. At low temperature (253 K) despite the predominant presence of methane in the gas phase the two components are almost quantitatively equally adsorbed up to a pressure of 300 kPa. Above this pressure carbon dioxide starts to be more adsorbed and replaces methane in the pores of silicalite. As the temperatures (277 K, 300 K, 333 K) increase, methane is initially more adsorbed than carbon dioxide. However, a reversal occurs. Interestingly, as the temperature increases this observed reversal is delayed and higher pressures are required for carbon dioxide to be more adsorbed. At 333 K methane is more adsorbed than carbon dioxide over the whole simulated pressure range. We can note that methane uptake is just about to level off, while carbon dioxide trend continues to increase. This means that reversal occurs beyond the studied pressure at 333 K.

Figure 4-8 shows the adsorption isotherms of mixtures of 80% carbon dioxide-20% methane. At all temperatures carbon dioxide is more strongly adsorbed than methane. As the temperature increases the amount of carbon dioxide adsorbed is relatively less in the high temperatures than lower temperatures, yet carbon dioxide is more adsorbed than methane. As for methane at high pressures as the temperature increases the amount adsorbed increases in very small amounts. This is surprising as the behaviour of all pure components is the opposite.

Carbon dioxide-ethane mixtures

The adsorption isotherms for carbon dioxide-ethane were calculated for their equimolar mixtures (50% each in the gas phase). Figure 4-9 shows the adsorption isotherms of the equimolar binary mixtures of carbon dioxide-ethane at different temperatures. Initially, ethane is preferentially more adsorbed than carbon dioxide. However, as the pressure increases carbon dioxide is adsorbed competitively displacing ethane, while ethane becomes less adsorbed and the trend expressing ethane adsorption starts to decline while carbon dioxide trend continues to increase. Interestingly, the initial difference between the amount adsorbed of ethane and carbon dioxide reduces as the temperature increases. The adsorption preference is delayed to higher pressures as the temperature increases and amount of carbon dioxide adsorbed becomes more than ethane at higher pressures.

The reason for the initial stronger adsorption of ethane at lower pressures is ethane's higher adsorption energy. Ethane has a higher heat of adsorption than carbon dioxide. As the pressure increases and the sites of the silicalite become filled. The dominant forces become those between adsorbate molecules and the entropy effects become more important resulting into the reversal where carbon dioxide starts to replace ethane molecules.

Methane-ethane mixtures

The adsorption isotherms of methane-ethane were calculated for their equimolar binary mixtures (50% each in the gas phase). Figure 4-10 shows the adsorption isotherms of the equimolar binary mixtures of methane-

ethane at different temperatures. At all temperatures ethane is much stronger adsorbed than methane. The difference between the amount of ethane adsorbed and the amount of methane adsorbed decreases as the temperature is increased with pressure. As the pressure increases the trend, describing ethane reaches a plateau; and particularly at 250 K it can be seen that at the highest pressure point ethane's isotherm is just about to start to decline, whereas for the other temperatures this is not observed possibly because it requires higher pressures which are not within the studied range. As for methane, it continues to adsorb even at higher pressures. The phenomenon of ethane being initially strongly more adsorbed may be attributed to the higher heat of adsorption of ethane, which is about 1.5 times that of methane. This is the reason why at higher pressures the small molecules displace the bigger ones which results in an increased adsorption of methane and slight decrease in the adsorption of ethane. This same observation has been found by Gallo (Gallo et al., 2006).

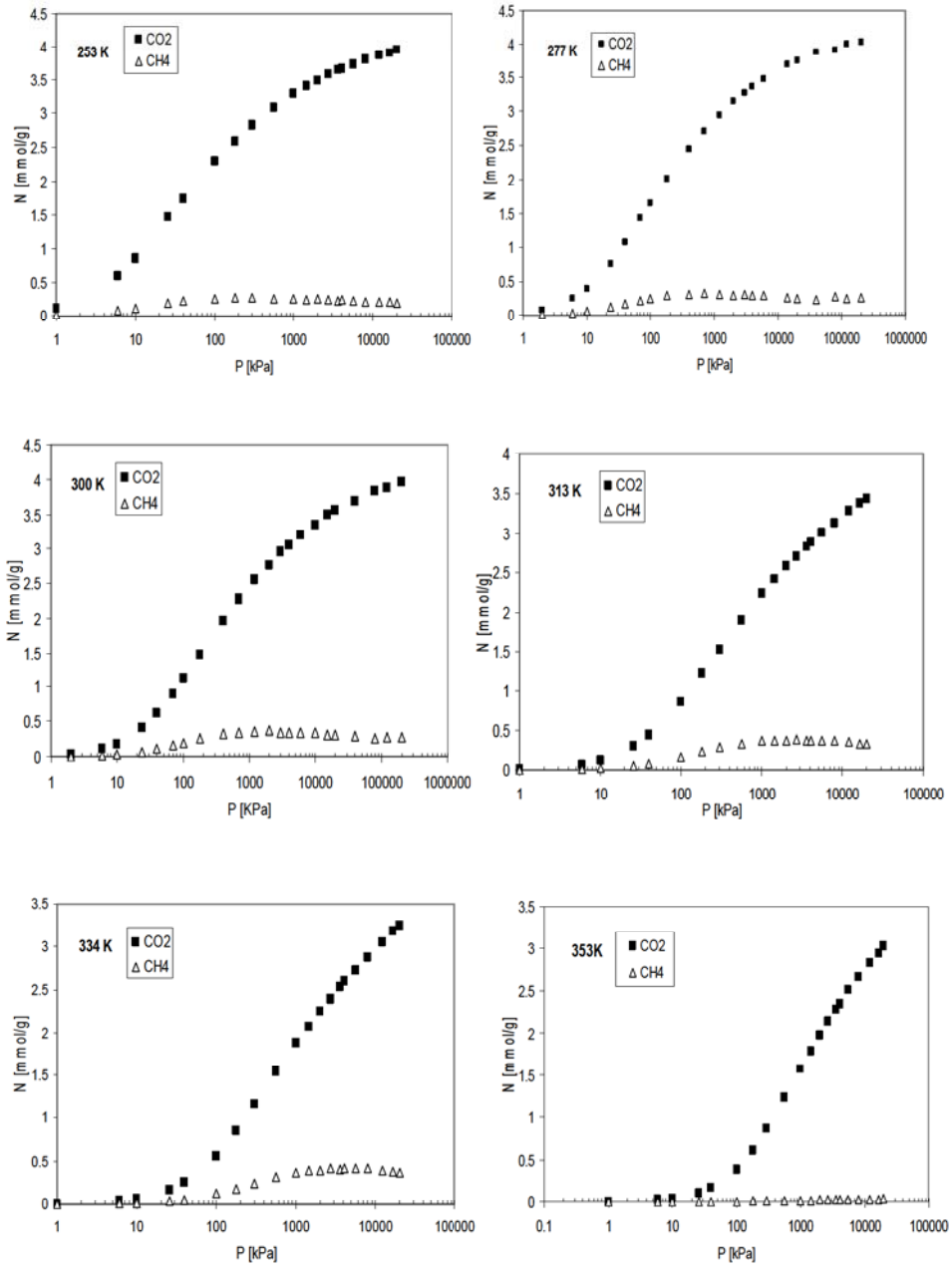

Figure 4-6 Adsorption isotherms of the equimolar binary mixtures of methane and carbon dioxide (50% each in the gas phase) in silicalite

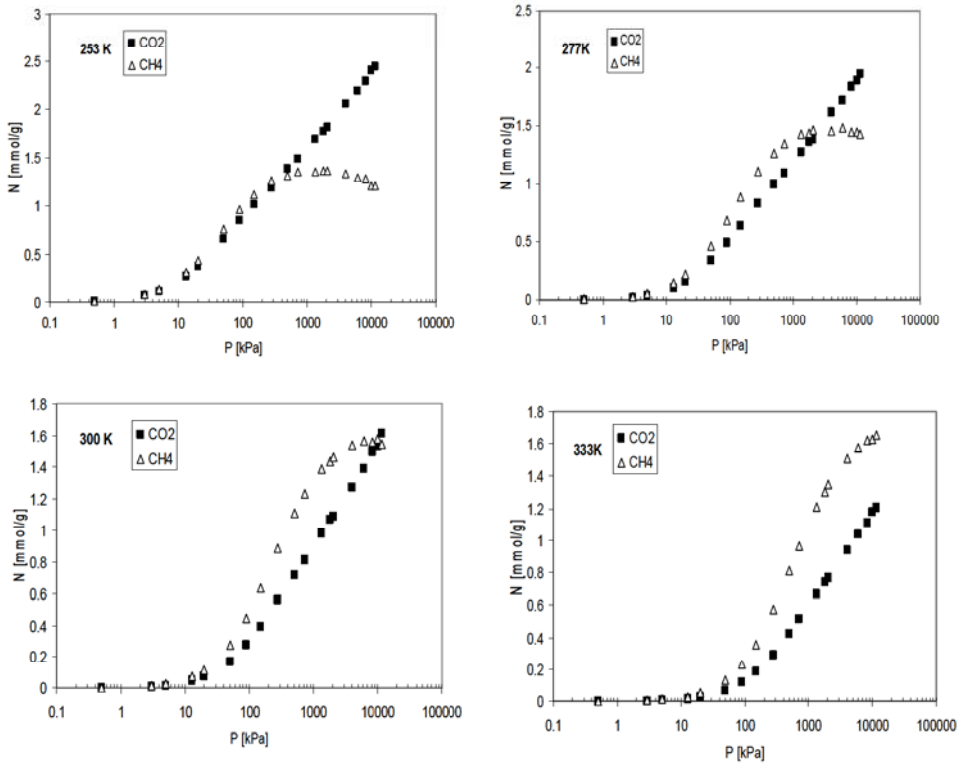

Figure 4-7 Adsorption isotherms of the binary mixtures of 10% carbon dioxide-90% methane in silicalite at various temperatures.

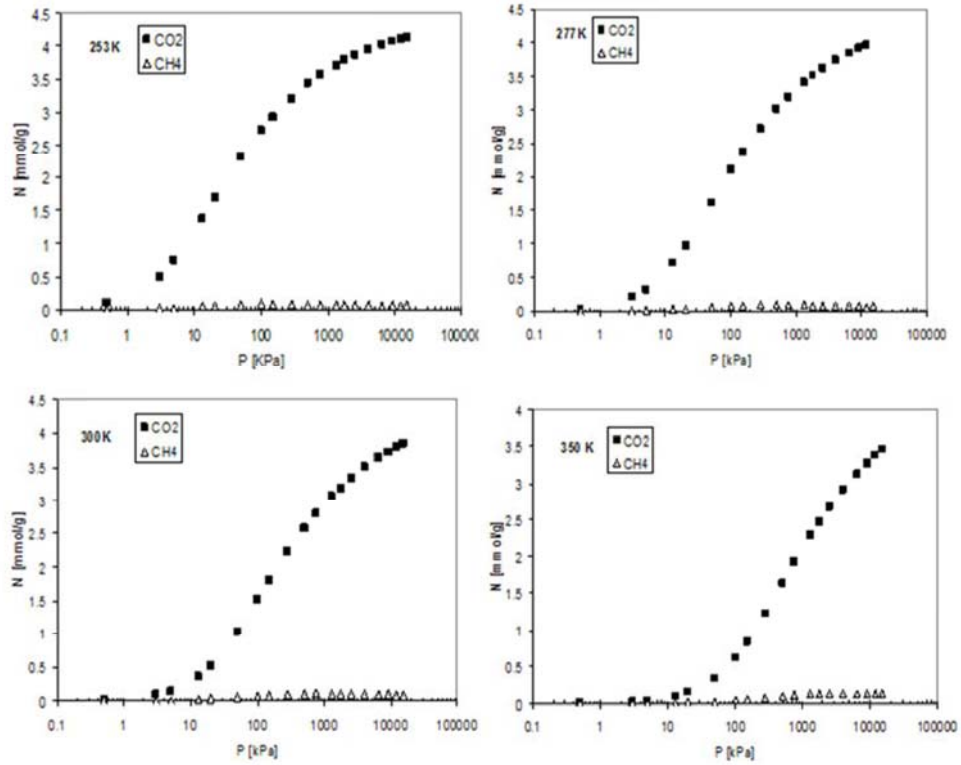

Figure 4-8 Adsorption isotherms of the binary mixtures of 80% carbon dioxide-20% methane in silicalite at various temperatures.

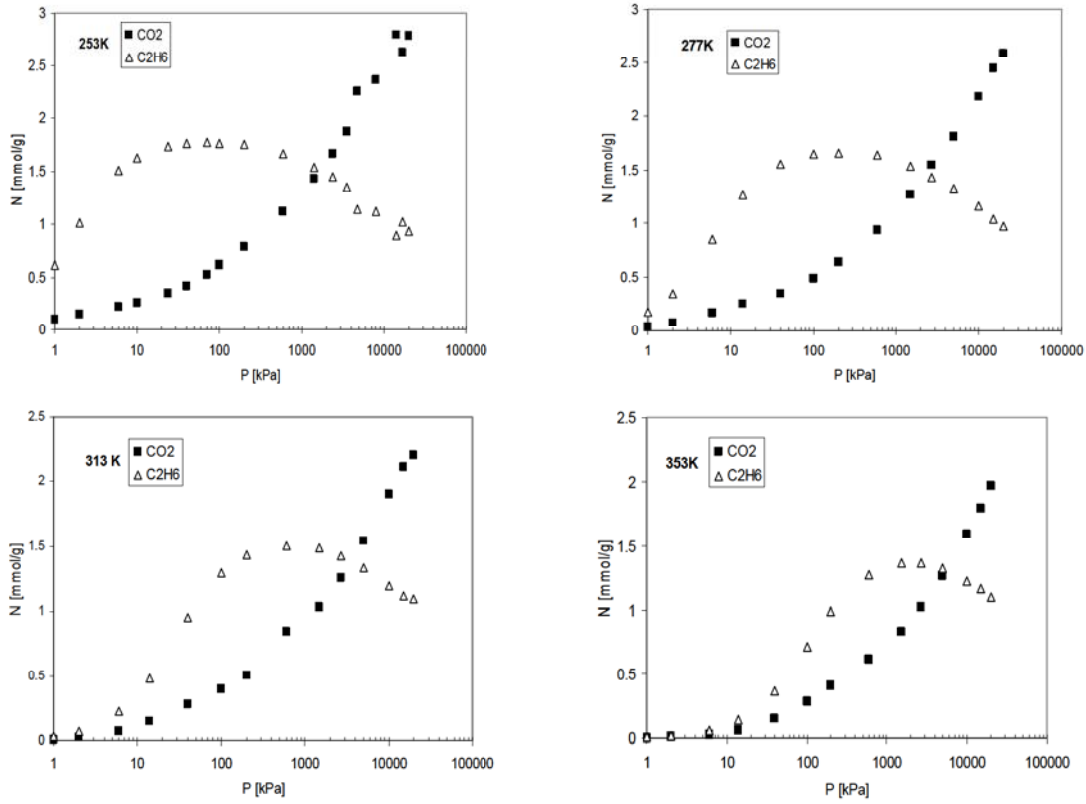

Figure 4-9 Adsorption isotherms of the equimolar binary mixtures (50% each in the gas phase) of carbon dioxide-ethane in silicalite at various temperatures.

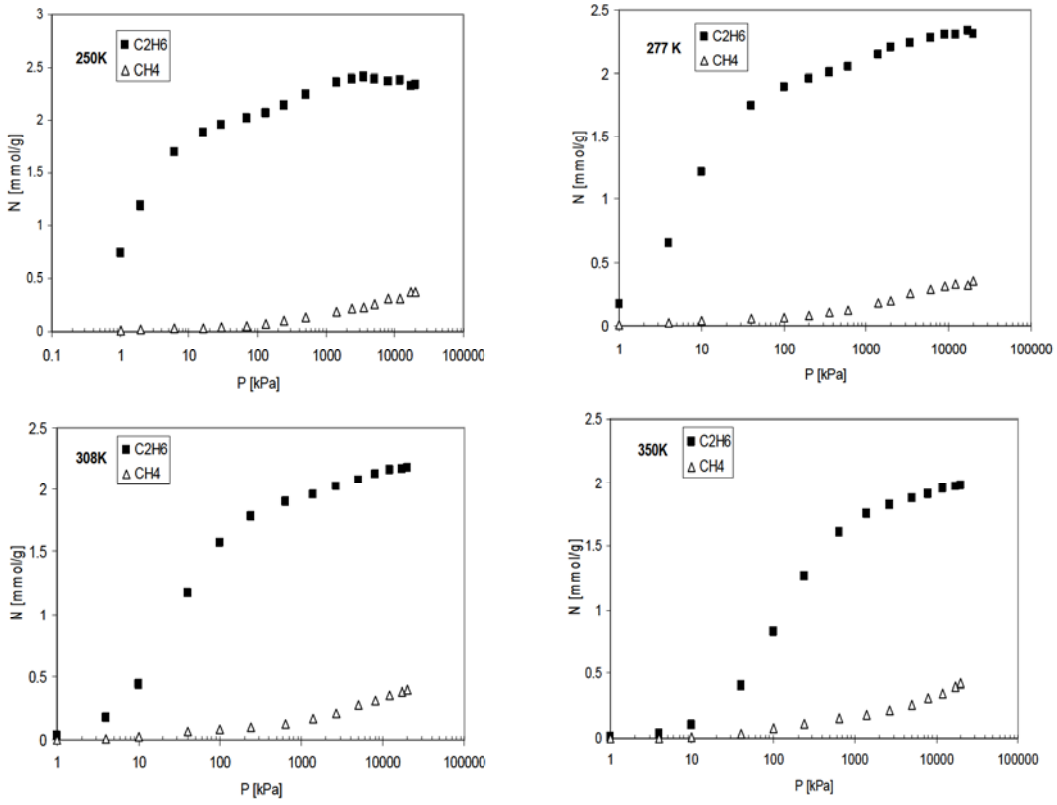

Figure 4-10 Adsorption isotherms of the equimolar binary mixtures (50% each in the gas phase) of methane-ethane in silicalite at various temperatures.

Figure 4-11, Figure 4-12 and Figure 4-13 are snapshots showing the distribution of equimolar mixtures of carbon dioxide-methane, carbon dioxide-ethane, and methane-ethane inside the silicalite channels. The ethane molecules are the atoms connected with red bonds. The zigzag channels are from left to right and the straight channels are from upper to lower. In all snapshots, the channels are more packed with molecules at higher pressure than lower pressures. It can be seen that at higher pressures molecules seem to preferentially adsorb more in the intersections of the zigzag and straight channels of the silicalite.

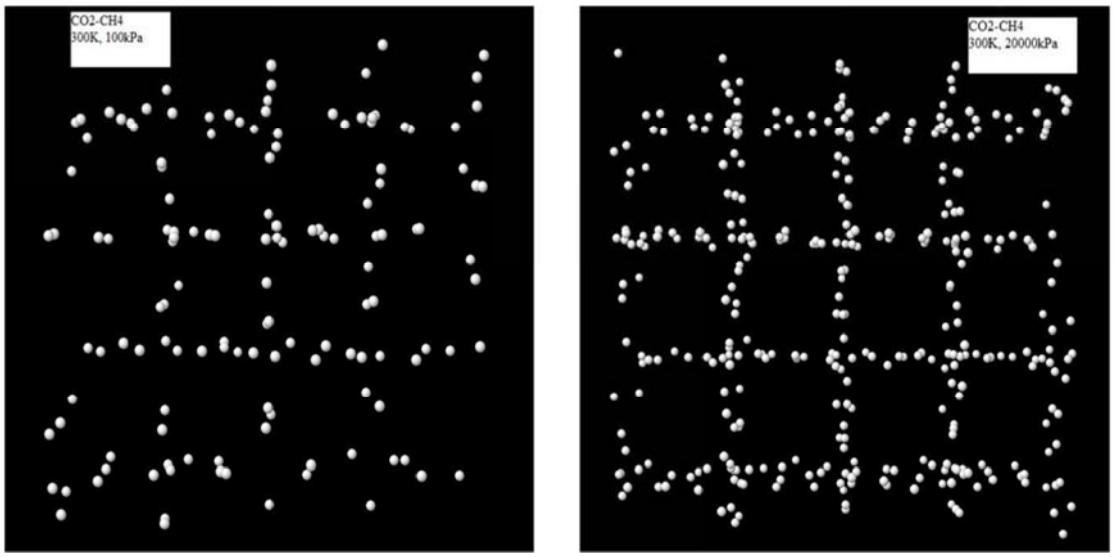

Figure 4-11 Snapshots of equimolar mixture of carbon dioxide-methane adsorption in silicalite at 300 K and 100 kPa (left), 20000 kPa (Right) showing their distribution inside the silicalite channels (Zigzag channels are from left to right and the straight channels are from upper to lower).

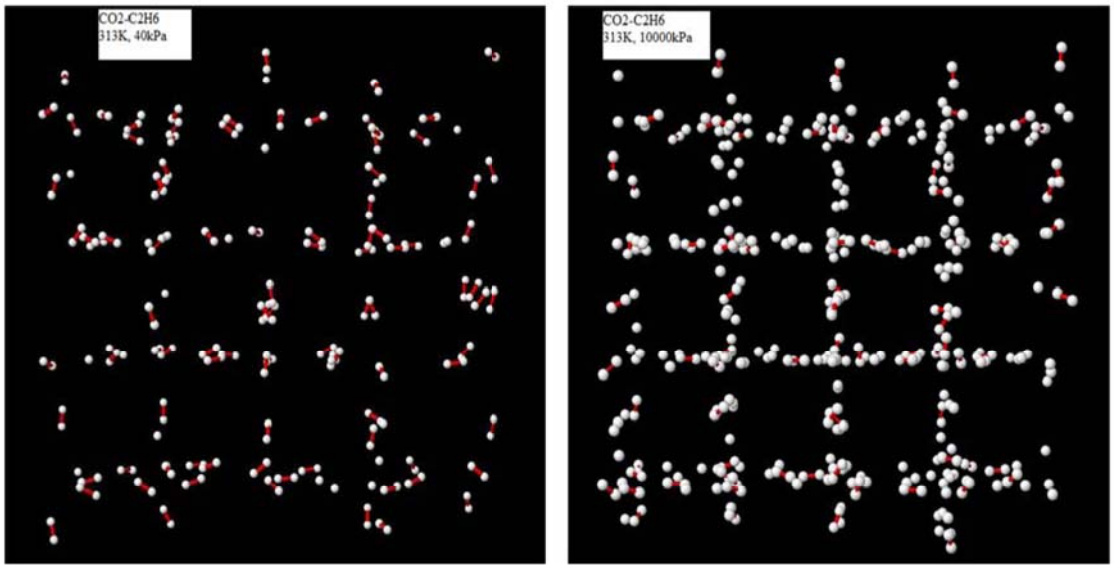

Figure 4-12 Snapshots of equimolar mixture of carbon dioxide-ethane adsorption in silicalite at313 K and 40 kPa (left), 10000 kPa (Right) showing their distribution inside the silicalite channels

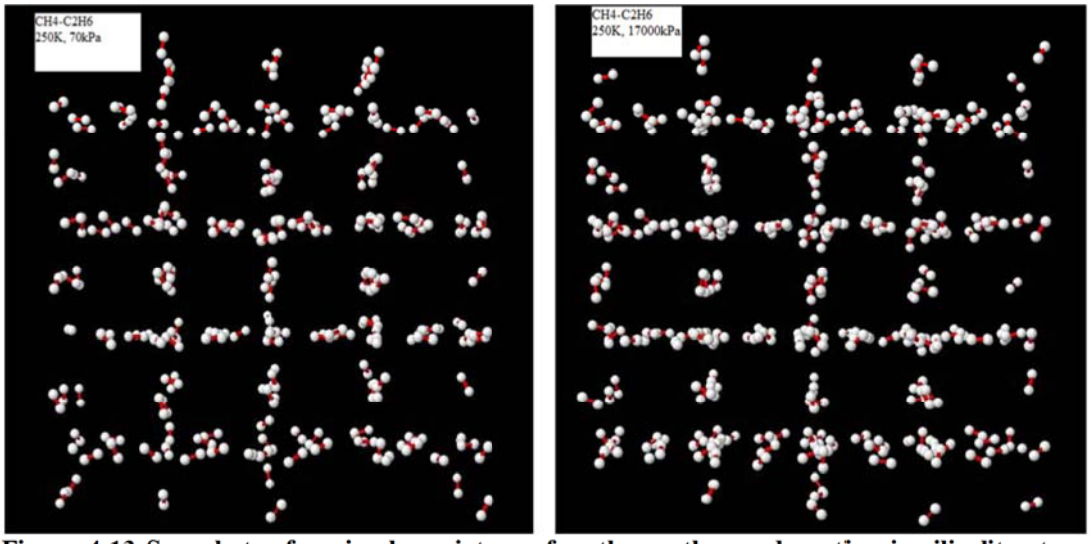

Figure 4-13 Snapshots of equimolar mixture of methane-ethane adsorption in silicalite at 250 K and 70 kPa (left), 17000 kPa (Right) showing their distribution inside the silicalite channels (Zigzag channels are from left to right and the straight channels are from upper to lower)The ethane molecules are the atoms connected with the red bonds.

Propane, n-butane and i-butane mixture

The adsorption isotherms of propane, n-butane and i-butane were calculated for their equimolar binary mixtures (50% each in the gas phase). Figure 4-14 shows the adsorption isotherms of the equimolar binary mixtures of propane and n-butane at different temperatures. Initially, n-butane is preferentially more adsorbed than propane. However, as the pressure increases propane is

adsorbed competitively displacing n-butane, while n-butane becomes less adsorbed and the trend expressing n-butane adsorption starts to decline while propane trend continues to increase.

Figure 4-15 shows the adsorption isotherms of the equimolar binary mixtures of n-butane and i-butane at different temperatures. n-butane is preferentially more adsorbed than i-butane. At lower temperature and at high pressures, i-butane is adsorbed competitively and it seems to displace n-butane but within the pressure range of the adsorption we are not going to see the phenomena of preferential adsorption.

Figure 4-16 shows the adsorption isotherms of the equimolar binary mixtures of propane and i-butane at different temperatures. Initially, i-butane is preferentially more adsorbed than propane. However, immediately as the pressure increases propane is adsorbed competitively displacing i-butane, while i-butane becomes less adsorbed and the trend expressing i-butane adsorption starts to decline while propane trend continues to increase.

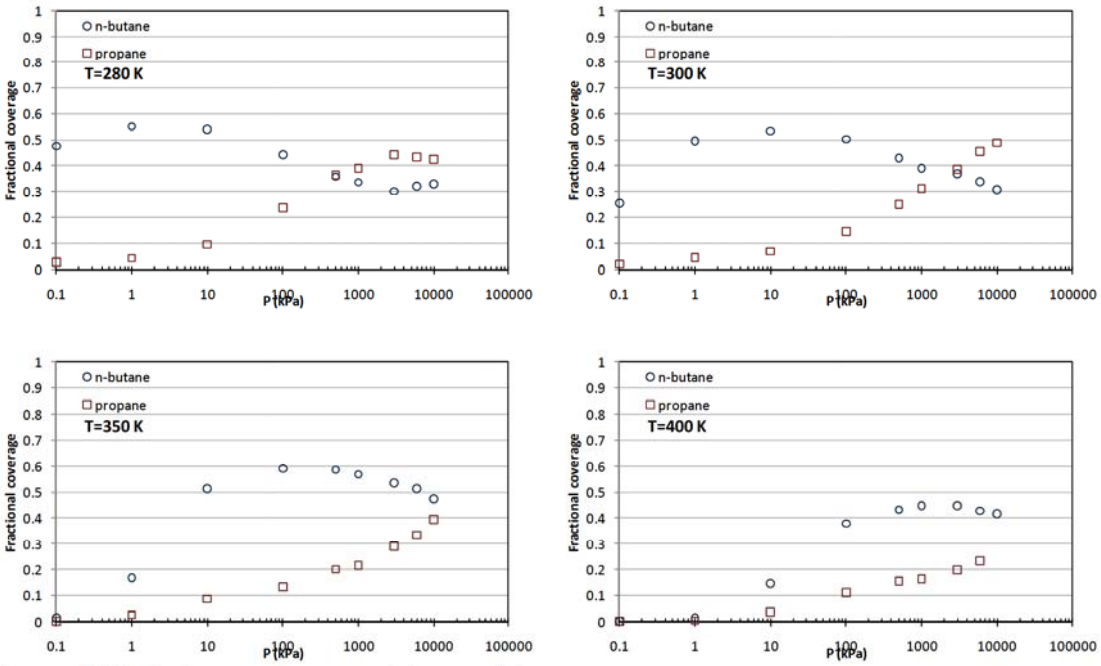

Figure 4-14 n-butane and propane binary mixture

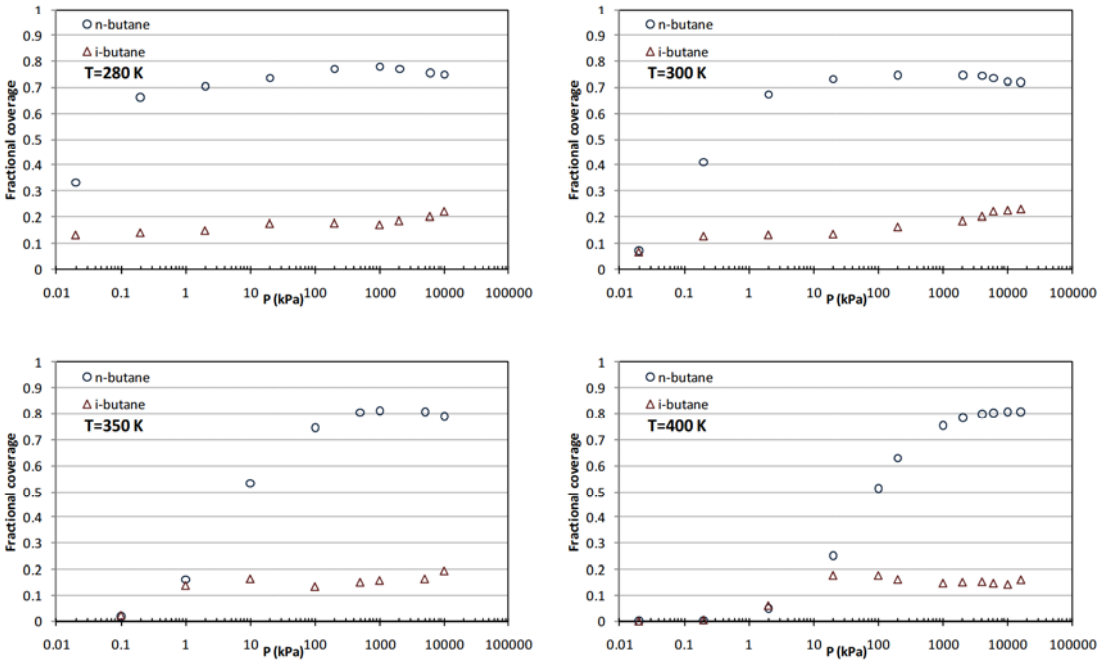

Figure 4-15 n-butane and i-butane binary mixture

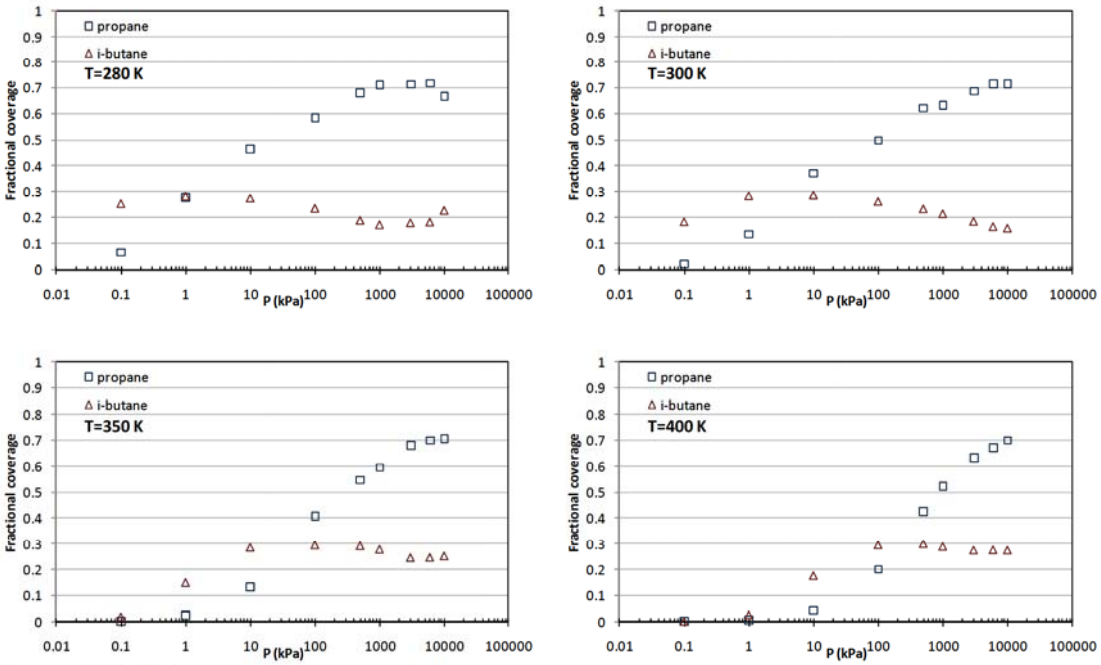

Figure 4-16 i-butane and propane mixture

4.3.4 Results of ternary mixtures

This research has also included studying the adsorption isotherms for ternary mixtures of methane-ethane-carbon dioxide. The study of these ternary components is of great interest particularly for the natural gas industry. The simulations were conducted for equimolar mixtures of methane (33.3%), ethane(33.3%) and carbon dioxide (33.3%) as well as mixture of methane (85%), ethane (10%) and carbon dioxide (5%).

Methane-ethane-carbon dioxide mixtures

Figure 4-17 shows the adsorption isotherms for an equimolar (33.3% each in the gas phase) ternary mixture of methane-ethane-carbon dioxide at 250 K, 298 K, and 350 K. At all temperatures and at lower pressures ethane is initially preferentially adsorbed more. As the temperature increases the difference between the amount of ethane adsorbed and the other components decreases. At higher pressures the other components mainly

CO_2 start to displace ethane. The reversal between ethane and carbon dioxide, the point where carbon dioxide becomes the most strongly adsorbed component moves to higher pressure as temperature increases. As for methane, it is the lowest adsorbed component. However, when the reversal between ethane and carbon dioxide occurs, methane also starts to displace ethane and continues to be adsorbed as the pressure increases despite the fact that it is being adsorbed in much smaller quantities compared with carbon dioxide. Interestingly, it is observed that the quantity of methane adsorbed at higher temperatures is higher than those at lower temperatures, whereas for the other components the contrary happens. This might be attributed to the fact that the other components are less adsorbed as the temperature is increased thus sites are emptier and become available for the adsorption of methane molecules.

Figure 4-18 illustrates an adsorption isotherm for a ternary mixture of 85% methane-10% ethane- 5% carbon dioxide at 298 K. This composition represents a typical composition of raw natural gas. Despite the fact that ethane content is only 10% (mole), it is initially preferentially more adsorbed than other components at lower pressures. However, the reversal between ethane and methane occurs at a pressure of 23000 kPa and the ethane molecules become displaced by the molecules of the other components. Interestingly, despite that carbon dioxide is the lowest adsorbed component because of its low presence (5% by vol); at very high pressures (about 200,000 kPa) it is noted that the reversal between carbon dioxide and ethane occurs and the reversal between carbon dioxide and methane is just

about to occur. This shows the high energetic attraction between carbon dioxide and the silicalite surface. This means that the use of silicalite as an adsorbent for the adsorption of this ternary mixture as means of separation is suitable, particularly if carbon dioxide is present in high percentages.

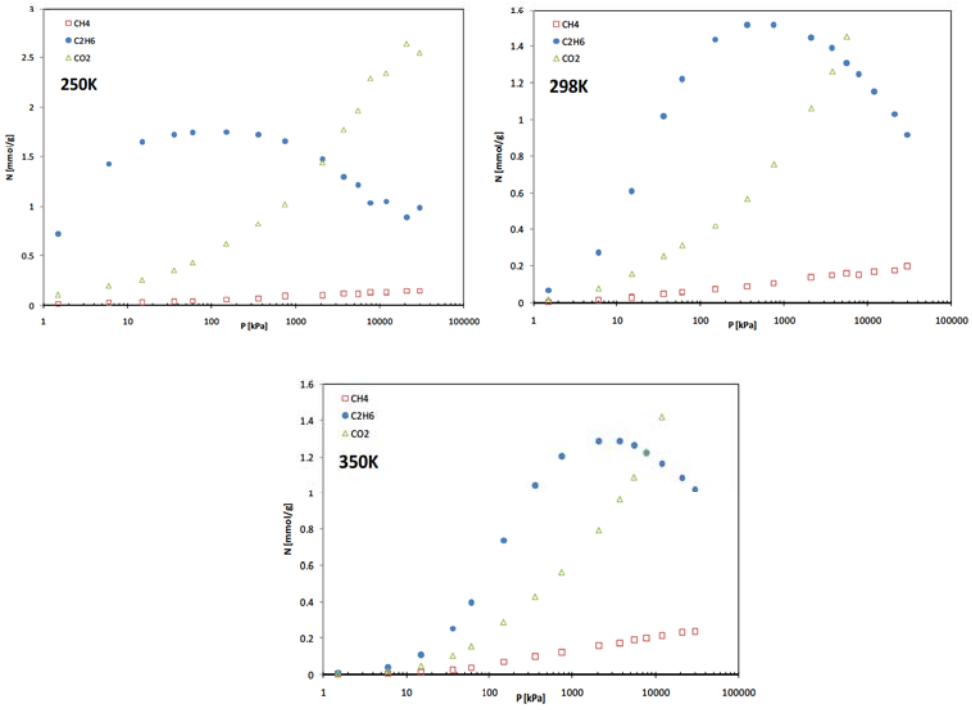

Figure 4-17 Adsorption isotherms for ternary equimolar mixtures (33.3% each in the gas phase)

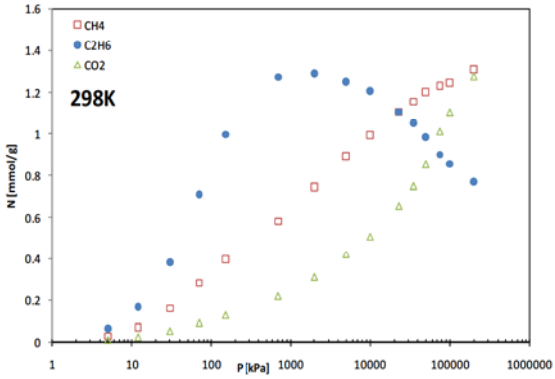

Figure 4-18 Adsorption isotherm for a ternary mixture of 85% methane-10% ethane-5% carbon dioxide at 298 K in silicalite.

Propane, n-butane and i-butane mixture

Figure 4-19 shows the adsorption isotherms for an equimolar (33.3% each in the gas phase) ternary mixture of propane, i-butane and n-butane at 277K, 300K, and 350K. At all temperatures and at lower pressures n-butane is initially preferentially more adsorbed and as the temperature increases the difference between the amount of ethane adsorbed and the other components becomes less. At higher pressures, propane start to displace n-butane and the reversal between n-butane and propane occurs where propane becomes the most strongly adsorbed component. As for i-butane, it is the lowest adsorbed component. At lower temperature, adsorption starts at relatively lower pressure. For instance at temperature equal to 277K, highest amount of n-butane is adsorbed at about 1 kPa but at 350K the peak adsorption for n-butane happens at about 100 kPa.

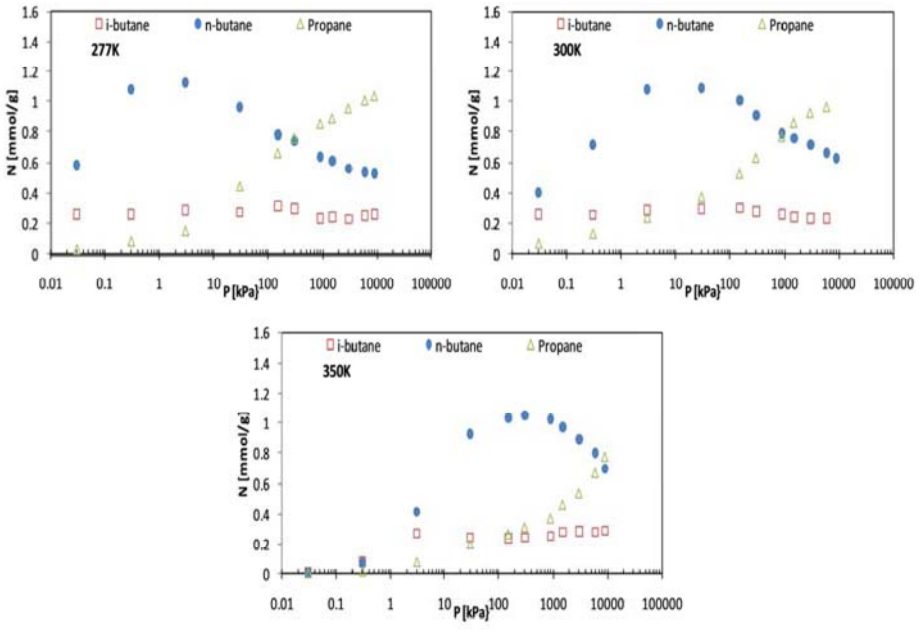

Figure 4-19 Adsorption isotherms for ternary equimolar mixtures of propane i-butane and n-butane (33.3% each in the gas phase).

5- LATTICE MODEL - HYDROCARBON AND CO_2 ADSORPTION IN SILICALITE

5.1 One-dimensional lattice model for the adsorption of CH_4, C_2H_6 and CO_2 mixtures

A lattice gas model based on mean-field theory successfully predicts experimental adsorption isotherms of short-chain alkanes at low coverage, but performs inadequately at high pressures. This is attributed in part to the poor representation of adsorbate–adsorbate interactions.

Since zeolites are crystalline alumino-silicates made up of repeating unit cells, the lattice presentation of adsorption sites is a realistic one.

Methane and ethane adsorption in zeolites based on lattice models has been studied before (Bell & Dunne, 1979;Dunne & Reuben, 1995b) and some results has been published by (Du et al., 1999).

5.1.1 The exact statistical mechanical one-dimensional lattice model

The process of adsorption of alkane mixtures in zeolites has been modelled using the Grand Canonical Monte-Carlo simulation method in various previous works (Du *et al.*, 1998;Smit, 1995a). The results from these

simulations display good agreement with the experimental data involving single-component adsorption isotherms.

Monte-Carlo simulations, however, do not allow a simple interpretation of the isotherms structure, despite their predictive capacity. This is why the exact calculation of the statistical mechanics of a lattice model is presented for the adsorption process of the mixtures we mentioned earlier to the one-dimensional pores of a zeolite structure as a means to understanding the characteristics shown in the Monte-Carlo simulations.

For this study, the Grand Partition function of the mixtures adsorbed in the silicalite pore is evaluated using the matrix method. The modes in which the molecules occupy the zeolite pores will be described at the beginning of the section for each mixture.

5.1.2 One-dimensional lattice model of mixtures

This one-dimensional lattice model has been used before to simulate the adsorption of alkane mixtures (Dunne et al., 2003). The results obtained by this work greatly resemble the ones that are obtained by the Monte-Carlo simulation method, and we can take this as a proof that this method will work for our case. For our study, the exact same method is implemented to simulate the mixtures that we consider.

The crystal structure of silicalite ZSM-5 has been presented previously in Figure 1-1. There is a well-known channel structure composed of zigzag and straight channels and the intersection (see Figure 1-3). It is widely assumed these channels house the adsorption sites. The channels in the three-

dimensional structure are made up of well-separated layers. Thus, the model is effectively that of two- types, zigzag and straight, of one-dimensional chains of sites which may be occupied by the alkane mixtures in various states. This representation, although not exact, is thought to be a realistic representation of the silicalite zeolite lattice.

A molecule that is approximated to be a sphere, in our case, CO_2 assumed to occupy a single lattice site (a monomer, where one site is occupied), while ethane can be assumed to be standing up (a monomer), or lying down (a dimer, where 2 sites are occupied).

In this study, we will assume the gas phase as ideal, (at ambient pressure and temperature P, T) in equilibrium with an adsorbed phase of mixture molecules in the silicalite pores. We consider a chain of N lattice points, each pair of neighbouring sites being separated by a spacing, which is a constant independent of pressure and temperature.

The Grand Partition function for a mixture in the adsorbed phase is given by:

$$\Xi = \sum_{n_a=0}^{\infty} \sum_{n_b=0}^{\infty} \exp(\mu_{as} \times \frac{n_a}{kT}) \times \exp(\mu_{bs} \times \frac{n_b}{kT}) \times Q(n_a, n_b, N, T) \qquad (5\text{-}1)$$

n_a and n_b are the number of adsorbed molecules, while μ_{as} and μ_{bs} are the chemical potentials. $Q(n_a, n_b, N, T)$ is the canonical partition function for n_a, n_b interacting molecules adsorbed on N sites in a zeolite channel.

For the mixtures of CO_2 and ethane, we assume that there are four species in the lattice, and the lattice model will be solved with 4x4 matrices. We label

ethane lying down as 1, ethane standing up as 2, CO_2, which is approximately a sphere, as 3 while 4 is a hole.

We assume cyclic boundary conditions[15] and consider the possible configurations of these species on a ring of N sites. We assume that occupation of sites by pairs of molecules is energetically forbidden, so that terms with more than N molecules on the same lattice do not contribute to the Grand Partition function. By inspection, it can be seen that Ξ may be written as the sum of the products of N factors given by:

$$\Xi = \sum_{\alpha=1,2,..,5} \sum_{\beta=1,2,..,5} \dots \sum_{\omega=1,2,..,5} A_{\alpha\beta} A_{\beta\gamma} A_{\gamma\delta} \dots A_{\omega\alpha} \tag{5-2}$$

Where

$$A_{\mu\nu} = (\phi_\mu \phi_\nu)^{1/2} \phi_{\mu\nu} \tag{5-3}$$

For the 4×4 matrix, the factors of $A_{\mu\nu}$ are given by:

$$\phi_1 = \exp\left[\frac{\mu_{as} - (\mu_{a_0 s} + \mu_0)}{k_B T}\right] \tag{5-4}$$

$$\phi_2 = \exp\left[\frac{\mu_{as} - \mu_{a_0 s}}{k_B T}\right] \tag{5-5}$$

$$\phi_3 = \exp\left[\frac{\mu_{bs} - \mu_{b_0 s}}{k_B T}\right] \tag{5-6}$$

$$\phi_4 = 1 \tag{5-7}$$

$$\phi_{\mu\nu} = \exp\left(\frac{-J_{\mu\nu}}{k_B T}\right) \tag{5-8}$$

[15] Cyclic or periodic boundary conditions are used when the physical geometry of interest has periodically repeating nature.

The parameter $J_{\mu\nu}$ is the interaction energy between the pairs of species μ and ν on nearest neighbour sites at the separation of the lattice sites. The separation distance of adsorbed nearest neighbour pairs of molecules may differ from the optimal distance of separation for pairs of free molecules. The interaction involving a vacant site is evidently zero. $U_{a_0 s}$ and $U_{b_0 s}$ are the free energies of the adsorbed molecules interacting with the lattice. These two phenomenological parameters can include changes in ro-vibrational free energies on adsorption of an isolated molecule onto the zeolite lattice from the gas phase.

Using the inner product rule $D_{ij} = \sum_k B_{ik} C_{kj}$ for matrix multiplication of a pair of matrices B and C, the Grand Partition function equation (5-2) can be expressed as:

$$\Xi = \sum_{\alpha=1,2,3,4,(5)} (A^N)_{\alpha\alpha} = Trace(A^N) = (\lambda_1)^N + (\lambda_2)^N + \ldots + (\lambda_5)^N \tag{5-9}$$

Where λ are the eigenvalues of the matrix A:

$$A = \begin{pmatrix} A_{11} & A_{12} & A_{13} & A_{14} \\ A_{21} & A_{22} & A_{23} & A_{24} \\ A_{31} & A_{32} & A_{33} & A_{34} \\ A_{41} & A_{42} & A_{43} & A_{44} \end{pmatrix} \tag{5-10}$$

For large N, we then obtain

$$\Xi = (\lambda_{\max})^N \tag{5-11}$$

Where $\lambda_{\max}$ is the largest eigenvalue of the matrix A. Hence, we have an exact evaluation of the Grand Partition function for the mixtures in the

quasi-one-dimensional zeolite pores. The mean density of adsorbed component a, (ρ_a) and component b, (ρ_b) are given by:

$$\rho_a = k_B T \frac{\partial}{\partial \mu_{as}} \ln(\lambda_{max}) \tag{5-12}$$

$$\rho_b = k_B T \frac{\partial}{\partial \mu_{bs}} \ln(\lambda_{max}) \tag{5-13}$$

The chemical potential of the a and b components in an ideal mixture are given by:

$$\mu_{as} = \mu_a^0 + k_B T \ln(x_a P) \tag{5-14}$$

$$\mu_{bs} = \mu_b^0 + k_B T \ln(x_b P) \tag{5-15}$$

Where μ_a^0 and μ_b^0 are the standard chemical potential of components a and b, respectively, given by equation (3-22).

The equations above are compiled using the Mathcad® mathematical software package (see appendix B) for a given set of variables and , total pressure and temperature , resulting in isotherms for the mixtures, which are compared to the ones obtained using the Monte-Carlo simulation (refer to chapter 4-).

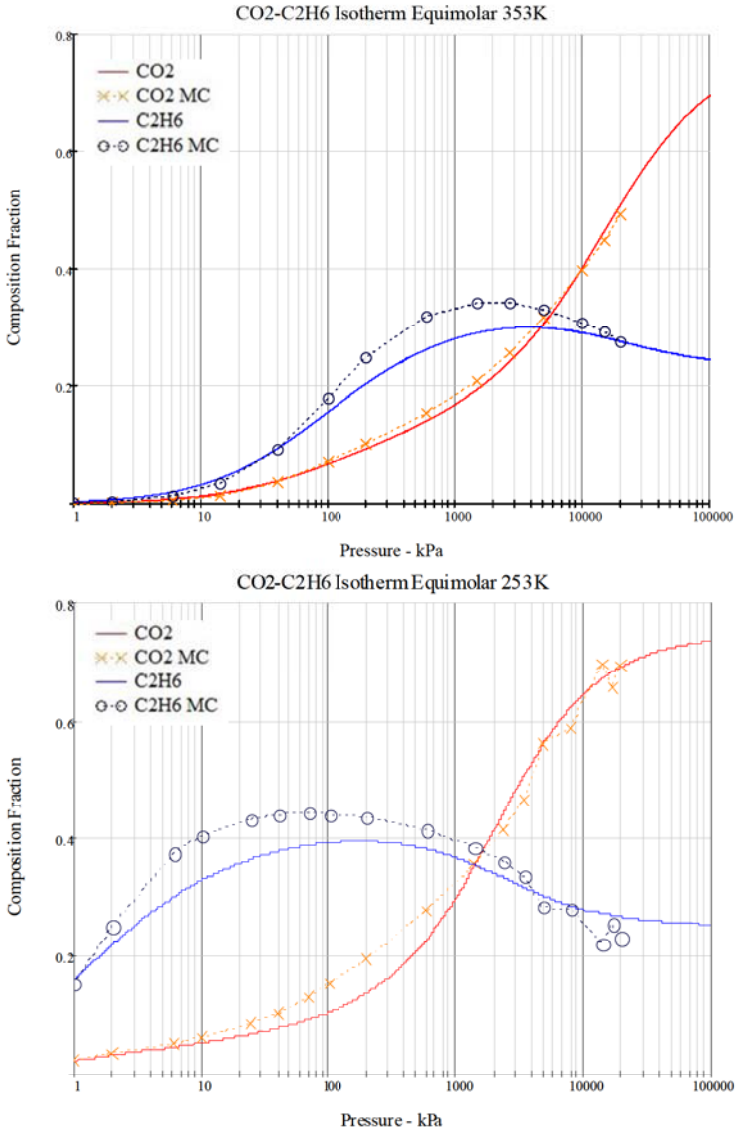

Figure 5-1 Lattice model adsorption isotherms for an equimolar $CO_2 - C_2H_6$ mixture on silicalite zeolite compared with Monte Carlo simulation

5.2 Propane, i-butane and n-butane binary adsorption in silicalite

The model is also used to simulate the adsorption isotherm for equimolar binary mixtures (50% each in the gas phase) of propane, i-butane and n-butane.

Figure 5-2 to Figure 5-4 show the adsorption isotherms of the equimolar binary mixtures at different temperatures calculated using the lattice model

with that of Monte Carlo simulations. The shape of the adsorption isotherms are in good agreement with the Monte Carlo results

Figure 5-2 shows n-butane is preferentially more adsorbed than i-butane. At lower temperature and at high pressures, i-butane is adsorbed competitively and it seems to displace n-butane but within the pressure range of the adsorption we are not going to see the phenomena of preferential adsorption.

As for n-butane/propane mixture, Figure 5-3 shows that n-butane is preferentially more adsorbed than propane. However, as the pressure increases propane is adsorbed competitively displacing n-butane, while n-butane becomes less adsorbed and the trend expressing n-butane adsorption starts to decline while propane trend continues to increase.

Figure 5-4 shows i-butane is preferentially more adsorbed than propane initially. However, immediately as the pressure increases propane is adsorbed competitively displacing i-butane, while i-butane becomes less adsorbed and the trend expressing i-butane adsorption starts to decline while propane trend continues to increase.

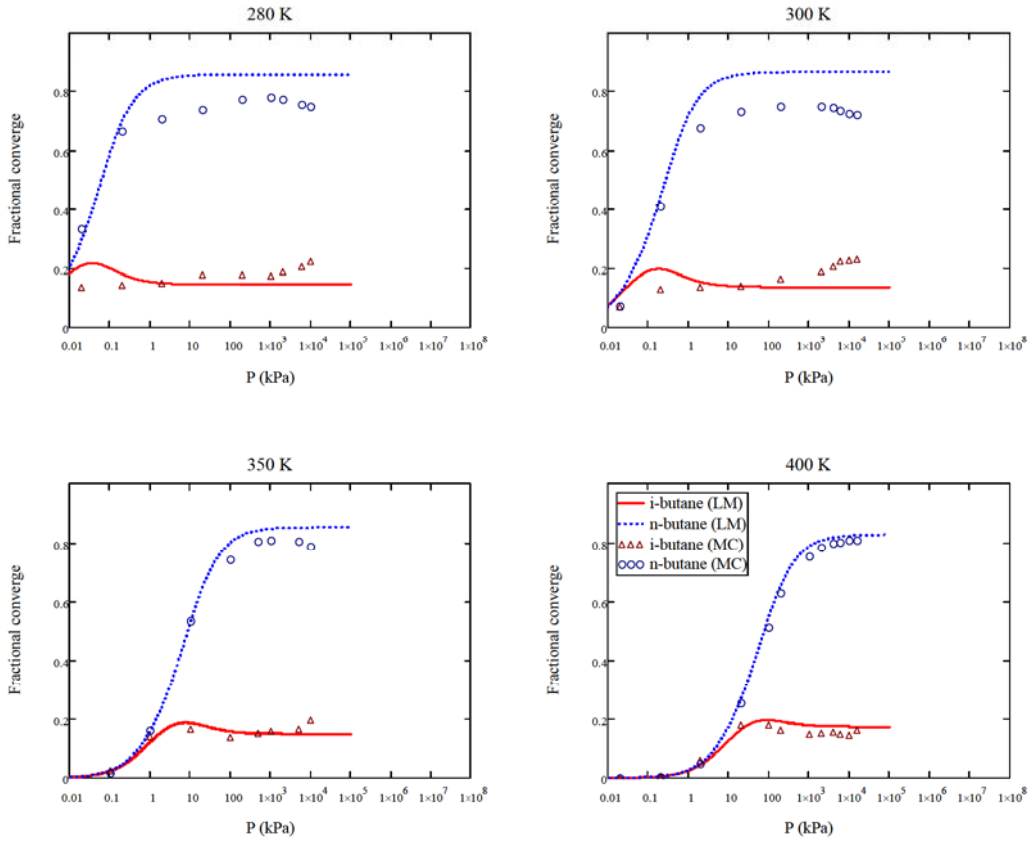

Figure 5-2 iso-butane and n-butane mixture adsorption. (LC= lattice model, MC=Monte carol)

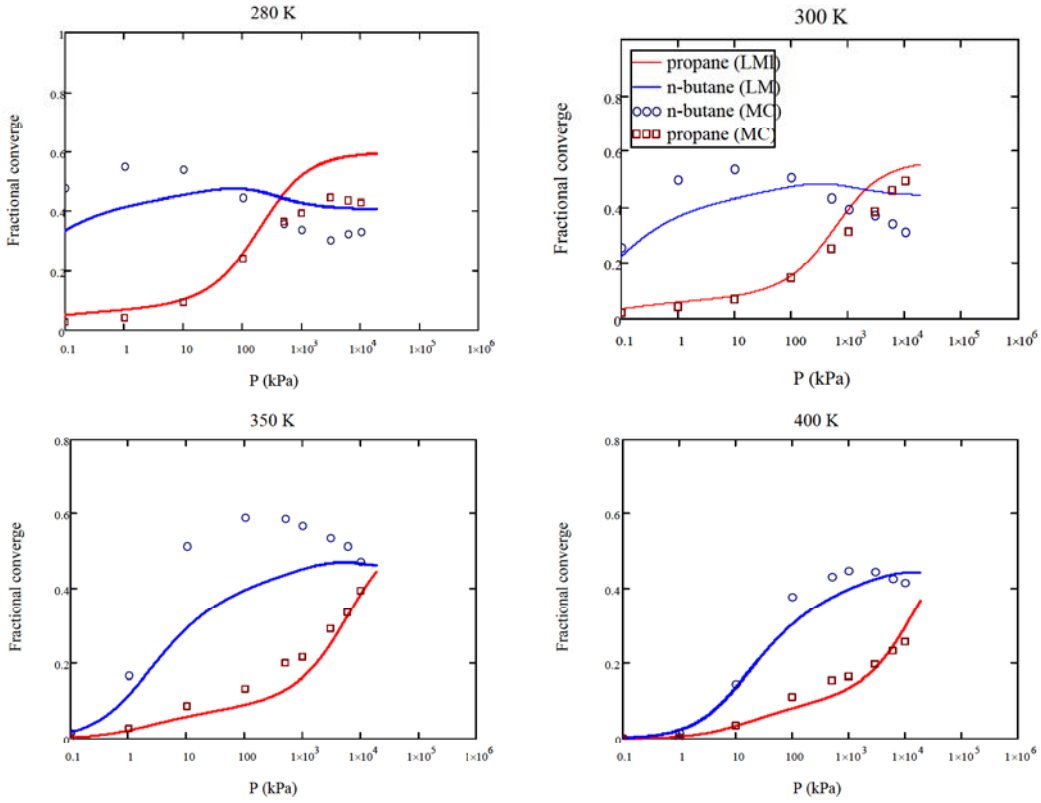

Figure 5-3 Propane and n-butane mixture adsorption. (LC= Lattice Model, MC=Monte carol)

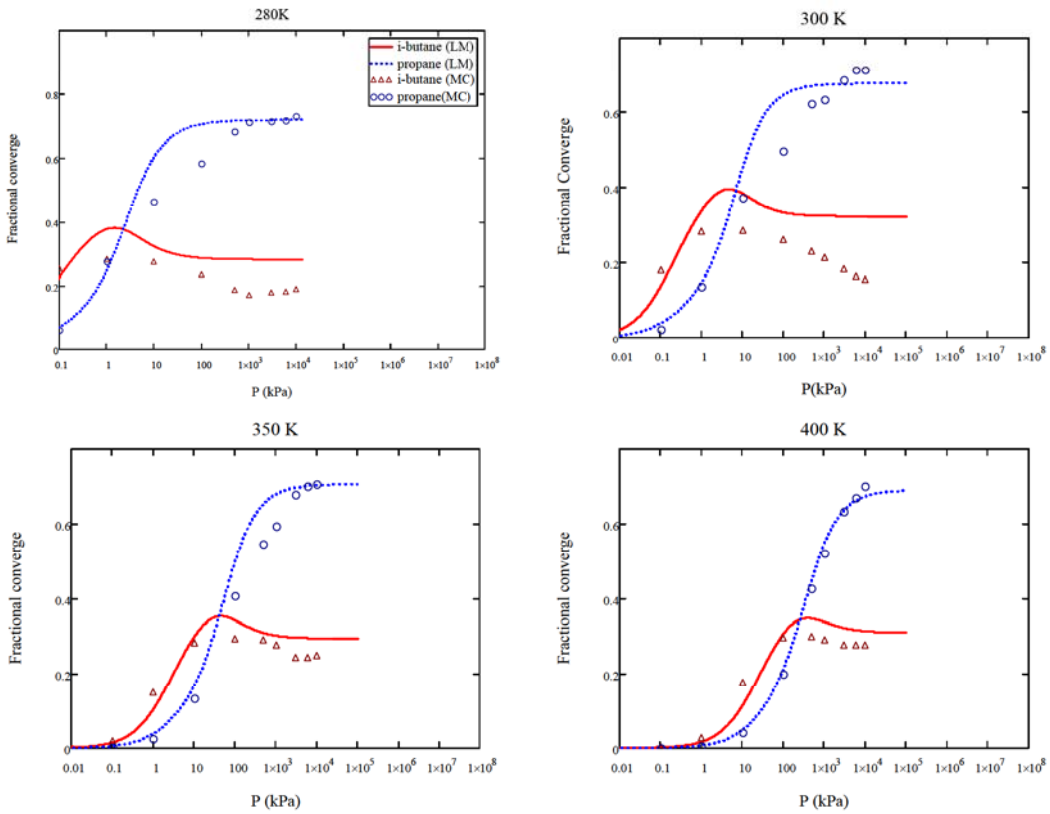

Figure 5-4 Propane and iso-butane mixture adsorption. (LC= lattice model, MC=Monte Carlo

5.3 One dimensional lattice model extension for ternary mixtures

In this section the quasi-one dimensional lattice model has been produced, which is an expanded version of a lattice model in the previous section.

The model again is obtained by considering an ideal mixture of gas at temperature T, and pressure P in equilibrium with an adsorbed phase of the same mixture of gases in the zeolite pores.

The grand partition function, Ξ, for the adsorbed phase for a ternary mixture of carbon dioxide (a), methane (b) and ethane (b) is given by

$$\Xi = \sum_{n_a=0}^{\infty}\sum_{n_b=0}^{\infty}\sum_{n_c=0}^{\infty} \exp\left(\mu_{as}.\frac{n_a}{k_BT}\right).\exp\left(\mu_{bs}.\frac{n_b}{k_BT}\right).\exp\left(\mu_{ac}.\frac{n_c}{k_BT}\right).Q(n_a,n_b,n_c,N,T) \qquad (5\text{-}16)$$

Where n_a, n_b and n_c are the numbers of adsorbed molecules of a, b and c respectively. μ_{as}, μ_{bs} and μ_{cs} are the chemical potentials. T is the temperature of the system. k_B is the Boltzmann constant[16].

$Q(n_a, n_b, n_c, N, T)$ is the canonical partition function of the three molecules adsorbed on N site within the zeolite lattice. In this work, there are six species that can be on the lattice; carbon dioxide and ethane are adsorbed in two possible configurations, methane is regarded as a ball and thus only ever adopts a maximum of one configuration, and the sixth specie is an empty zeolite pore.

For the model of 6 species the numbering is:

Configurations molecules

1. CO_2 (Lying)
2. CO_2 (Standing)
3. Methane (Ball)
4. C_2H_6 (Lying)
5. C_2H_6 (Standing)
6. Zeolite Pore

The chemical potential of an ideal gas mixture is given by

$$\mu_{is} = \mu_i^0 + k_B T \ln(x_i P) \qquad (5\text{-}17)\#$$

[16] The physical constant that relates temperature with energy. It is the molar gas constant R divided by Avogadro's number of molecules per mol N_A. $k_B = \frac{R}{N_A} = 1.38 \times 10^{-23}\ JK^{-1}$

7he parameter x_i is the molar fraction of the component in the gas phase. The value μ_i^0 is the standard chemical potential for component i, given by equation (3-22).

The model assumes cyclic boundary conditions. In effect the lattice is a ring containing N adsorption sites. It is assumed that it is energetically unstable to have more than one molecule adsorbed on to one lattice site, and therefore if there is more than N molecules on the lattice this configuration does not contribute to the Grand Partition Function. By inspection it can be seen that the Grand Partition Function, Ξ, can be written as the sum of the products of N factors for the 6 species.

$$\Xi = \sum_{\alpha=1,2,\ldots,6} \sum_{\beta=1,2,\ldots,6} \ldots \sum_{\omega=1,2,\ldots,6} A_{\alpha\beta} A_{\beta\gamma} A_{\gamma\delta} \ldots A_{\omega\alpha} \tag{5-18}$$

where

$$A_{\mu\nu} = \left(\phi_\mu \phi_\nu\right)^{1/2} . \phi_{\mu\nu} \tag{5-19}$$

The factors of $A_{\mu\nu}$ are given by

$$\phi_1 = \exp\left[\frac{\left(\mu_{as} - u_{a_0 s}\right)}{k_B T}\right] \tag{5-20}$$

$$\phi_2 = \exp\left[\frac{\left[\mu_{as} - \left(u_{a_0 s} + u_{a_0}\right)\right]}{k_B T}\right] \tag{5-21}$$

$$\phi_3 = \exp\left[\frac{\left(\mu_{bs} - u_{b_0 s}\right)}{k_B T}\right] \tag{5-22}$$

$$\phi_4 = \exp\left[\frac{\left(\mu_{cs} - u_{c_0 s}\right)}{k_B T}\right] \tag{5-23}$$

$$\phi_5 = \exp\left[\frac{\left[\mu_{cs} - \left(u_{c_0 s} + u_{c_0}\right)\right]}{k_B T}\right] \tag{5-24}$$

$$\phi_6 = 1 \tag{5-25}$$

$$\phi_{\mu\nu} = \exp\left(\frac{-J_{\mu\nu}}{k_B T}\right) \tag{5-26}$$

The parameters $u_{a_0 s}$, $u_{b_0 s}$ and $u_{c_0 s}$ are the free energies of adsorption for carbon dioxide, methane and ethane respectively, u_{a_0} and u_{c_0} are the penalty value for the free energy of a molecule in the standing configuration. The interaction energy between pairs of species μ and ν on neighbouring sites is denoted by $J_{\mu\nu}$.

Using the inner product rule for matrix multiplication for a pair of matrices the Grand Partition Function, can be expressed as

$$\Xi = \sum_{\alpha=1,2,\ldots,6} \left(A^N\right)_{\alpha\alpha} = Trace\left(A^N\right) = \left(\lambda_1\right)^N + \left(\lambda_2\right)^N + \ldots + \left(\lambda_6\right)^N \tag{5-27}$$

Where $\lambda_1, \lambda_2, \ldots, \lambda_6$ are the eigenvalues of the matrix A given below

$$A = \begin{pmatrix} A_{11} & A_{12} & A_{13} & A_{14} & A_{15} & A_{16} \\ A_{21} & A_{22} & A_{23} & A_{24} & A_{25} & A_{26} \\ A_{31} & A_{32} & A_{33} & A_{34} & A_{35} & A_{36} \\ A_{41} & A_{42} & A_{43} & A_{44} & A_{45} & A_{46} \\ A_{51} & A_{52} & A_{53} & A_{54} & A_{55} & A_{56} \\ A_{61} & A_{62} & A_{63} & A_{64} & A_{65} & A_{66} \end{pmatrix} \tag{5-28}$$

For large values of N the Grand Partition Function can be obtained from the maximum eigenvalue of matrix A, $\lambda_{\max}$.

$$\Xi = \left(\lambda_{\max}\right)^N \tag{5-29}$$

The mean density of each adsorbed molecule can be evaluated by a step change in the chemical potential of that molecule.

$$\rho_i = k_B T \frac{\partial}{\partial \mu_{is}} \ln\left(\lambda_{\max}\right) = k_B T \frac{\ln\left(\frac{\lambda_{\max}}{\lambda_{\max i}}\right)}{step} \qquad (5\text{-}30)$$

Where $\lambda_{\max,i}$ is the maximum eigenvalue for A produced by the step change in the chemical potential, μ_i.

The mean density obtained is the number of molecules of each component per N sites. In order for this to be compared against other work this value has to be scaled. For this work the Monte Carlo data was converted to allow comparison.

The Monte Carlo isotherms produced in chapter 4- are described in amount of gas adsorbed per site $(mmol/g)$. Therefore to compare these results, where the lattice model produce isotherms, in terms of fractional coverage of the zeolite, the Monte Carlo data has been scaled by a factor of 4 to represent the largest amount of sites.

Calculation procedure

The diagram below describes the steps taken to produce the isotherm and comparison with the Monte Carlo results.

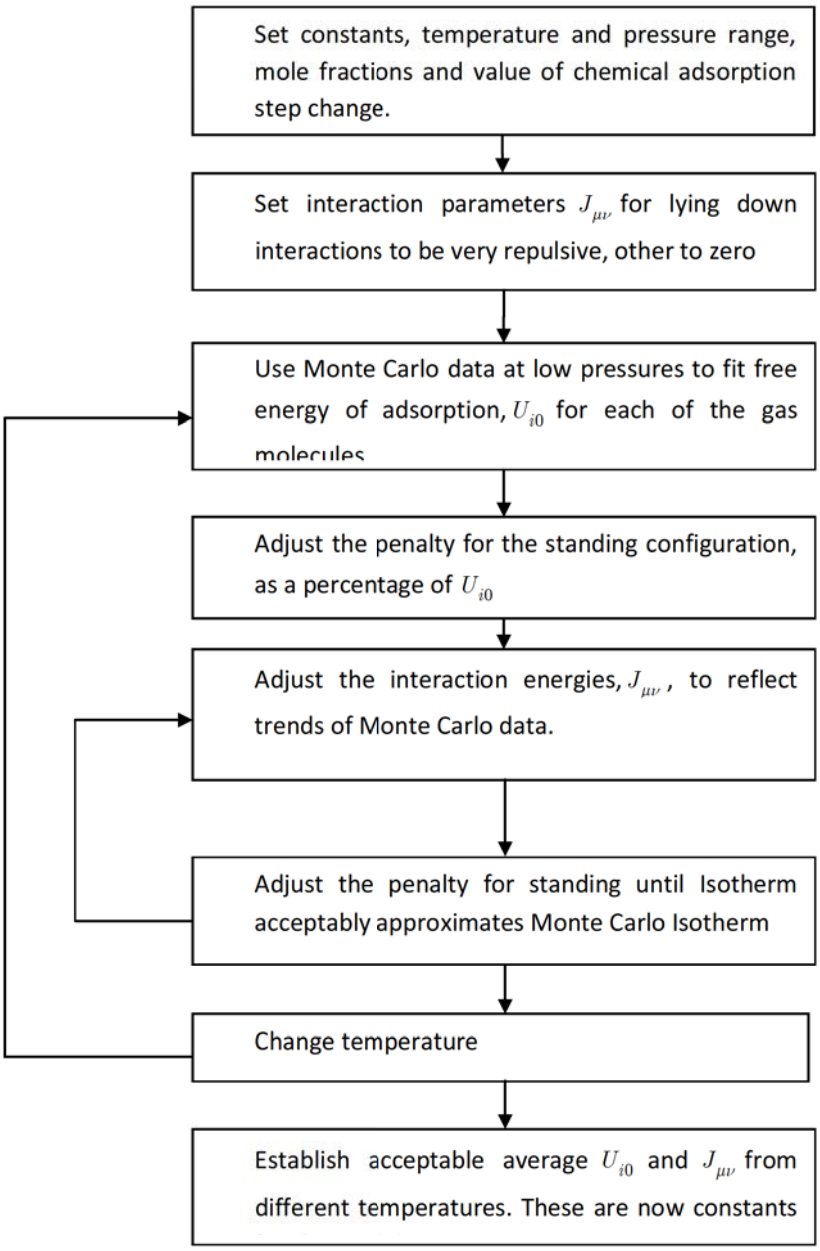

Figure 5-5 Flow chart describing method for determining isotherm interactions

5.4 Results

To investigate the isotherms produced by Monte Carlo simulations for ternary mixtures a lattice model of spherical molecules was produced. This model allows for the investigation of the effect that the value for the free energy of adsorption of each molecule has on the shape of the isotherms. As previously mentioned this model uses an interaction matrix of 6×6 parameters. The modelling procedure described in the previous section was

implemented to obtain the values of U_{a0}, U_{b0} & U_{c0} at low pressures. Establishing these values allowed for the effect of the intermolecular interactions $J_{\mu\nu}$ to be investigated. These interactions determine the rates of adsorptions, and also the adsorption preference reversal for carbon dioxide and ethane shown in the Monte Carlo simulations (see Figure 5-6 and Figure 5-7).

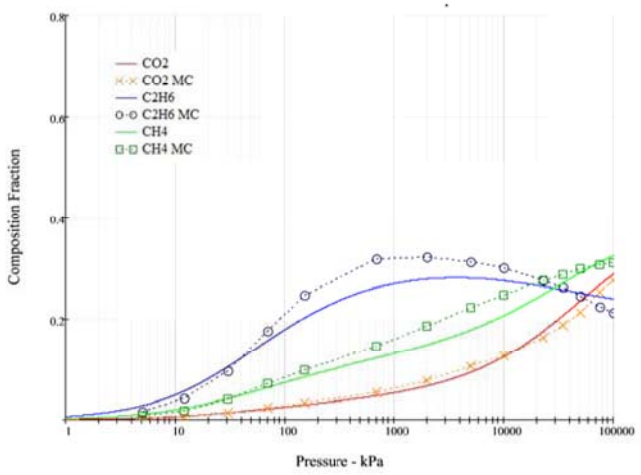

Figure 5-6 isotherms for natural gas mixture composition at 298K compared with Monte Carlo simulation.

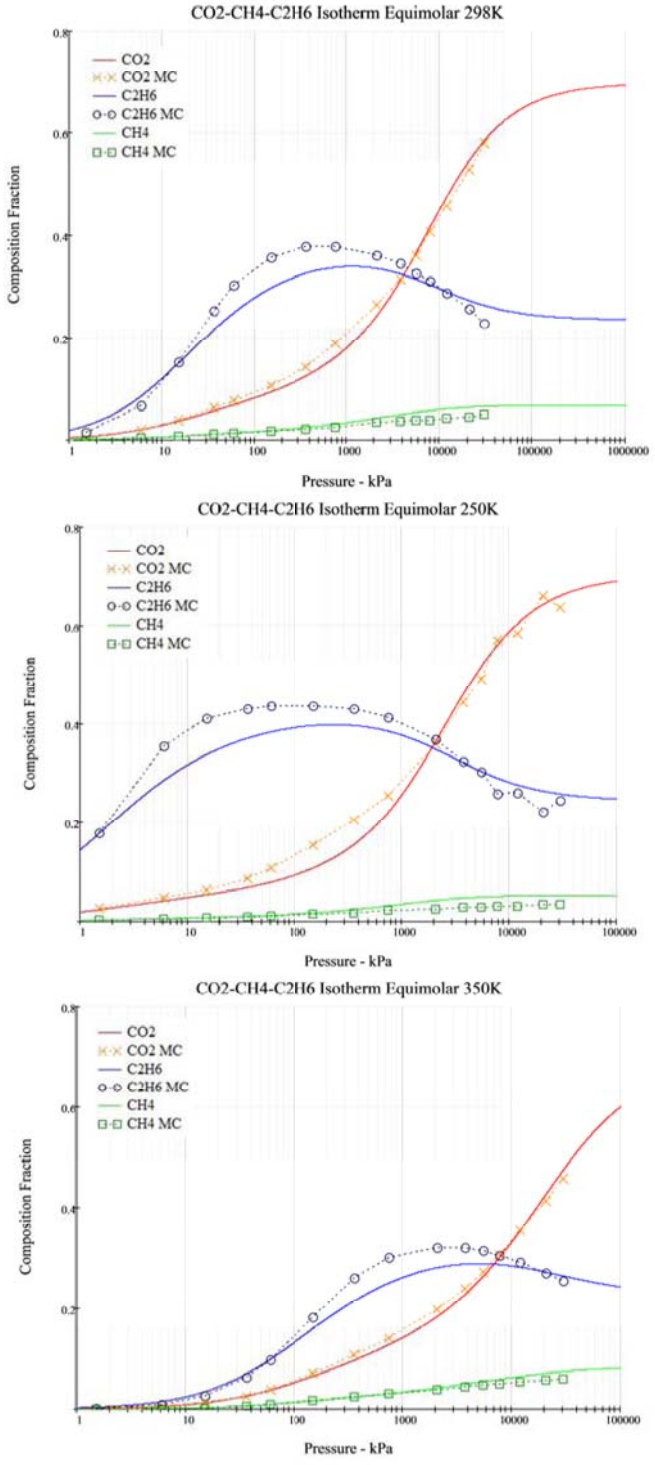

Figure 5-7 isotherms for equimolar mixtures of carbon dioxide, methane and ethane at various temperatures 250K, 298K & 350K compared with Monte Carlo simulation data over the same range.

FUTURE WORK

- Global warming has been identified as one of the world's major environmental issues. While it is impossible to completely stop the effects of anthropological global warming, it is possible to mitigate these effects via a variety of options. One such option is the reduction of greenhouse gas emissions by the capture of carbon dioxide from power plant flue gases with a typical composition of 15 to 20 percent N2 and 60-70 percent CO2. Therefore, it is suggested that future work should be focused on nitrogen and carbon dioxide mixture adsorption in silicalite.
- Adsorption of large molecules in silicalite such as pentane and hexane should also be focused on for future work. The configurational-bias Monte Carlo technique may present some difficulties, for example, the growth of the molecules may be stuck. Therefore, some modification may be needed. Some related techniques have been developed and discussed in section 2.15, which may solve such

problem. The same technique could be used for obtaining adsorption information of larger molecules (e.g. polymers and proteins) as they play a significant role in industrial processes, for example, in petroleum processing and catalytic process, etc.

- Statistical mechanical lattice model has proved that can be relied on to predict the adsorption isotherms for single and mixture of relatively small molecules. The model should be extended to calculate adsorption isotherm for larger molecules such as pentane and hexane.

REFERENCES

Abdul-Rehman, H. B., Hasanain, M. A. & Loughlin, K. F. (1990) "Quaternary, ternary, binary, and pure component sorption on zeolites. 1. Light alkanes on Linde S-115 silicalite at moderate to high pressures" *Industrial & Engineering Chemistry Research* **29**, 1525-1535.

Alexandrowicz, Z. (1998) "Simulation of polymers with rebound selection" *Journal of Chemical Physics* **109**, 5622.

Allen, M. P. & Tildesley, D. J. (1987) *"Computer simulation of liquids"* : Clarendon Press, Oxford, New York.

Aranovich, G. & Donohue, M. (1998b) "Analysis of adsorption isotherms: Lattice theory predictions, classification of isotherms for gas-solid equilibria, and similarities in gas and liquid adsorption behavior" *Journal of Colloid and Interface Science* **200**, 273-290.

Aranovich, G. & Donohue, M. (1998a) "Analysis of adsorption isotherms: Lattice theory predictions, classification of isotherms for gas-solid equilibria, and similarities in gas and liquid adsorption behavior" *Journal of Colloid and Interface Science* **200**, 273-290.

Atkins, P. W. (1998) *"Physical chemistry"* Oxford: Oxford University Press.

Aziz, R. A. & Chen, H. H. (1977) "Accurate Intermolecular Potential for Argon" *Journal of Chemical Physics* **67**, 5719-5726.

Babarao, R., Hu, Z., Jiang, J., Chempath, S. & Sandler, S. I. (2006a) "Storage and separation of CO2 and CH4 in silicalite, C168 schwarzite, and IRMOF-1: A comparative study from Monte Carlo simulation" *Langmuir* **23**, 659-666.

Babarao, R., Hu, Z., Jiang, J., Chempath, S. & Sandler, S. I. (2006b) "Storage and separation of CO2 and CH4 in silicalite, C168 schwarzite, and IRMOF-1: A comparative study from Monte Carlo simulation" *Langmuir* **23**, 659-666.

Bancroft, W. D. (1918) "Adsorption in vacuum tubes" *Journal of Physical Chemistry*.

Barker, J. A. & Henderson, D. (1971) "Monte Carlo values for radial distribution function of a system of fluid hard spheres" *Molecular Physics* **21**, 187-191.

Bassett, D. R., Boucher, E. A. & Zettlemoyer, A. C. (1968a) "Adsorption studies on hydrated and dehydrated silicas" *Journal of Colloid and Interface Science* **27**, 649-658.

Bassett, D. R., Boucher, E. A. & Zettlemoyer, A. C. (1968b) "Adsorption studies on hydrated and dehydrated silicas" *Journal of Colloid and Interface Science* **27**, 649-658.

Beebe, R. A. & Taylor, H. S. (1924) "Determination of heat of adsorption and some values for hydrogen on nickel and copper" *Journal of the American Chemical Society* **46**, 44.

Bell, G. M. (1969) "One dimensional bonded fluids" *Journal of Mathematical Physics* **10**, 1753.

Bell, G. M. & Dunne, L. J. (1978) "Theory of anomalous temperature dependence in spin labeled lipid monolayers" *Journal of the Chemical Society-Faraday Transactions Ii* **74**, 149-159.

Bell, G. M. & Dunne, L. J. (1979) "Statistical mechanics of anomalous thermal effects in monolayers" *Journal of Physics C: Solid State Physics* **12**, 4137-4149.

Bell, G. M. & Salt, D. W. (1973) "Bulk and boundary effects in a one dimensional water like fluid" *Molecular Physics* **26**, 887-903.

Berzelius, J. J. (1836) *Jahresber* **15**, 237-245.

Bezus, A. G., Kiselev, A. V., Lopatkin, A. A. & Du, P. Q. (1978) "Molecular statistical calculation of thermodynamic adsorption characteristics of zeolites using atom-atom approximation .1. Adsorption of methane by zeolite Nax" *Journal of the Chemical Society, Faraday Transactions 2: Molecular and Chemical Physics* **74**, 367-379.

Blinder, S. M. (1969) "Advanced Physical Chemistry: A Survey of Modern Theoretical Principles" *Journal of Chemical Education* **46**, A894.

Bomchil, G., Harris, N., Leslie, M., Tabony, J., White, J. W., Gamlen, P. H., Thomas, R. K. & Trewern, T. D. (1979) "Structure and Dynamics of Ammonia Adsorbed on Graphitized Carbon-Black .1. Adsorption-Isotherms and Thermodynamic Properties" *Journal of the Chemical Society, Faraday Transactions 1: Physical Chemistry in Condensed Phases* **75**, 1535-1541.

Brady, B. O., Kao, C. P. C., Dooley, K. M., Knopf, F. C. & Gambrell, R. P. (1987) "Supercritical Extraction of Toxic Organics from Soils" *Industrial & Engineering Chemistry Research Res* **26**, 261-268.

British Zeolite Association (2006) http://www.bza.org/

Brunauer, S. (1945) *"The adsorption of gases and vapors"* : Princeton, Princeton University Press.

Brunauer, S., Deming, L. S., Deming, E. & Teller, E. (1940) "On a theory of the Van der Waals adsorption of gases" *Journal of the American Chemical Society*.

Brunauer, S., Emmett, P. H. & Teller, E. (1938) "Adsorption of gases in multi molecular layers" *Journal of the American Chemical Society* **60**, 309-319.

Bruno, E., Marconi, M. B. & Evans, R. (1987) "Phase-transitions in a confined lattice gas - Prewetting and capillary condensation" *Physica A* **141**, 187-210.

Catlow, C. R. A. (1992a) *"Modelling of structure and reactivity in zeolites"* : Academic Press Inc.

Catlow, C. R. A. (1992b) *"Modelling of structure and reactivity in zeolites"* : Academic Press Inc.

Catlow, C. R. A., Freeman, C. M., Vessal, B., Tomlinson, S. M. & Leslie, M. (1991b) "Molecular dynamics studies of hydrocarbon diffusion in zeolites" *Journal of the Chemical Society-Faraday Transactions* **87**, 1947.

Catlow, C. R. A., Freeman, C. M., Vessal, B., Tomlinson, S. M. & Leslie, M. (1991a) "Molecular dynamics studies of hydrocarbon diffusion in zeolites" *Journal of the Chemical Society-Faraday Transactions* **87**, 1947.

Champion, W. M. & Halsey, G. D. (1953) "Physical adsorption on uniform surfaces" *Journal of Physical Chemistry* **57**, 646-648.

Chiang, A. S. T., Lee, C. K., Rudzinski, W., Narkiewicz-Michalek, J. & Szabelski, P. (1997) "Energy and structure heterogeneities for the adsorption in zeolites" *Equilibria and Dynamics of Gas Adsorption on Heterogeneous Solid Surfaces* **104**, 519-572.

Consta, S., Vlugt, T. J. H., Hoeth, J. W., Smit, B. & Frenkel, D. (1999) "Recoil growth algorithm for chain molecules with continuous interactions" *Molecular Physics* **97**, 1243-1254.

Consta, S., Wilding, N. B., Frenkel, D. & Alexandrowicz, Z. (1998) "Recoil growth: An efficient simulation method for multi-polymer systems" *Journal of Chemical Physics* **110**, 3220-3228.

Cracknell, R. F. & Nicholson, D. (1994) "Grand canonical Monte Carlo study of Lennard Jones mixtures in slit pores. Part 3. Mixtures of 2 molecular fluids: ethane and propane" *Journal of the Chemical Society, Faraday Transactions* **90**, 1487-1493.

Cuadros, F., Cachadiña, I. & Ahumada, W. (1996) "Determination of Lennard-Jones interaction parameters using a new procedure" *Molecular Engineering* **V6**, 319-325.

Cundy, C. S. & Cox, P. A. (2003) "The hydrothermal synthesis of zeolites: History and development from the earliest days to the present time" Chemical Reviews **103**, 663-702.

DeFilippi, R. P., Robey, R. J. & Industrial Environmental Research Laboratory (Research Triangle Park (1983) *"Supercritical fluid regeneration of adsorbents"* Research Triangle Park, NC: U.S. Environmental Protection Agency, Industrial Environmental Research Laboratory.

Delara, E. C., Kahn, R. & Goulay, A. M. (1989b) "Molecular dynamics by numerical simulation in zeolites - Methane in Naa" *Journal of Chemical Physics* **90**, 7482-7491.

Delara, E. C., Kahn, R. & Goulay, A. M. (1989a) "Molecular dynamics by numerical simulation in zeolites - Methane in Naa" *Journal of Chemical Physics* **90**, 7482-7491.

Demontis, P., Suffritti, G. B. & Mura, P. (1992b) "A molecular dynamics study of diffusion of methane in silicalite molecular sieve at high dilution" *Chemical Physics Letters* **191**, 553-560.

Demontis, P., Suffritti, G. B. & Mura, P. (1992a) "A molecular dynamics study of diffusion of methane in silicalite molecular sieve at high dilution" *Chemical Physics Letters* **191**, 553-560.

Deoliveira, M. J. & Griffiths, R. B. (1978) "Lattice gas model of multiple layer adsorption" *Surface Science* **71**, 687-694.

Depablo, J. J., Laso, M. & Suter, U. W. (1992) "Estimation of the chemical potential of chain molecules by simulation" *Journal of Chemical Physics* **96**, 6157-6162.

Do, D. D. (1998) *"Adsorption analysis: equilibria and kinetics"* : Imperial College Press.

Du, Z. M., Dunne, L. J., Chaplin, M. F. & Manos, G. (1999) "Comparative study of mean-field theory and Monte Carlo simulation of supercritical methane adsorption in zeolites" *Chemical Physics Letters* **307**, 413-418.

Du, Z. M., Dunne, L. J., Manos, G. & Chaplin, M. F. (2000) "Exact statistical mechanical treatment of benzene adsorption in a zeolite twin-pore one-dimensional lattice model" *Chemical Physics Letters* **318**, 319-324.

Du, Z. M., Manos, G., Vlugt, T. J. H. & Smit, B. (1998) "Molecular simulation of adsorption of short linear alkanes and their mixtures in silicalite" *Aiche Journal* **44**, 1756-1764.

Dunne, J. A., Mariwala, R., Rao, M., Sircar, S., Gorte, R. J. & Myers, A. L. (1996b) "Calorimetric heats of adsorption and adsorption isotherms. 1. O2, N2, Ar, CO2, CH4, C2H6, and SF6 on silicalite" *Langmuir* **12**, 5888-5895.

Dunne, J. A., Mariwala, R., Rao, M., Sircar, S., Gorte, R. J. & Myers, A. L. (1996a) "Calorimetric heats of adsorption and adsorption isotherms. 1. O2, N2, Ar, CO2, CH4, C2H6, and SF6 on silicalite" *Langmuir* **12**, 5888-5895.

Dunne, J. A., Mariwala, R., Rao, M., Sircar, S., Gorte, R. J. & Myers, A. L. (1996d) "Calorimetric heats of adsorption and adsorption isotherms. 1. O2, N2, Ar, CO2, CH4, C2H6, and SF6 on silicalite" *Langmuir* **12**, 5888-5895.

Dunne, J. A., Mariwala, R., Rao, M., Sircar, S., Gorte, R. J. & Myers, A. L. (1996c) "Calorimetric heats of adsorption and adsorption isotherms. 1. O2, N2, Ar, CO2, CH4, C2H6, and SF6 on silicalite" *Langmuir* **12**, 5888-5895.

Dunne, L. J. & Bell, G. M. (1980) "Theory of cooperative phenomena in monolayers of hydroxyhexadecanoic acid isomers" *Journal of the Chemical Society, Faraday Transactions 2: Molecular and Chemical Physics* **76**, 431-440.

Dunne, L. J. & Manos, G. (2004) "Exact statistical mechanical treatment of a toroidal lattice model of narrow-bore nanotube alkane adsorption isotherms and comparison with Monte-Carlo simulations" *Chemical Physics Letters* **390**, 14-19.

Dunne, L. J., Manos, G. & Du, Z. M. (2003) "Exact statistical mechanical one-dimensional lattice model of alkane binary mixture adsorption in zeolites and comparison with Monte-Carlo simulations" *Chemical Physics Letters* **377**, 551-556.

Dunne, L. J. & Reuben, B. G. (1995b) "Application of the field theoretic method of Bohm and Pines to the determination of the activity coefficients of strong 1/1 electrolytes" *Chemical Physics Letters* **242**, 560-569.

Dunne, L. J. & Reuben, B. G. (1995a) "Application of the field theoretic method of Bohm and Pines to the determination of the activity coefficients of strong 1/1 electrolytes" *Chemical Physics Letters* **242**, 560-569.

Ebner, C. (1980) "Film formation on a weakly attractive substrate within the lattice gas model" *Physical Review A* **22**, 2776-2781.

Ertl, G. & Koch, J. (1970) "Adsorption of Co on a Palladium(III) surface" *Zeitschrift fur Naturforschung Part A-Astrophysik Physik und Physikalische Chemie* **A 25**, 1906.

Faraday, M. (1834) "Experimental researches in electricity. Sixth series" *Philosophical Transactions of the Royal Society of London* **124**, 55-76.

Favre, P. A. (1874) *Ann Chim Phys* **1**, 209.

Flory, P. J. (1969) *"Statistical mechanics of chain molecules"* New York: Interscience.

Fontana, F. (1777) *Memorie di Matematica e Fisica della Società Italiana*, 679.

Fowler, R. H. (1935) "A statistical derivation of the Langmuir adsorption isotherm". p. 260: Proceedings of the Cambridge Philosophical Society.

Frenkel, D. & Smit, B. (2002) *"Understanding molecular simulation from algorithms to applications"* : Academic Press.

Funke, H. H., Argo, A. M., Falconer, J. L. & Noble, R. D. (1997a) "Separations of cyclic, branched, and linear hydrocarbon mixtures through silicalite membranes" *Ind Eng Chem Res* **36**, 137-143.

Funke, H. H., Frender, K. R., Green, K. M., Wilwerding, J. L., Sweitzer, B. A., Falconer, J. L. & Noble, R. D. (1997b) "Influence of adsorbed molecules on the permeation properties of silicalite membranes" *Journal of Membrane Science* **129**, 77-82.

Galassi, G. & Tildesley, D. J. (1994) "Phase diagrams of diatomic molecules using the Gibbs ensemble Monte Carlo method" *Molecular Simulation* **13**, 11-24.

Gallo, M., Nenoff, T. M. & Mitchell, M. C. (2006) "Selectivities for binary mixtures of hydrogen/methane and hydrogen/carbon dioxide in silicalite and ETS-10 by Grand Canonical Monte Carlo techniques" *Fluid Phase Equilibria* **247**, 135-142.

Garcia-Perez, E., Parra, J., Ania, C., Garcia-Sanchez, A., van Baten, J., Krishna, R., Dubbeldam, D. & Calero, S. (2007) "A computational study of CO2, N2, and CH4 adsorption in zeolites" *Adsorption* **13**, 469-476.

Golden, T. C. & Sircar, S. (1994c) "Gas adsorption on silicalite" *Journal of Colloid and Interface Science* **162**, 182-188.

Golden, T. C. & Sircar, S. (1994a) "Gas adsorption on silicalite" *Journal of Colloid and Interface Science* **162**, 182-188.

Golden, T. C. & Sircar, S. (1994b) "Gas adsorption on silicalite" *Journal of Colloid and Interface Science* **162**, 182-188.

Gregg, S. J. & Sing, K. S. W. (1982) *"Adsorption, surface area and porosity"* : Academic Press, London.

Guggenheim, E. A. & Mcglashan, M. L. (1960) "Interaction between argon atoms" *Proceedings of the Royal Society of London Series A-Mathematical and Physical Sciences* **255**, 456-476.

Gump, C. J., Noble, R. D. & Falconer, J. L. (1999) "Separation of hexane isomers through nonzeolite pores in ZSM-5 zeolite membranes" *Industrial & Engineering Chemistry Research* **38**, 2775-2781.

Hill, T. L. (1960) *"An introduction to statistical thermodynamics"* Reading (Mass.): Addison-Wesley.

Hill, T. L. (1949) "Extension of fowler treatment of surface tension to physical adsorption" *Journal of Chemical Physics* **17**, 668-669.

Huang, K. (1988) *"Statistical mechanics"* : John Wiley & Sons.

International Zeolite Association (2010a) http://www.iza-online.org

International Zeolite Association (2010b) http://www.iza-online.org

Ising, E. (1925) "Beitrag zur Theorie des Ferromagnetismus" *Zeitschrift für Physik* **31**, 253-258.

Jaroniec, M. & Madey, R. (1988) "Adsorption theory of volume filling of micropores for structurally heterogeneous solids" *Journal of the Chemical Society, Faraday Transactions 2: Molecular and Chemical Physics* **84**, 1139-1148.

Johnston, K. P. & Haynes, C. (1987) "Extreme solvent effects on reaction rate constants at supercritical fluid conditions" *Aiche Journal* **33**, 2017-2026.

Jorgensen, W. L., Madura, J. D. & Swenson, C. J. (1984) "Optimized intermolecular potential functions for liquid hydrocarbons" *Journal of the American Chemical Society* **106**, 6638-6646.

June, R. L., Bell, A. T. & Theodorou, D. N. (1990) "Prediction of low occupancy sorption of alkanes in silicalite" *Journal of Physical Chemistry* **94**, 1508-1516.

June, R. L., Bell, A. T. & Theodorou, D. N. (1992b) "Molecular dynamics studies of butane and hexane in silicalite" *Journal of Physical Chemistry* **96**, 1051-1060.

June, R. L., Bell, A. T. & Theodorou, D. N. (1992a) "Molecular dynamics studies of butane and hexane in silicalite" *Journal of Physical Chemistry* **96**, 1051-1060.

Kayser, H. (1881) *Wiederman's Ann Phys Chem*, 451.

Kramers, H. A. & Wannier, G. H. (1941) "Statistics of the two dimensional ferromagnet. Part I" *Physical Review* **60**, 252-262.

Kretschmer, Rolf G., Fiedler & Klause (1977) "Calculation of the thermodynamic functions of n-alkanes absorbed in zeolites using the Monte Carlo method" *Zeitschrift fuer Physikalische Chemie (Leipzig)* **258**, 1045-1058.

Krishna, R. & Paschek, D. (2001b) "Molecular simulations of adsorption and siting of light alkanes in silicalite-1" *Physical Chemistry Chemical Physics*, 453-462.

Krishna, R. & Paschek, D. (2001a) "Molecular simulations of adsorption and siting of light alkanes in silicalite-1" *Physical Chemistry Chemical Physics*, 453-462.

Krishna, R. & Paschek, D. (2001c) "Molecular simulations of adsorption and siting of light alkanes in silicalite-1" *Physical Chemistry Chemical Physics*, 453-462.

Lachet, V., Boutin, A., Tavitian, B. & Fuchs, A. H. (1997) "Grand canonical Monte Carlo simulations of adsorption of mixtures of xylene molecules in faujasite zeolites" *Faraday Discussions*, 307-323.

Langmuir, I. (1913) "Chemical reactions at very low pressures. I. The clean up of oxygen in a tungsten lamp" *Journal of the American Chemical Society* **35**, 105-127.

Langmuir, I. (1915) "Chemical reaction at low pressures" *Journal of the American Chemical Society* **37**, 1139-1167.

Langmuir, I. (1918) "The adsorption of gases on plane surfaces of glass, mica and platinum" *Journal of the American Chemical Society* **40**, 1361-1403.

Leach, A. R. (2001) *"Molecular modelling - principles and applications"* Harlow, England ; New York: Prentice Hall.

Lee, C. K., Chiang, A. S. T. & Wu, F. Y. (1992) "Lattice model for the adsorption of benzene in silicalite-I" *Aiche Journal* **38**, 128-135.

Lee, T. D. & Yang, C. N. (1952) "Statistical theory of equations of state and phase transitions .II. lattice gas and Ising model" *Physical Review* **87**, 410-419.

Lennard-Jones, J. E. (1925) "On the forces between atoms and ions" *Proceedings of the Royal Society of London* **109**, 584-597.

Lifshitz, E. M. (1956) "The theory of molecular attractive forces between solid" *Soviet Physics JETP* **2**, 73-83.

Lin, X., Falconer, J. L. & Noble, R. D. (1998) "Parallel pathways for transport in ZSM-5 zeolite membranes" *Chem Mater* **10**, 3716-3723.

Maitland, G. C., Rigby, M., Smith, E. B. & Wakeham, W. A. (1987) *"Intermolecular forces: Their origin and determination"* : Clarendon Press.

Maitland, G. C. & Smith, E. B. (1973) "Simplified representation of intermolecular potential energy" *Chemical Physics Letters* **22**, 443-446.

Makri, M., Jiang, Y., Yentekakis, I. V. & Vayenas, C. G. (1996) "Oxidative coupling of methane to ethylene with 85% yield in a gas recycle electrocatalytic or catalytic reactor-separator" *11Th International Congress on Catalysis - 40Th Anniversary, Pts A and B* **101**, 387-396.

Maris, T., Vlugt, T. J. H. & Smit, B. (1998) "Simulation of alkane adsorption in the aluminophosphate molecular sieve AlPO4-5" *Journal of Physical Chemistry B* **102**, 7183-7189.

Maxwell, I. E. & Stork, W. H. J. (2001) Hydrocarbon processing with zeolites In *Introduction to zeolite science and practice*, 2nd completely rev. and expanded edn. Edited by H. v. Bekkum, P. A. Jacobs, E. M. Flanigen & J. C. Jansen. Amsterdam: Elsevier.

McBain, J. W. & Britton, G. T. (1930) "The nature of the sorption by charcoal of gases and vapors under great pressure" *Journal of the American Chemical Society* **52**, 2198.

Mclachlan, A. D. (1964) "Van der Waals forces between an atom and a surface" *Molecular Physics* **7**, 381.

Meirovitch, H. (1988) "Statistical properties of the scanning simulation method for polymer chains" *Journal of Chemical Physics* **89**, 2514-2522.

Mentzen, B. F. & Lefebvre, F. (1997) "Flexibility of the MFI silicalite framework upon benzene adsorption at higher pore-fillings: A study by X-ray powder diffraction, NMR and molecular mechanics" *Materials Research Bulletin* **32**, 813-821.

Metropolis, N., Rosenbluth, A. W., Rosenbluth, M. N., Teller, A. H. & Teller, E. (1953) "Equation of state calculations by fast computing machines" *Journal of Chemical Physics* **21**, 1087-1092.

Mooij, G. C. A. M., Frenkel, D. & Smit, B. (1992) "Direct Simulation of Phase-Equilibria of Chain Molecules" *Journal of Physics-Condensed Matter* **4**, L255-L259.

Morozzo, C. L. (1783) *Observations Sur La Physique, Sur l'Historie Naturelle Et Sur Les Arts* **23**, 58.

Nicholas, J. B., Trouw, F. R., Mertz, J. E., Iton, L. E. & Hopfinger, A. J. (1993a) "Molecular dynamics simulation of propane and methane in silicalite" *Journal of Physical Chemistry* **97**, 4149-4163.

Nicholas, J. B., Trouw, F. R., Mertz, J. E., Iton, L. E. & Hopfinger, A. J. (1993b) "Molecular dynamics simulation of propane and methane in silicalite" *Journal of Physical Chemistry* **97**, 4149-4163.

Nicholson, D. (1975) "Molecular theory of adsorption in pore spaces .1. Isotherms for simple lattice models" *Journal of the Chemical Society, Faraday Transactions I* **71**, 238-255.

Nicholson, D. (1976) "Molecular theory of adsorption in pore spaces .2. Thermodynamic and molecular lattice model descriptions of capillary condensation" *Journal of the Chemical Society, Faraday Transactions I* **72**, 29-39.

Nicholson, D. & Gubbins, K. E. (1996) "Separation of carbon dioxide-methane mixtures by adsorption: Effects geometry and energetics on selectivity" *Journal of Chemical Physics* **104**, 8126-8134.

Nicholson, D. & Parsonage, G. (1982a) *"Computer simulation and the statistical mechanics of adsorption"* : Academic Press.

Nicholson, D. & Parsonage, G. (1982b) *"Computer simulation and the statistical mechanics of adsorption"* : Academic Press.

Nicholson, D. & Silvester, R. G. (1977) "Investigation of step formation in multilayer adsorption isotherms using a lattice model" *Journal of Colloid and Interface Science* **62**, 447-453.

Okayama, T., Yoneya, J. & Nitta, T. (1995) "Monte Carlo simulations of adsorption in a slitlike pore for binary mixtures of butane and carbon dioxide at supercritical conditions" *Fluid Phase Equilibria* **104**, 305-316.

Olson, D. H., Kokotailo, G. T., Lawton, S. L. & Meier, W. M. (1981) "Crystal structure and structure related properties of Zsm-5" *Journal of Physical Chemistry* **85**, 2238-2243.

Onsager, L. (1944) "A two dimensional model with an order disorder transition" *Physical Review* **65**, 117-149.

Pan, D. F. & Mersmann, A. (1990) "Multilevel Adsorption and Hysteresis in Well-Defined Zeolite Sorbents" *Zeolites* **10**, 210-212.

Panagiotopoulos, A. Z. (1987b) "Direct determination of phase coexistence properties of fluids by Monte Carlo simulation in a new ensemble" *Molecular Physics* **61**, 813-826.

Panagiotopoulos, A. Z. (1987a) "Direct determination of phase coexistence properties of fluids by Monte Carlo simulation in a new ensemble" *Molecular Physics* **61**, 813-826.

Panagiotopoulos, A. Z. (1992) "Direct determination of fluid phase equilibria by simulation in the Gibbs ensemble - A review" *Molecular Simulation* **9**, 1-23.

Panagiotopoulos, A. Z., Quirke, N., Stapleton, M. & Tildesley, D. J. (1988) "Phase equilibria by simulation in the Gibbs ensemble - Alternative derivation, generalization and application to mixture and membrane equilibria" *Molecular Physics* **63**, 527-545.

Pope, C. G. (1986) "Sorption of benzene, toluene, and para-xylene on silicalite and H-Zsm-5" *Journal of Physical Chemistry* **90**, 835-837.

Press, W. H. & Flannery, B. P. (1994) *"Numerical recipes in FORTRAN : the art of scientific computing"* Cambridge [England]: Cambridge University Press.

Putnam, F. A. & Fort, T. (1975) "Physical adsorption on patchwise heterogeneous surfaces .1. heterogeneity, 2-dimensional phase transitions, and spreading pressure of krypton-graphitized carbon black system near 100 K" *Journal of Physical Chemistry* **79**, 459-467.

Rabo, J. A. (1976) *"Zeolite chemistry and catalysis"* Washington: American Chemical Society.

Richardson, L. B. (1917) "The adsorption of carbon dioxide and ammonia by charcoal" *Journal of the American Chemical Society* **39**, 1892.

Roberts, J. K. (1930) Exchange of energy between gas atoms and solid surface In *Proceedings of the Royal Society*, p. 146: Royal Society (Great Britain).

Rosenbluth, M. N. & Rosenbluth, A. W. (1955) "Monte Carlo calculation of the average extension of molecular chains" *Journal of Chemical Physics* **23**, 356-359.

Ross, S. & Winkler, W. (1955) "Physical adsorption VIII monolayer adsorption of Argon and Nitrogen on Graphitised Carbon". 10 edn, p. 319.

Rouppe, H. W. & Norden (1799) *Annales de chimie--science des materiaux, ser 1* **32**, 3.

Ryckaert, J. P. & Bellemans, A. (1978) "Molecular dynamics of liquid alkanes" *Faraday Discussions*, 95-106.

sabatier-Reid, P. (1922) *"Catalysis in organic chemistry"* : Van Nostrand Company, New York.

Scheele C.W. (1780) *"Chemical observations on air and fire"* .

Shen, D. M. & Rees, L. V. C. (1991) "Adsorption and diffusion of n-butane and 2-butane in silicalite-1" *Zeolites* **11**, 684-689.

Siepmann, J. I., Martin, M. G., Mundy, C. J. & Klein, M. L. (1997) "Intermolecular potentials for branched alkanes and the vapour-liquid phase equilibria of n-heptane, 2-methylhexane, and 3-ethylpentane" *Molecular Physics* **90**, 687-693.

Sing, K. S. W. (1985) "IUPAC Commission on Colloid and Surface Chemistry Including Catalysis" *Pure and Applied Chemistry* **57**, 603-619.

Smit, B. (1995a) "Grand canonical Monte Carlo simulations of chain molecules - Adsorption isotherms of alkanes in zeolites" *Molecular Physics* **85**, 153-172.

Smit, B. (1995b) "Simulating the adsorption isotherms of methane, ethane, and propane in the zeolite silicalite" *Journal of Physical Chemistry* **99**, 5597-5603.

Smit, B. & Siepmann, J. I. (1994) "Simulating the adsorption of alkanes in zeolites" *Science* **264**, 1118-1120.

Smith, J. M. (1981) *"Chemical engineering kinetics"* Boston: McGraw-Hill.

Snurr, R. Q., Bell, A. T. & Theodorou, D. N. (1993) "Prediction of adsorption of aromatic hydrocarbons in silicalite from grand canonical Monte Carlo simulations with biased insertions" *Journal of Physical Chemistry* **97**, 13742-13752.

Soto, J. L. & Myers, A. L. (1981) "Monte Carlo studies of adsorption in molecular sieves" *Molecular Physics* **42**, 971-983.

Stach, H., Thamm, H., Janchen, J., Fiedler, K. & Schirmer, W. (1984) New developments in zeolite science and technology In *Proceedings of the Sixth International Zeolite Conference : Reno, USA 10-15 July 1983*, p. 225. Edited by D. Olson & A. Bisio: Butterworth.

Stroud, H. J. F., Richards, E., Limcharoen, P. & Parsonage, N. G. (1976) "Thermodynamic study of linde sieve 5A + methane system" *Journal of the Chemical Society-Faraday Transactions I* **72**, 942-954.

Sun, M. S., Shah, D. B., Xu, H. H. & Talu, O. (1998d) "Adsorption equilibria of C1 to C4 alkanes, CO2, and SF6 on silicalite" *The Journal of Physical Chemistry B* **102**, 1466-1473.

Sun, M. S., Shah, D. B., Xu, H. H. & Talu, O. (1998g) "Adsorption equilibria of C1 to C4 alkanes, CO2, and SF6 on silicalite" *The Journal of Physical Chemistry B* **102**, 1466-1473.

Sun, M. S., Shah, D. B., Xu, H. H. & Talu, O. (1998f) "Adsorption equilibria of C1 to C4 alkanes, CO2, and SF6 on silicalite" *The Journal of Physical Chemistry B* **102**, 1466-1473.

Sun, M. S., Shah, D. B., Xu, H. H. & Talu, O. (1998e) "Adsorption equilibria of C1 to C4 alkanes, CO2, and SF6 on silicalite" *The Journal of Physical Chemistry B* **102**, 1466-1473.

Sun, M. S., Shah, D. B., Xu, H. H. & Talu, O. (1998c) "Adsorption equilibria of C1 to C4 alkanes, CO2, and SF6 on silicalite" *The Journal of Physical Chemistry B* **102**, 1466-1473.

Sun, M. S., Shah, D. B., Xu, H. H. & Talu, O. (1998b) "Adsorption equilibria of C1 to C4 alkanes, CO2, and SF6 on silicalite" *The Journal of Physical Chemistry B* **102**, 1466-1473.

Sun, M. S., Shah, D. B., Xu, H. H. & Talu, O. (1998a) "Adsorption equilibria of C1 to C4 alkanes, CO2, and SF6 on silicalite" *The Journal of Physical Chemistry B* **102**, 1466-1473.

Tan, C. S. & Liou, D. C. (1988) "Desorption of ethyl acetate from activated carbon by supercritical carbon dioxide" *Industrial & Engineering Chemistry Research* **27**, 988-991.

Temkin, M. I. & Pyzhez, V. (1940) "Kinetica of Ammonia synthesis on promoted Iron catalysts" *Acta Physiochim, USSR* **12**, 217.

Ter-Minassian-Saraga, L. (1985) "IUPAC commission on colloid and surface chemistry including catalysis". 57 edn, pp. 621-632.

Titov, A. (1911) "The adsorption of gases by charcoal" *Z Physik Chem* **74**, 641.

Toth, J. (1962) "Gas- (Dampf-)Adsorption An Festen Oberflachen Inhomogener Aktivitat .2" *Acta Chimica Academiae Scientarium Hungaricae* **31**, 393.

Valenzuela, D. P. & Meyers, A. L. (1989) *"Adsorption equilibrium data handbook"* : Prentice Hall Englewood Cliffs, NJ.

van de Graaf, J. M., Kapteijn, F. & Moulijn, J. A. (1999) "Modeling permeation of binary mixtures through zeolite membranes" *Aiche Journal* **45**, 497-511.

Vanderploeg, P. & Berendsen, H. J. C. (1982) "Molecular dynamics simulation of a bilayer membrane" *Journal of Chemical Physics* **76**, 3271-3276.

Vanmegen, W. & Snook, I. (1980) "The grand canonical ensemble Monte Carlo method applied to the electrical double layer" *Journal of Chemical Physics* **73**, 4656-4662.

Vantassel, P. R., Davis, H. T. & McCormick, A. V. (1994) "New lattice model for adsorption of small molecules in zeolite micropores" *Aiche Journal* **40**, 925-934.

Verlet, L. & Weis, J. J. (1972) "Perturbation theory for thermodynamic properties of simple liquids" *Molecular Physics* **24**, 1013.

Vlugt, T. J. H., Krishna, R. & Smit, B. (1999) "Molecular simulations of adsorption isotherms for linear and branched alkanes and their mixtures in silicalite" *Journal of Physical Chemistry B* **103**, 1102-1118.

Vlugt, T. J. H., Martin, M. G., Smit, B., Siepmann, J. I. & Krishna, R. (1998) "Improving the efficiency of the configurational-bias Monte Carlo algorithm" *Molecular Physics* **94**, 727-733.

von Saussure, T. (1814) "Beobachtungen über die Absorption der Gasarten durch verschiedene Körper" *Annalen der Physik (Leipzig)* **47**, 113.

Vuong, T. & Monson, P. A. (1996b) "Monte Carlo simulation studies of heats of adsorption in heterogeneous solids" *Langmuir* **12**, 5425-5432.

Vuong, T. & Monson, P. A. (1996a) "Monte Carlo simulation studies of heats of adsorption in heterogeneous solids" *Langmuir* **12**, 5425-5432.

Wang, Y., Hill, K. & Harris, J. G. (1993b) "Thin films of n-octane confined between parallel solid surfaces - structure and adhesive forces vs film thickness from molecular dynamics simulations" *Journal of Physical Chemistry* **97**, 9013-9021.

Wang, Y., Hill, K. & Harris, J. G. (1993a) "Thin films of n-octane confined between parallel solid surfaces - structure and adhesive forces vs film thickness from molecular dynamics simulations" *Journal of Physical Chemistry* **97**, 9013-9021.

Wang, Y., Hill, K. & Harris, J. G. (1993c) "Thin films of n-octane confined between parallel solid surfaces - structure and adhesive forces vs film thickness from molecular dynamics simulations" *Journal of Physical Chemistry* **97**, 9013-9021.

Whitehouse, J. S., Nicholson, D. & Parsonage, N. G. (1983) "A grand ensemble Monte Carlo study of krypton adsorbed on graphite" *Molecular Physics* **49**, 829-847.

Woods, G. B. & Rowlinson, J. S. (1989) "Computer simulations of fluids in zeolite-X and zeolite-y" *Journal of the Chemical Society, Faraday Transactions 2* **85**, 765-781.

Yang, C. N. (1952) "The spontaneous magnetization of a 2-dimensional Ising model" *Physical Review* **85**, 808-815.

APPENDIX A – METHANE AND ETHANE ADSORPTION

LATTICE GAS MODEL - METHANE AND ETHANE ADSORPTION IN SILICALITE

The comparisons for methane adsorption in silicalite with experimental data are shown in Figure A-1 to Figure A-4. It is clear that simulated results slightly underestimate the adsorbed amount of methane for all temperatures. Considering the accuracy of the experimental data however, the agreement can be considered satisfactory. It shows that the model of methane adsorption presented above is suitable for a wide range of temperatures.

The results for ethane are presented in Figure A-5, to Figure A-8. Similarly, the agreement between the simulations and experiment is good. It is interesting to note that at low temperatures (275K and 300K), both experiments and simulations show that there is a small kink in the adsorption isotherms at high loading and this kink disappears at higher temperatures. It could be explained that at low pressures ethane molecules move freely and distributed uniformly over the various channels of zeolites.

However, at higher pressures ethane molecules are locked in the zig-zag channels between two intersections. The molecules no longer move freely. The size of the ethane molecules gives a structure that is commensurate with the Zeolites structure.

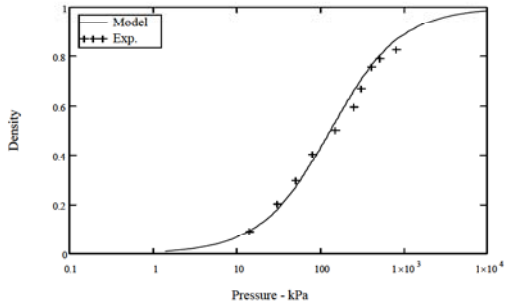

Figure A-1 comparison of methane adsorption isotherm predicted by lattice gas model and experiment at 275K

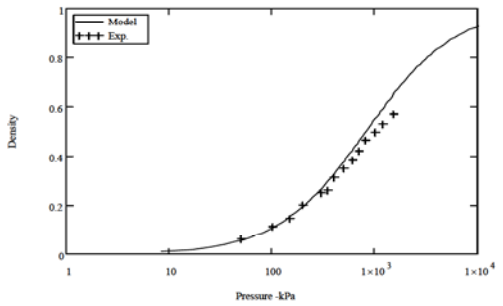

Figure A-4 comparison of methane adsorption isotherm predicted by lattice gas model and experimental at 350K

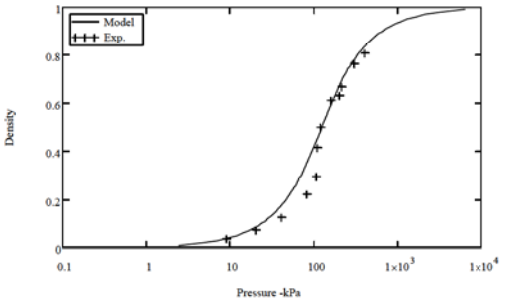

Figure A-2comparison of methane adsorption isotherm predicted by lattice gas model and experiment at 300K

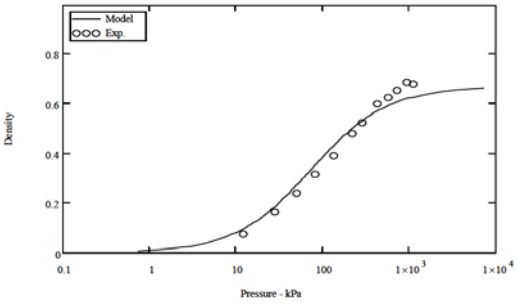

Figure A-5 comparison of ethane adsorption isotherm predicted by lattice gas model and the experimental at 275K.

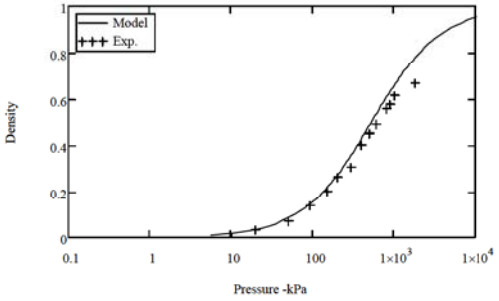

Figure A-3 comparison of methane adsorption isotherm predicted by lattice gas model and experiment at 325K.

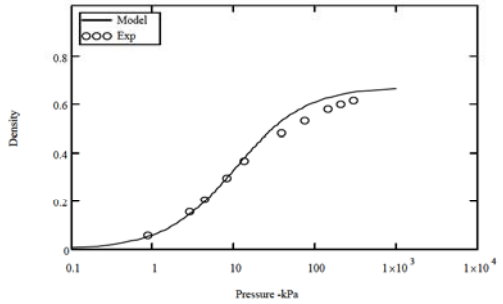

Figure A-6 comparison of ethane adsorption isotherm predicted by lattice gas model and experimental at 300K.

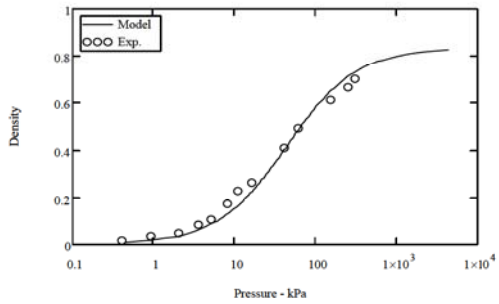

Figure A-7 comparison of ethane adsorption isotherm predicted by lattice gas model and experimental at 325K.

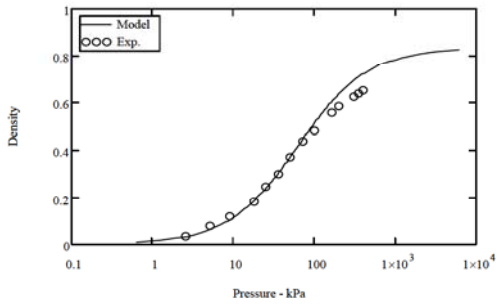

Figure A-8 comparison of ethane adsorption isotherm predicted by lattice gas model and experiment at 350K

Monte Carlo simulation – Methane and ethane adsorption in silicalite

The adsorption isotherms for methane are shown in Figure A-9, the Monte Carlo simulations were also conducted for the temperatures 277 K, 304 K, 308 K, 314 K, 334.4 K, 343 K, and 353 K and they were compared to the same experimental data (Dunne *et al.*, 1996d;Golden & Sircar, 1994c;Sun *et al.*, 1998d). The simulation results match closely to the experimental data for all temperatures. However, it is observed that there is a slight underestimation of the amount of methane adsorbed at high pressures at 277 K. The study of Smit (Smit, 1995b) which included the comparison of different experimental data for the adsorption on silicalite showed that most of experimental results seem to agree closely at low pressures and deviate at high pressures. He also found that in the compared experiments the theoretical maximum loading of methane varies between 2.7 and 3.75 mmol/g. This shows that it is very difficult to determine the loading at high pressures. Therefore, it is concluded that at low pressures accurate experimental data exist and can be compared with the simulation results.

The amount of methane adsorbed is proportional to the increase of pressure, while it is inversely proportional with the increase of temperature.

Comparing methane with carbon dioxide at the same conditions of adsorption; it is noted that carbon dioxide is more adsorbed. This is discussed more in the binary mixtures adsorption isotherms.

The adsorption isotherms for ethane are presented in Figure A-10. The simulations were carried for the temperatures 277 K, 296 K, 308 K, 314 K, and 353 K. Similarly, there is a good agreement between the simulations and the experimental data (Dunne *et al.*, 1996c). However, there is some deviation between the simulation results and the experimental data (Sun *et al.*, 1998c). Du (Du et al., 1998) carried out Monte Carlo simulation and compared their results with the experiment work of Abdul-Rehman (Abdul-Rehman et al., 1990) reported deviations of their ethane adsorption isotherms results with the work of Sun (Sun *et al.*, 1998b).

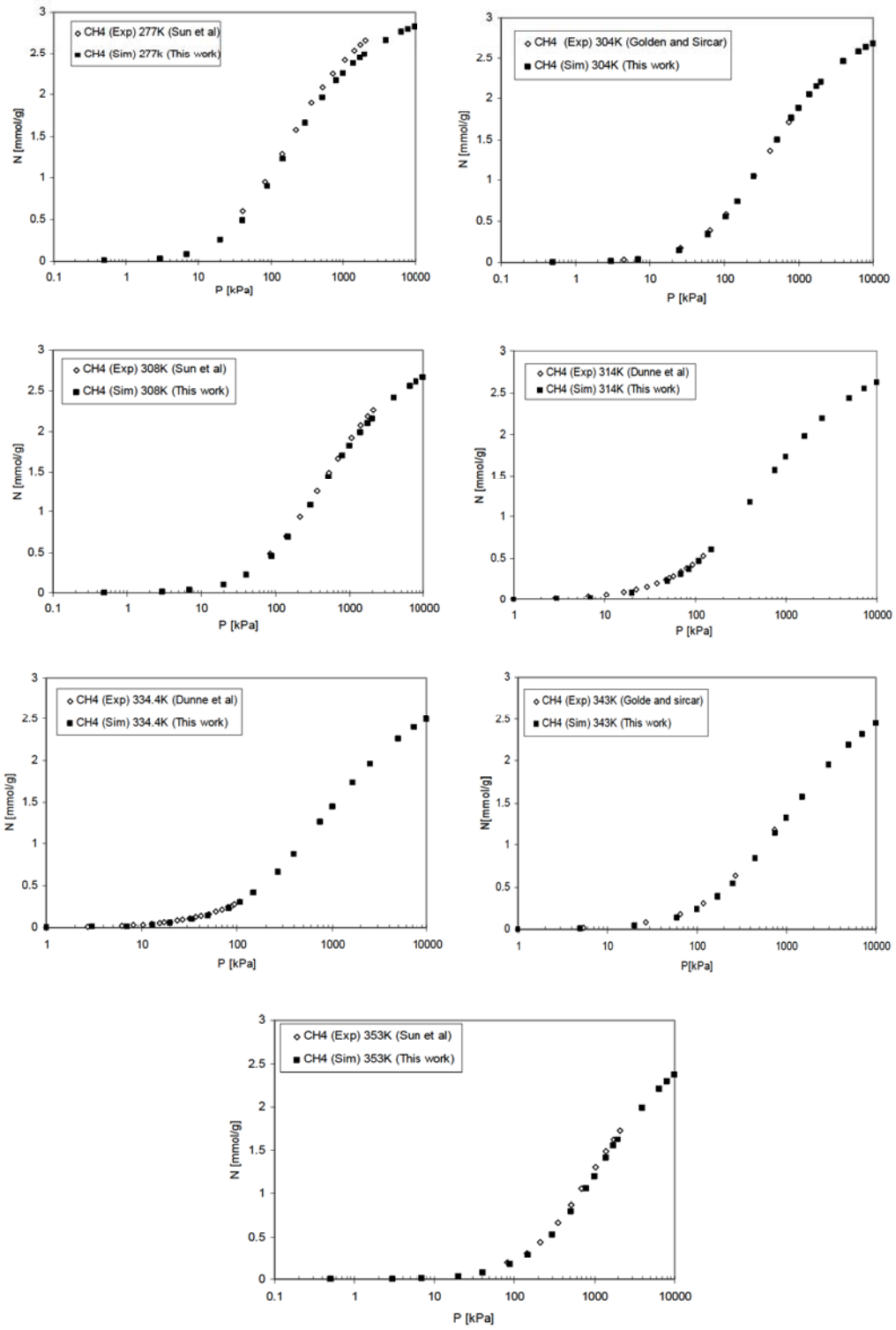

Figure A-9 Monte Carlo simulations (Sim) and experimental (Exp) adsorption isotherms of pure methane in silicalite at various temperatures.

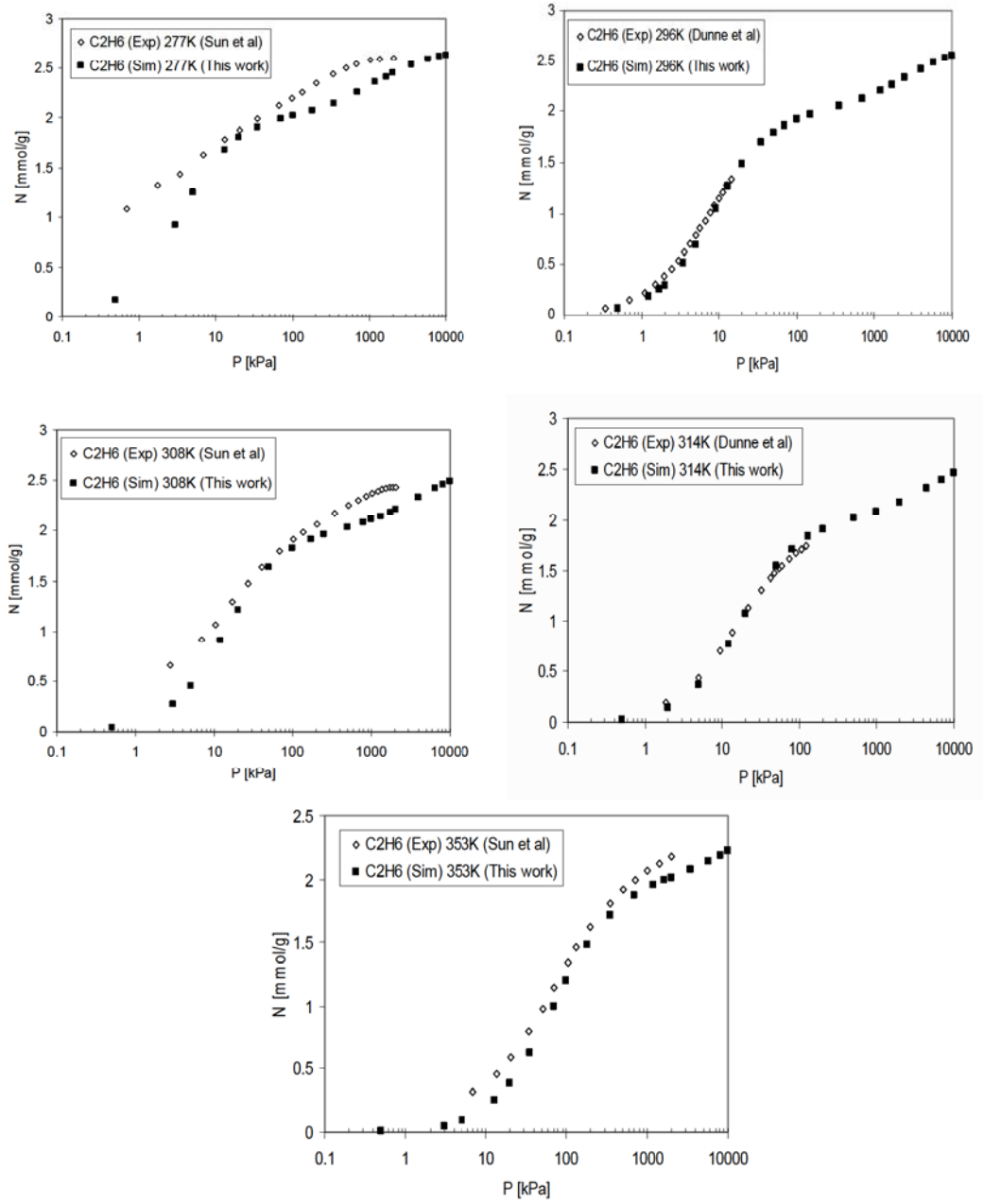

Figure A-10 Monte Carlo simulations (Sim) and experimental (Exp) adsorption isotherms of pure ethane in silicalite at various temperatures.

APPENDIX B – MATHCAD® CODE

Mathcad® code – Lattice Model for propane and i-butane equimolar mixture at 300 K

Planck's constant	$h := 6.625 \times 10^{-34}$
Boltzman's constant	$k := 1.38 \times 10^{23}$
Mass of a proton	$m := 1.67 \times 10^{-27}$
a is propane	$mwa := 44$
b is iso-butane	$mwb := 58$
Temperature	$Temp := 300$

Setting interaction parameters $ua0$, $ub0$, Jaa, Jbb and Jab

$ua0 := -7.3 \times 10^{-20}$ $u0 := -1.4 \times 10^{-20}$ $ub0 := -9.45 \times 10^{-20}$

$J11 := 1.0 \times 10^{-21}$ $J12 := -6.0 \times 10^{-21}$ $J13 := 5.0 \times 10^{-21}$ $J14 := 0$

$J21 := J12$ $J22 := -10.0 \times 10^{-21}$ $J23 := 5.0 \times 10^{-21}$ $J24 := 0$

$J31 := J13$ $J32 := J23$ $J33 := 6.0 \times 10^{-21}$ $J34 := 0$

$J41 := 0$ $J42 := J24$ $J43 := J34$ $J44 := 0$

$J11 := \frac{J11}{k \cdot Temp}$ $J12 := \frac{J12}{k \cdot Temp}$ $J13 := \frac{J13}{k \cdot Temp}$ $J14 := \frac{J14}{k \cdot Temp}$

$J21 := J12$ $J22 := \frac{J22}{k \cdot Temp}$ $J23 := \frac{J23}{k \cdot Temp}$ $J24 := \frac{J24}{k \cdot Temp}$

$J31 := J13$ $J32 := J23$ $J33 := \frac{J33}{k \cdot Temp}$ $J34 := \frac{J34}{k \cdot Temp}$

$J41 := 0$ $J42 := J24$ $J43 := J34$ $J44 := \frac{J44}{k \cdot Temp}$

Mole fraction:

$Xa := 0.5$ $\quad$ $Xb := 1 - Xa$

Scaling up of J and $u0$

$$uaos := \frac{ua0}{k \cdot Temp} \qquad ubos := \frac{ub0}{k \cdot Temp} \qquad uo := \frac{u0}{k \cdot Temp}$$

Chemical potential (scaled) of gas phase:

$Aa := 2 \cdot \pi \cdot (mwa \cdot mass) \cdot k \cdot Temp$ $\quad$ $Ab := 2 \cdot \pi \cdot (mwb \cdot mass) \cdot k \cdot Temp$

$BB := h^2$ $\quad$ $Ci := k \cdot Temp$

$$Da := \left(\frac{Aa}{BB}\right)^{\frac{3}{2}} \cdot Ci \qquad Db := \left(\frac{Ab}{BB}\right)^{\frac{3}{2}} \cdot Ci$$

$\mu aos := -\ln(Da)$ $\quad$ $\mu bos := -\ln(Db)$

$n := 1,2 \ldots 10000$ $\quad$ $P_n := n^{\frac{n}{5000}}$

$\mu as_n := \mu aos + \ln(Xa \cdot P_n)$ $\quad$ $\mu bs_n := \mu bos + \ln(Xb \cdot P_n)$

1 is a lying down, 2 is a standing up, 3 is b approximately sphere and 4 is a hole.

$\phi 1_n := \exp\left(\mu as_n - (uasos + u0)\right)$ $\quad$ $\phi 2_n := \exp\left(uas_n + uaos\right)$

$\phi 3_n := \exp\left(ubs_n + ubos\right)$ $\quad$ $\phi 4_n := 1.0$

$A11_n := (\phi 1_n)^{\frac{1}{2}} \cdot (\phi 1_n)^{\frac{1}{2}} \cdot \exp(-J11)$ $\quad$ $A21_n := A12_n$

$A12_n := (\phi 1_n)^{\frac{1}{2}} \cdot (\phi 2_n)^{\frac{1}{2}} \cdot \exp(-J12)$ $\quad$ $A22_n := (\phi 2_n)^{\frac{1}{2}} \cdot (\phi 2_n)^{\frac{1}{2}} \cdot \exp(-J22)$

$A13_n := (\phi 1_n)^{\frac{1}{2}} \cdot (\phi 3_n)^{\frac{1}{2}} \cdot \exp(-J13)$ $\quad$ $A23_n := (\phi 2_n)^{\frac{1}{2}} \cdot (\phi 3_n)^{\frac{1}{2}} \cdot \exp(-J23)$

$A14_n := (\phi 1_n)^{\frac{1}{2}} \cdot (\phi 4_n)^{\frac{1}{2}} \cdot \exp(-J14)$ $\quad$ $A24_n := (\phi 2_n)^{\frac{1}{2}} \cdot (\phi 4_n)^{\frac{1}{2}} \cdot \exp(-J24)$

$A31_n := A13_n$ $\quad$ $A41_n := A14_n$

$A32_n := A23_n$ $\quad$ $A42_n := A24_n$

$A33_n := (\phi 3_n)^{\frac{1}{2}} \cdot (\phi 3_n)^{\frac{1}{2}} \cdot \exp(-J33)$ $\quad$ $A43_n := A34_n$

$A34_n := (\phi 3_n)^{\frac{1}{2}} \cdot (\phi 4_n)^{\frac{1}{2}} \cdot \exp(-J34)$ $\quad$ $A44_n := (\phi 4_n)^{\frac{1}{2}} \cdot (\phi 4_n)^{\frac{1}{2}} \cdot \exp(-J44)$

$$B_n := \begin{pmatrix} A11_n & A12_n & A13_n & A14_n \\ A21_n & A22_n & A23_n & A24_n \\ A31_n & A32_n & A33_n & A34_n \\ A41_n & A42_n & A43_n & A44_n \end{pmatrix}$$

$eig1_n := \max\left(eigenvals\left(B_n\right)\right)$

$$en := P_n \frac{\left(100 \cdot 10^{-30}\right)}{Ci}$$

$step := 0.000001 \cdot \mu aos$

$$\phi 1_n := \exp \mu as_n - (uaos + u) + step$$
$$\phi 3_n := \exp(\mu bs_n - ubos)$$
$$A11_n := (\phi 1_n)^{\frac{1}{2}} \cdot (\phi 1_n)^{\frac{1}{2}} \cdot \exp(-J11)$$
$$A12_n := (\phi 1_n)^{\frac{1}{2}} \cdot (\phi 2_n)^{\frac{1}{2}} \cdot \exp(-J12)$$
$$A13_n := (\phi 1_n)^{\frac{1}{2}} \cdot (\phi 3_n)^{\frac{1}{2}} \cdot \exp(-J13)$$
$$A14_n := (\phi 1_n)^{\frac{1}{2}} \cdot (\phi 4_n)^{\frac{1}{2}} \cdot \exp(-J14)$$
$$A31_n := A13_n$$
$$A32_n := A23_n$$
$$A33_n := (\phi 3_n)^{\frac{1}{2}} \cdot (\phi 3_n)^{\frac{1}{2}} \cdot \exp(-J33)$$
$$A34_n := (\phi 3_n)^{\frac{1}{2}} \cdot (\phi 4_n)^{\frac{1}{2}} \cdot \exp(-J34)$$
$$B2_n := \begin{pmatrix} A11_n & A12_n & A13_n & A14_n \\ A21_n & A22_n & A23_n & A24_n \\ A31_n & A32_n & A33_n & A34_n \\ A41_n & A42_n & A43_n & A44_n \end{pmatrix}$$
$$\phi 1_n := \exp \mu as_n - (uaos + u0) + step$$
$$\phi 3_n := \exp(\mu bs_n - ubos + step)$$
$$A11_n := (\phi 1_n)^{\frac{1}{2}} \cdot (\phi 1_n)^{\frac{1}{2}} \cdot \exp(-J11)$$
$$A12_n := (\phi 1_n)^{\frac{1}{2}} \cdot (\phi 2_n)^{\frac{1}{2}} \cdot \exp(-J12)$$
$$A13_n := (\phi 1_n)^{\frac{1}{2}} \cdot (\phi 3_n)^{\frac{1}{2}} \cdot \exp(-J13)$$
$$A14_n := (\phi 1_n)^{\frac{1}{2}} \cdot (\phi 4_n)^{\frac{1}{2}} \cdot \exp(-J14)$$
$$A31_n := A13_n$$
$$A32_n := A23_n$$
$$A33_n := (\phi 3_n)^{\frac{1}{2}} \cdot (\phi 3_n)^{\frac{1}{2}} \cdot \exp(-J33)$$
$$A34_n := (\phi 3_n)^{\frac{1}{2}} \cdot (\phi 4_n)^{\frac{1}{2}} \cdot \exp(-J34)$$
$$B3_n := \begin{pmatrix} A11_n & A12_n & A13_n & A14_n \\ A21_n & A22_n & A23_n & A24_n \\ A31_n & A32_n & A33_n & A34_n \\ A41_n & A42_n & A43_n & A44_n \end{pmatrix}$$
$$kPr_n := \left(\frac{P_n}{1000}\right)$$

$$\phi 2_n := \exp(\mu as_n - uaos + step)$$
$$\phi 4_n := 1.0$$
$$A21_n := A12_n$$
$$A22_n := (\phi 2_n)^{\frac{1}{2}} \cdot (\phi 2_n)^{\frac{1}{2}} \cdot \exp(-J22)$$
$$A23_n := (\phi 2_n)^{\frac{1}{2}} \cdot (\phi 3_n)^{\frac{1}{2}} \cdot \exp(-J23)$$
$$A24_n := (\phi 2_n)^{\frac{1}{2}} \cdot (\phi 4_n)^{\frac{1}{2}} \cdot \exp(-J24)$$
$$A41_n := A14_n$$
$$A42_n := A24_n$$
$$A43_n := A34_n$$
$$A44_n := (\phi 4_n)^{\frac{1}{2}} \cdot (\phi 4_n)^{\frac{1}{2}} \cdot \exp(-J44)$$
$$eig2_n := \max(eigenvals(B2_n))$$
$$rhoa_n := \frac{\ln\left(\frac{eig2_n}{eig1_n}\right)}{step}$$
$$\phi 2_n := \exp(\mu as_n - uaos)$$
$$\phi 4_n := 1.0$$
$$A21_n := A12_n$$
$$A22_n := (\phi 2_n)^{\frac{1}{2}} \cdot (\phi 2_n)^{\frac{1}{2}} \cdot \exp(-J22)$$
$$A23_n := (\phi 2_n)^{\frac{1}{2}} \cdot (\phi 3_n)^{\frac{1}{2}} \cdot \exp(-J23)$$
$$A24_n := (\phi 2_n)^{\frac{1}{2}} \cdot (\phi 4_n)^{\frac{1}{2}} \cdot \exp(-J24)$$
$$A41_n := A14_n$$
$$A42_n := A24_n$$
$$A43_n := A34_n$$
$$A44_n := (\phi 4_n)^{\frac{1}{2}} \cdot (\phi 4_n)^{\frac{1}{2}} \cdot \exp(-J44)$$
$$eig3_n := \max(eigenvals(B3_n))$$
$$rhob_n := \frac{\ln\left(\frac{eig3_n}{eig1_n}\right)}{step}$$
$$\log kPr_n := \log\left(\frac{P_n}{1000}\right)$$

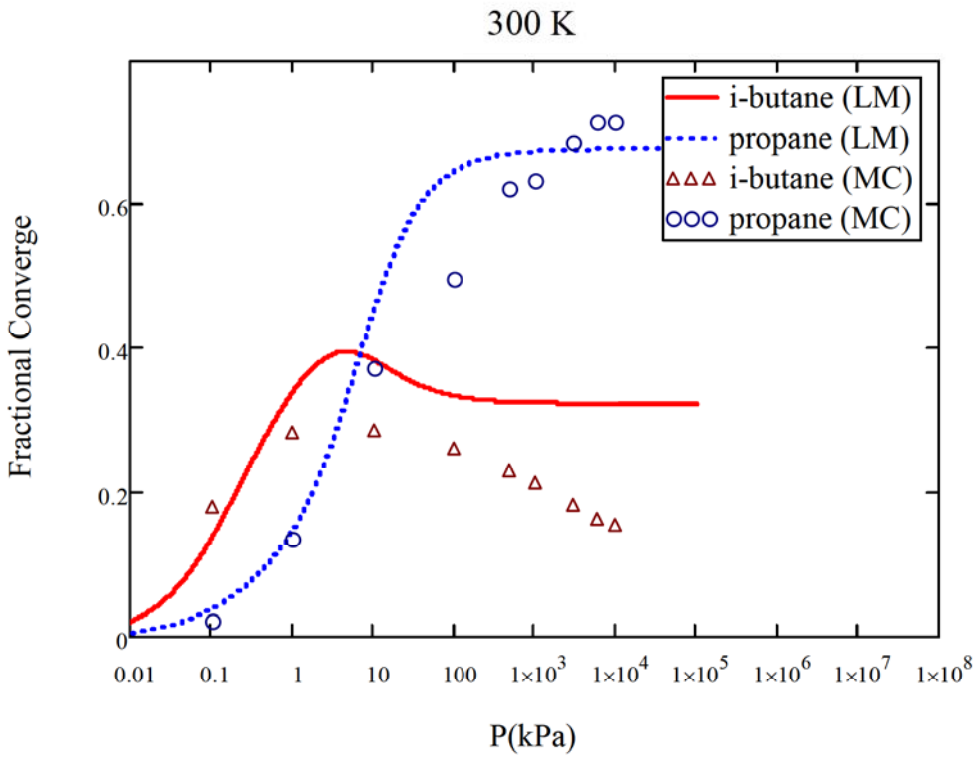

Lattice model adsorption of propane and i-butane equimolar at 300 K comparing with Monte Carlo results (see chapter 4).